

1919
TECHNICAL LIBRARY
REFERENCE COPY



346

AD 723403

TECHNICAL REPORT M-68-1

DYNAMICS OF WHEELED VEHICLES

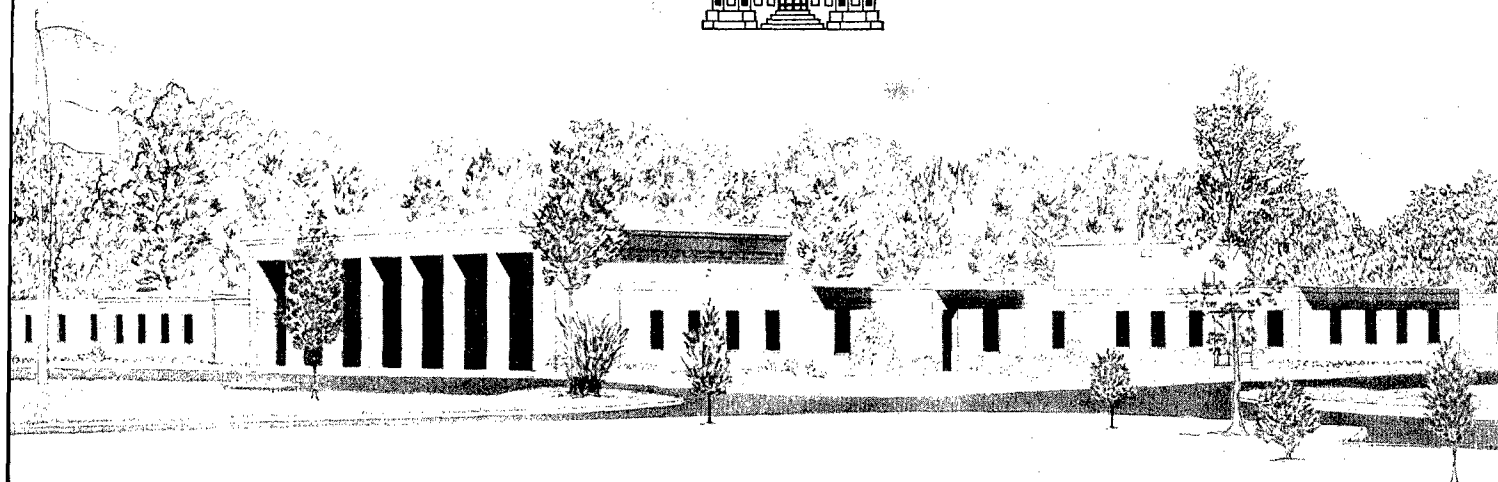
Report 2

IMPLEMENTATION OF WIENER-BOSE THEORY AND APPLICATION TO RIDE DYNAMICS

by

A. S. Lessem

20020724079



March 1971

Reproduced From
Best Available Copy

Sponsored by U. S. Army Materiel Command

Conducted by U. S. Army Engineer Waterways Experiment Station, Vicksburg, Mississippi

**Destroy this report when no longer needed. Do not return
it to the originator.**

**The findings in this report are not to be construed as an official
Department of the Army position unless so designated
by other authorized documents.**



DEPARTMENT OF THE ARMY
WATERWAYS EXPERIMENT STATION, CORPS OF ENGINEERS
P. O. BOX 631
VICKSBURG, MISSISSIPPI 39180

IN REPLY REFER TO: WESTR

7 May 1971

SUBJECT: Transmittal of Publications

Commanding General
U.S. Army Tank Automotive Center
ATTN: AMSTA-BSL
Warren, Michigan 48090

Technical Report M-68-1, "Dynamics of Wheeled Vehicles," Report 2, "Implementation of Wiener-Bose Theory and Application to Ride Dynamics," and Report 3, "A Statistical Analysis of Terrain Vehicle-Speed Systems," along with Technical Memorandum No. 3-240, "Trafficability of Soils; Nineteenth Supplement, Effects of Surface Conditions on Drawbar Pull of a Wheeled Vehicle," are inclosed.

FOR THE DIRECTOR:

2 Incl (dupe)

1. T. R. M-68-1, Rpts 2 and 3
2. T. M. 3-240, Nineteenth Supplement

W. W. GEDDINGS, JR.
Engineer
Information Services Branch



TECHNICAL REPORT M-68-1

DYNAMICS OF WHEELED VEHICLES

Report 2

IMPLEMENTATION OF WIENER-BOSE THEORY AND APPLICATION TO RIDE DYNAMICS

by

A. S. Lessem



March 1971

Sponsored by U. S. Army Materiel Command

Project IT061102B52A-01

Conducted by U. S. Army Engineer Waterways Experiment Station, Vicksburg, Mississippi

ARMY-MRC VICKSBURG, MISS.

This document has been approved for public release and sale; its distribution is unlimited

FOREWORD

This report was prepared by Dr. Allan S. Lessem of the Mobility Research Branch, Mobility and Environmental Division, U. S. Army Engineer Waterways Experiment Station. The report is essentially a thesis submitted by Dr. Lessem in partial fulfillment of the requirements for the degree of Doctor of Philosophy in Engineering to the Graduate Faculty of Mississippi State University, and is a study of the application of Wiener-Bose Theory to vehicle ride dynamics studies. The study described herein was conducted under DA Project 1T061102B52A, "Research in Military Aspects of Terrestrial Sciences," Task 01, "Military Aspects of Off-Road Mobility," under the sponsorship and guidance of the Research, Development and Engineering Directorate, U. S. Army Materiel Command. The program of tests was accomplished under the general direction of Messrs. A. J. Green, S. J. Knight, and W. G. Shockley.

COL Levi A. Brown, CE, and COL Ernest D. Peixotto, CE, were Directors of the Waterways Experiment Station during the period of preparation and publication of this report. Mr. F. R. Brown was Technical Director.

ACKNOWLEDGEMENTS

It is a pleasure to acknowledge the assistance of Dr. Willie L. McDaniel, Jr., in the conduct of a pertinent special problems course that marked the beginning of this study and in guiding its subsequent development. It also is a pleasure to acknowledge the assistance of Mr. Richard B. Ahlvin in many phases of this study.

The work reported in this dissertation was undertaken as one of the author's assignments with the Mobility and Environmental Division of the U. S. Army Engineer Waterways Experiment Station, Vicksburg, Mississippi. It is a pleasure to express appreciation to Messrs. A. J. Green, S. J. Knight, and W. G. Shockley for permission to pursue an unusual topic and for their support of ongoing education for their subordinates.

TABLE OF CONTENTS

	<u>Page</u>
FOREWORD	iii
ACKNOWLEDGEMENTS	v
LIST OF FIGURES	viii
LIST OF SYMBOLS	xi
 I. INTRODUCTION	
Background: Wiener-Bose Theory	1
Background: Ride Dynamics	4
Statement of the Problem	7
Purpose and Scope of This Dissertation	9
 II. THE BASIC IDEAS OF WIENER-BOSE THEORY	
General Considerations	10
Wiener's Theory of Nonlinear Systems: An Operations Point of View	11
Bose's Contribution to the Wiener Theory	28
 III. IMPLEMENTATION OF WIENER-BOSE THEORY	
Transition to a Practical Form	34
Nature and Determination of Characterizing Coefficients	48
Bose Noise	51
System Settling Time	55
Determination of Coefficients for Bose Noise Probe	57
Examples	58
 IV. APPLICATION TO RIDE DYNAMICS	
General Considerations	80
Selection of the Vehicle and the Wiener-Bose Models	82
Test Setup and Procedures	85
Results	94
Discussion	105
 V. CONCLUSIONS	
Some Guidelines for Constructing WBT Models	111
Conclusions	118
Recommendations	118
REFERENCES	120
ABSTRACT	122

LIST OF FIGURES

<u>Figure</u>		<u>Page</u>
1	Elements of Ride Dynamics Models	5
2	The Basic Idea of the Wiener Theory	15
3	Representation of the Past of the Input	16
4	Process Flow for Wiener Analysis	21
5	Process Flow for Wiener Synthesis	22
6	General Wiener Analysis and Synthesis Procedures	23
7	Hermite Function of Index 5	25
8	Hermite Function of Index 10	26
9	Bose Analysis and Synthesis Procedures	29
10	Gate Functions	30
11	Bose Analysis Process with Generalized Probe . . .	35
12	WBT Analysis and Synthesis Procedures	38
13	WBT Analysis for Zero-Memory System	39
14	Zero-Memory System of Example 1	41
15	Hysteretic System of Example 2	43
16	WBT Coefficients, Example 2	45
17	System Response to Specific Input, Example 2 . . .	46
18	Model Response to Specific Input, Example 2 . . .	47
19	Configuration Diagram, Example 2	54
20	Initial Part of Bose Noise Sequence, Example 2 . .	56
21	System of Example 3	59
22	Configuration Diagram, Example 3	62
23	Excerpts from Bose Noise Sequence, Example 3 . . .	63

<u>Figure</u>		<u>Page</u>
24	State Diagram, Example 3	65
25	Comparison of System and Model Responses, Example 3	66
26	System for Example 4	70
27	Model Parameters, Example 4	71
28	Configuration Diagram, Example 4	75
29	State Diagram, Example 4	76
30	Comparison of System and Model Responses, Example 4	77
31	Configuration Diagram, M37 Model	84
32	Representative Obstacle	86
33	Representative Obstacle	87
34	Representative Obstacle	88
35	Traversal of Last Step of an Obstacle	89
36	12-Obstacle Test Course	90
37	Complete Isolation of Front Wheel from Rear Wheel.	91
38	Incomplete Isolation of Rear Wheel from Front Wheel	92
39	Benchmark Model	96
40	Benchmark State Diagrams	97
41	Specific Inputs for Benchmark and WBT Models . . .	99
42	Vehicle and WBT (Benchmark) Responses	100
43	Vehicle and WBT (Benchmark) Responses	101
44	M37 State Diagrams	102
45	M37 Responses	103
46	M37 Responses	104
47	Comparison of Actual and Predicted RMS Pitch Time Histories	106
48	WBT Parameter Selection Flow Chart	112

LIST OF SYMBOLS

<u>Symbol</u>	<u>Meaning</u>
a_i	i^{th} WBT coefficient
$\text{avg}(\cdot)$	Time average operator
B_i	Dashpot compliances, example 4
$E(\cdot \cdot)$	Conditional expectation operator
F_i	Compliance forces, example 4
$G(x)$	WBT weighting function on system input
h_i	i^{th} Laguerre function
I	Moment of inertia, example 4
K_i	Spring compliances, example 4
ℓ_i	Characteristic lengths, example 4
M_i	Lumped masses, example 4
m_i	Number of gate functions on the i^{th} delay line tap
N_t	Number of delay line taps
N_c	Number of coefficients
N_B	Number of amplitude levels in Bose Noise sequence
s	Amplitude spread parameter
$\text{sat}(\cdot)$	Saturation operator, example 3
T_s	System settling time
ΔT	Time increment between delay line taps
u_i	i^{th} Laguerre coefficient
x	System input
y	System output
z_n	Approximation to system output

<u>Symbol</u>	<u>Meaning</u>
β_i	i^{th} Wiener coefficient
Δ_i	Compliance deflections, example 4
ε	Mean square error
η_i	i^{th} Hermite polynomial
θ_i	i^{th} Laguerre polynomial
ϕ_i	i^{th} gate function

I. INTRODUCTION

Background: Wiener-Bose Theory

Wiener-Bose Theory is a theory of nonlinear systems analysis first assembled by Norbert Wiener [1] and modified later by A. G. Bose [2]. Its purpose is to obtain a mathematical model of standard form of any nonlinear system taken from a broad class of applicable systems. The model is in terms of a set of "characterizing coefficients" which are obtained through the agency of a certain testing program carried out on the specific system. Once the coefficients have been determined they may be used in a rational synthesis procedure to predict responses to inputs of interest. The principal appeal of Wiener-Bose Theory is that it requires very little knowledge of the physics of the system. No dynamical equations need be written. In essence the physics of the system is incorporated into the characterizing coefficients.

Wiener-Bose Theory is based upon the use of a series expansion of orthogonal functionals. The use of expansions in series of polynomials to represent functions that are not amenable to concise mathematical expression is a familiar and fruitful method of analysis.[3] An extension of this technique involves the use of orthogonal polynomials.[4] In both cases, polynomials, $p_i(x)$, are used in some way to represent a function, $y(x)$, and both p and y are "no-memory" functions of their arguments in the sense that each entry of a value for x immediately produces corresponding values for p and for y . Algebraic expressions are of this nature. In contrast, expressions involving implicit derivatives or integrals are not of this kind. For example

the solution of

$$\frac{dy}{dx} + g(x)y = f(x)$$

is

$$y = e^{-F(x)} \left(\int e^{F(\xi)} f(\xi) d\xi + c \right)$$

where

$$F(x) = \int g(\xi) d\xi$$

We see that all values of x from the origin of integration to its present value are involved in finding the present value of y . In this case y is a functional of x and may be thought of as a function "with memory."

Much work has been done to formulate a calculus of series expansions in functionals that parallels, at least conceptually, the use of series expansions for functions.[5] One approach expands the functional, $y(x)$, in a series of iterated convolution integrals (Volterra functionals) as follows:

$$y[x(t)] = h_0 + \sum_{i=1}^N \underbrace{\int \int \dots \int}_i h(\tau_1, \tau_2, \dots, \tau_i) \prod_{j=1}^i x(t - \tau_j) d\tau_j$$

For the case of linear systems, this series reduces to the familiar convolution integral of linear theory. We may go further and formulate expansions in series of orthogonal functionals as well.[6] It was Norbert Wiener's contribution to formulate a strategy for producing a

series of orthogonal Volterra functionals when the argument, $x(t)$, is white Gaussian noise. He recognized the equivalence of such a series to a multivariate series expansion of Hermite functions having white Gaussian arguments. He consolidated these factors into a strategy where the Gaussian noise was used as a "probe" for the nonlinear system in the same sense as an impulse is a probe for a linear system. The characterizing coefficients referred to above are the coefficients of the Hermite function expansion, whose orthogonality permits their separate determination.

Wiener presented his work to a group of graduate students during a series of summer lectures in the early 1950's. Except for a brief monograph, Wiener's own exposition of this theory was unpublished. Descriptions, discussions of, and additions to the theory were accomplished as dissertations by his students. No practical applications of the theory were reported.

A significant modification of the theory was made by Bose.[2] The basic idea of empirical characterization was retained but the characterizing agent was not required to be Gaussian noise. Bose defined a multivariate expansion, a "gate-function" expansion, different from the Hermite expansion used by Wiener. The Wiener expansion gives a continuous approximation to the desired response; the Bose expansion gives a staircase approximation. Through a procedure analogous to Wiener's, Bose obtained separately determinable characterizing coefficients for the nonlinear system. Although no implementation was attempted the potential exists for simpler realization than the original Wiener theory allows.

In recent years, Harris has attempted an application [7] of a

truncated form of Wiener-Bose Theory with encouraging success. With suitable restraints on the nature of the inputs that can be accommodated, he was able to significantly reduce the number of coefficients required for satisfactory model performance.

Wiener-Bose Theory has not seen abundant application to systems of engineering interest because of formidable demands upon computer capacity and because of practical difficulties of coefficient determination. The original Wiener Theory is especially liable to difficulties of implementation but Bose's form of the theory fares better. Certain additional modifications are suggested in this dissertation that are potentially capable of bringing application effort within reasonable limits for many nonlinear systems.

Background: Ride Dynamics

Ride dynamics refers to the vibratory motion of vehicles in response to traversal of irregular terrain. For many military, commercial, and agricultural vehicles operating in an on- and off-road environment, overall mobility is limited by such vibratory motion. Simulation studies of ride dynamics are used for rational design and evaluation of vehicles. These studies are accomplished through the use of mathematical models that reflect the structure and interaction of vehicles and terrains.

At present, ride dynamics models are constructed as required from a common set of building blocks.[8] These are illustrated in fig. 1 with a representative coupling scheme, and reflect the fact that there are five principal problem areas: representation of the terrain, the vehicle, their interaction, and the identification and use of outputs.

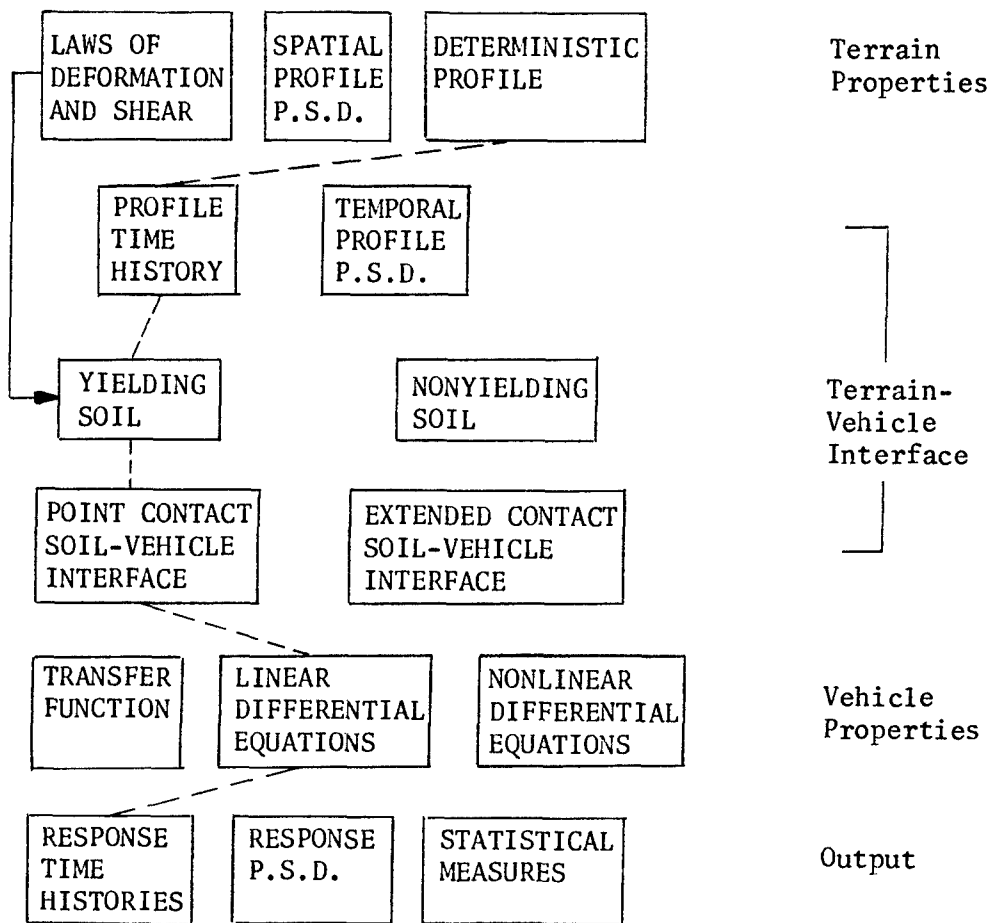


Figure 1 Elements of Ride Dynamics Models

The central problem for ride analysis is the representation of the vehicle. A physically motivated mathematical model that properly accounts for significant structural flexing is too unwieldy for practical applications. The use of rigid-body mechanics has become the standard approach. Vehicles are represented as collections of masses, springs, and damping elements suitably configured for the job at hand. These give rise to sets of differential equations which describe motions throughout the vehicle. Nonlinearities are inevitable. They arise, for example, from the physics of suspension components, from limitations on suspension travel, and from large pitch and roll motions. A trade-off is required between the inclusion of these important nonlinearities and the added complexity of analysis.

Another important problem for ride analysis is the representation of terrain. The property of principal interest is the terrain profile--a record of changes in elevation encountered along the path of the vehicle. This profile is used as a displacement time history or is converted to a power spectral density for input to the vehicle model. Most models imagine that the soil-vehicle interface is nonyielding; this is easy to do since no additional equations are required. It is also reasonable because for purposes of ride analysis it represents a worst-case situation. Some models have attempted more realism in this respect and have included yielding interfaces. This increases the complexity of the model, but permits a realistic and desirable coupling of ride analysis and mobility analysis in one package. The tradeoff between realism and complexity also influences the choice of an easily implemented point-contact soil-vehicle interface or a more realistic

extended-contact interface.

The generation of outputs from vehicle models is a relatively simple task. These consist of time histories of various responses and their counterpart power spectral densities and statistical measures. These outputs represent dynamic inputs to drivers, passengers, and cargo. It is the responses of these elements of the man-machine system that usually govern the contribution of ride dynamics to vehicle mobility.

Methods of analysis have developed along two complementary lines: time history and frequency response. The first uses differential equations which are "driven" by time dependent forcing functions and produce time dependent responses. The second displays properties of interest, typically statistical properties such as root mean square elevation or acceleration, against a frequency parameter. An analysis predicated on time histories can be used for frequency response at little extra cost. Most vehicle dynamics models reflect this fact by being set up to exercise both options. The great appeal of frequency response analysis is that under conditions such that linearity is a reasonable assumption, it is possible to bypass the use of differential equations entirely (and thus the detailed workings of the vehicle) and deal directly with input-output correspondences.

Statement of the Problem

The state of the art of current practice in mathematical modeling for ride dynamics gives the impression that there are few problems of concept and implementation. The vehicles appear to be assemblages of

several mechanical subsystems, each of which appears to be amenable to straightforward mathematical modeling through the use of structure-oriented mass-spring-dashpot concepts.

This appearance is, however, quite deceptive. Although there are many examples of carefully written ride dynamics models, some of which are very elaborate and would seem to include every reasonable dynamical contribution, the problem of correct simulation remains unsolved. When comparing the actual motions of a vehicle measured in the field and the motions predicted by its model, the usual result is that the model does a poor job until it has been carefully "tuned." The tuning process involves making changes in a priori estimates of parameters to bring model responses into accord with the field responses. When compared against another set of field responses the tuning process must be invoked again. Thus the use of current vehicle dynamics models involves a basically irrational parameter adjustment process that is accepted as a necessary evil of the modeling strategy.

It would be of value to develop another, completely different, strategy for ride dynamics studies. Wiener-Bose Theory can provide this new approach. The principal difficulty with conventional ride analysis is the (necessarily) incomplete modeling of the physics of the vehicle. Wiener-Bose Theory requires no detailed knowledge of the vehicle. We know the physics of the vehicle as the empirical response of the vehicle to traversal of a special obstacle course. Once the vehicle has been characterized its response to specific terrain profiles may be determined.

The basic problem to which this dissertation is addressed is to learn how to bring Wiener-Bose Theory to bear upon the specific nonlinear

systems of interest in vehicle ride dynamics.

Purpose and Scope of This Dissertation

This dissertation has two principal goals:

- a. Elucidation: to uncover and solve problems of implementation of Wiener-Bose Theory.
- b. Application: to apply Wiener-Bose Theory to a specific ride dynamics problem.

The first goal was sought by making an extensive computer study of the original Wiener Theory and of the modified one due to Bose. Several additional useful modifications of the basic theory became apparent and a practical form evolved. A series of increasingly complex examples was studied and experience gained was summed up in a set of guidelines for constructing Wiener-Bose models.

The second goal was sought through a field test program in which characterizing coefficients for a wheeled vehicle were determined using concepts developed earlier in the computer study. The test program involved the design and construction of an obstacle course whose traversal by the vehicle became the probing process required by the model. Once the coefficients were obtained, comparisons of model predictions and actual vehicle responses were made for traversals of several terrain profiles of interest.

II. THE BASIC IDEAS OF WIENER-BOSE THEORY

General Considerations

We want to recognize from the outset that Wiener-Bose Theory (WBT) is difficult to use. It is addressed to the characterization of such a broad class of systems that we could hardly expect otherwise. In general, systems that are independent of the remote past of their inputs are treated. This means that responses to impulsive or step-function inputs relax to equilibrium levels and that oscillations damp out and do not occur spontaneously. We must make a judgement of "remoteness" in each case.

The system parameters must remain constant. Because WBT is not predicated on some a priori model for the system, there is no way to account for varying parameters. If the rate of variation were slow compared with the duration of probing, it would be possible to obtain several ensembles of coefficient sets for system characterization. However, as shall become apparent in subsequent discussions of probing effort, this approach would probably be unreasonable.

WBT requires no detailed insight into the physics of the nonlinear system. This fact is at once the greatest strength and the greatest weakness of the theory. On the one hand, WBT provides a possible method of analysis in cases where the complexity of the system precludes acceptable structure-oriented modeling. On the other, we require a copy of the system at our disposal to bring the theory to bear. The analysis is in terms of input-output quantities and gives no insight into the internal workings of the system.

The ability to define inputs and outputs is of central importance for successful application of WBT. In many cases the determination of what is an input and what is an output and, indeed, what is the system will be the most difficult tasks. In what follows we will be discussing single input-single output systems.

Wiener's Theory of Nonlinear Systems: An Operations Point of View

Several excellent detailed discussions of Wiener's theory are in the literature.[2,4,9] The presentation given below is not intended to duplicate these discussions but, instead, to give the flavor of the theory, its working formulas and an idea of the effort involved in implementation.

To get the basic point of Wiener's theory, consider the following example: We have a function, $f(x)$, in the form of a graph or set of data points for which we want an analytic expression in terms of an expansion in a series of orthogonal polynomials. We will use normalized Hermite polynomials defined by

$$\eta_i(x) = \left(\sqrt{2^{i-1} (i-1)! \sqrt{\pi}} \right)^{-1} (-1)^{i-1} e^{x^2} \frac{d^{(i-1)}}{dx} e^{-x^2} \quad i = 1, 2, 3 \dots$$

These have the properties of orthogonality and normality over the interval $(-\infty < x < \infty)$ with respect to the weighting function $\exp(-x^2)$:

$$\int_{-\infty}^{\infty} \eta_i(x) \eta_j(x) e^{-x^2} dx = \begin{cases} 0 & i \neq j \\ 1 & i = j \end{cases} \quad (1)$$

Our series expansion is to be

$$f(x) = \sum_{i=1}^{\infty} \beta_i \eta_i(x) e^{-x^2/2} \quad (2)$$

and we want to find the set of coefficients, $\{\beta_i\}$. To do this we multiply both sides of equation 2 by the j^{th} Hermite function

$$\eta_j(x) e^{-x^2/2}$$

and integrate to get

$$\int_{-\infty}^{\infty} f(x) \eta_j(x) e^{-x^2/2} dx = \sum_{i=1}^{\infty} \int_{-\infty}^{\infty} \beta_i \eta_i(x) \eta_j(x) e^{-x^2} dx \quad (3)$$

With reference to equation 1 we see that only when $i=j$ is there a non-zero term on the right side of equation 3 and that

$$\beta_i = \int_{-\infty}^{\infty} f(x) \eta_i(x) e^{-x^2/2} dx \quad (4)$$

This is our desired rule for finding $\{\beta_i\}$.

We may find the coefficients another way. Suppose x is a function of time $x(t)$ and that the function is random with Gaussian amplitude probability density and unity variance. Then its probability density function is

$$p(x) = \frac{1}{\sqrt{2\pi}} e^{-x^2/2}$$

We can write equation 4 as follows:

$$\beta_i = \sqrt{2\pi} \int_{-\infty}^{\infty} f(x) \eta_i(x) \frac{e^{-x^2/2}}{\sqrt{2\pi}} dx$$

which may be interpreted as the expected value of the random function $f(x)\eta_i(x)$. If we confine our attention to random functions that are stationary and erogodic we may write

$$\sqrt{2\pi} \int_{-\infty}^{\infty} f(x) \eta_i(x) \frac{e^{-x^2/2}}{\sqrt{2\pi}} dx = \sqrt{2\pi} \left[\lim_{T \rightarrow \infty} \frac{1}{T} \int_0^T f(x) \eta_i(x) dt \right]$$

or

$$\beta_i = \sqrt{2\pi} \text{ avg } [f(x)\eta_i(x)]$$

in which we are expressing the fact that each β_i is obtained from the time average of the product of $f(x)$ and $\eta_i(x)$ when the argument is the Gaussian random function $x(t)$.

This second method for finding $\{\beta_i\}$ illustrates the essence of Wiener's theory. The function, $f(x)$, represents the response of a certain nonlinear system to its input, x . We want to use equation 2 as a model for this system and will characterize the system by the coefficient set, $\{\beta_i\}$. Wiener has shown that we may "probe" the system with Gaussian noise, form averages of products of the response and the Hermite polynomials, $\eta_i(x)$, and thus find the $\{\beta_i\}$. Note that we are committed to the use of the Hermite polynomials with the Gaussian probe because the weighting function for orthogonality of the polynomials and the probability density of the probe must be of the same form.

The function, $f(x)$, in the foregoing example represented the response of a "zero-memory" system. To each value of the input, x , corresponds a single response regardless of earlier inputs. Most systems of interest will be of "finite memory" which means that present responses depend upon both present and earlier inputs. Wiener's theory was intended to characterize such finite-memory, nonlinear systems. Wiener does this by expressing the present response as a function of the "past of the input." Figure 2 illustrates this idea.

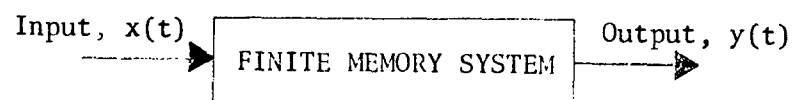
Both the past of $x(t)$ and the function $f(\cdot)$ are represented by polynomial expansions. The past of the input, $x(t)$, is represented by a polynomial expansion of the form

$$x(t-\tau) = \sum_{i=1}^{\infty} u_i(t) \theta_i(\tau) \quad (5)$$

Equation 5 expresses the idea that at a certain time, t , we can go into the past by an amount, τ , and express x at that time in terms of an expansion in polynomials, $\theta_i(\tau)$, with coefficients $u_i(t)$. Figure 3 illustrates this idea using a finite number of terms in equation 5. As time, t , advances the coefficients, $u_i(t)$, change. They must be computed continuously as $x(t)$ changes. Within the desirable constraint that they be orthogonal, the choice of polynomials, $\theta_i(\tau)$, is free. When the polynomials are orthogonal, the coefficients satisfy a minimum mean squared error criterion.[10] Wiener chose the Laguerre polynomials

$$\theta_i(\tau) = \frac{1}{(i-1)!} e^{\tau} \frac{d^{(i-1)}}{d\tau} \left(\tau^{i-1} e^{-\tau} \right) \quad i = 1, 2, 3, \dots$$

If these polynomials are multiplied by $e^{-\tau/2}$ they become the normalized



$$y(t) = f(\text{past of } x(t))$$

Figure 2 The Basic Idea of The Wiener Theory

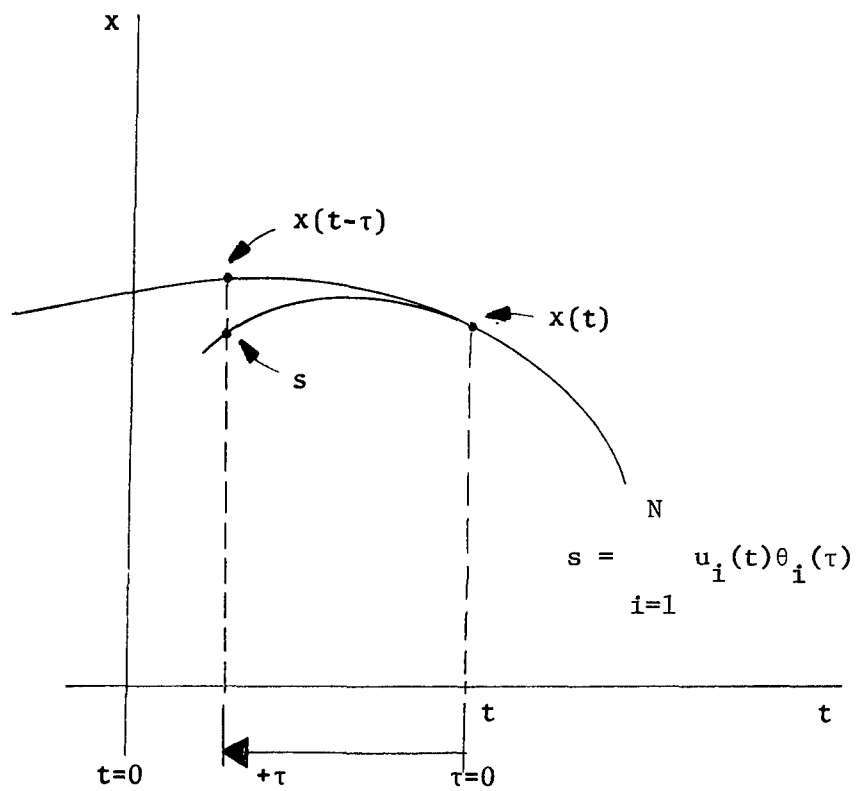


Figure 3 Representation of the Past of the Input

Laguerre functions and amenable to straightforward implementation.[11]

Writing

$$h_i(\tau) = \theta_i(\tau) e^{-\tau/2}$$

our expansion of the past of the input is

$$x(t-\tau) = \sum_{i=1}^{\infty} u_i(t) h_i(\tau)$$

The coefficients, $u_i(t)$, for this expansion may be obtained by solving the set of equations:[7]

$$\dot{u}_1(t) = -\frac{u_1(t)}{2} + x(t) \quad (6)$$

$$\dot{u}_i(t) = -\frac{u_i(t)}{2} - \sum_{j=1}^{i-1} u_j(t) + x(t) \quad i = 2, 3, \dots \quad (7)$$

Equations 6 and 7 give the method for continuously computing the coefficients, $u_i(t)$, of the Laguerre function expansion of $x(t)$. The past of the input now consists of a large set of time varying coefficients which may be used to reconstruct $x(t-\tau)$.

To represent the functional dependence of the present output on the past of the input, Wiener used the Hermite polynomial expansion discussed above. In this instance we are expanding a function of the many variables, $\{u_i(t)\}$, and Wiener's expression is the multivariate expansion

$$z_n(t) = \sum_{i=1}^{\infty} \sum_{j=1}^{\infty} \dots \sum_{k=1}^{\infty} \beta_{i,j, \dots, k} \eta_i(u_1) \eta_j(u_2) \dots \eta_k(u_n) \exp \left(- \sum_{i=1}^n \frac{u_i^2}{2} \right) \quad (8)$$

$$y(t) = \lim_{n \rightarrow \infty} z_n(t) \quad (9)$$

If our system is in fact independent of the past there is no need for the Laguerre function expansion and equations 8 and 9 reduce to equation 2.

The coefficients $\{\beta_{i,j, \dots, k}\}$ are calculated according to the following rule when $x(t)$ is Gaussian noise:

$$\beta_{i,j, \dots, k} = (\sqrt{2\pi})^n \text{avg} [y(t) \eta_i(u_1) \eta_j(u_2) \dots \eta_k(u_n)] \quad (10)$$

Bose [2] shows that equation 10 corresponds to a minimum weighted mean square error criterion between $y(t)$ and $z_n(t)$ as follows:

$$\epsilon = \text{avg} \left[\left[y(t) - z_n(t) \right]^2 \exp \left(\sum_{i=1}^n \frac{u_i^2}{2} \right) \right] = \text{minimum}$$

Equations 8, 9, and 10 represent the main result of Wiener's theory.

Any effort to use these equations must involve a finite number of terms so that in practice our working formula is

$$y(t) = \sum_{i=1}^{m_1} \sum_{j=1}^{m_2} \dots \sum_{k=1}^{m_n} \beta_{i,j,\dots,k} \eta_i(u_1) \eta_j(u_2) \dots \quad (11)$$

$$\eta_k(u_n) \exp \left[- \sum_{i=1}^n \frac{u_i^2}{2} \right]$$

where n is the number of Laguerre coefficients representing the past of the input and m_i is the number of Hermite polynomials used to expand the i^{th} Laguerre coefficient.

To illustrate the experimental process involved in computing the $\{\beta_{i,j,\dots,k}\}$ consider an especially simple case. Let $n = 2$, $m_1 = 2$, and $m_2 = 2$. Thus we are representing the past of the input by two Laguerre coefficients, and each Laguerre coefficient is expanded in a series of two Hermite polynomials. For this case equation 11 becomes

$$y(t) = [\beta_{11} \eta_1(u_1) \eta_1(u_2) + \beta_{12} \eta_1(u_1) \eta_2(u_2) + \beta_{21} \eta_2(u_1) \eta_1(u_2) + \beta_{22} \eta_2(u_1) \eta_2(u_2)] \exp \left[- \frac{u_1^2 + u_2^2}{2} \right]$$

The β 's are evaluated using equation 10

$$\begin{aligned} \beta_{11} &= 2\pi \text{ avg } [y(t) \eta_1(u_1) \eta_1(u_2)] \\ \beta_{12} &= 2\pi \text{ avg } [y(t) \eta_1(u_1) \eta_2(u_2)] \\ \beta_{21} &= 2\pi \text{ avg } [y(t) \eta_2(u_1) \eta_1(u_2)] \\ \beta_{22} &= 2\pi \text{ avg } [y(t) \eta_2(u_1) \eta_2(u_2)] \end{aligned} \quad (12)$$

Equation 12 may be implemented as illustrated in fig. 4. These β 's are used to synthesize specific responses to specific inputs as indicated in fig. 5. In terms of parallel mathematical operations, we can see that the analysis process requires two integrations in the Laguerre coefficient generator and four integrations to perform the averaging process for a total of six integrations. We require four function generations, four multiplications, and a source of Gaussian noise. The synthesis process requires two integrations, four multiplications, and four function generations.

In general, selections of n, m_1, m_2, \dots, m_n will produce N_c coefficients where

$$N_c = \prod_{i=1}^n m_i$$

Even modest selections for n and the m 's produce very large N_c 's. A block diagram for the characterization process is shown in fig. 6a. Once the coefficients have been established they are used to synthesize responses as indicated in fig. 6b. Once again, in terms of parallel mathematical operations, analysis requires $(n + N_c)$ integrations, N_c multiplications, and N_c function generations. Synthesis requires n integrations, N_c multiplications, and N_c function generations. When we realize that the practical applications of this theory will call for thousands of coefficients to be determined, we can appreciate the severe demands made upon computer facilities regardless of whether they are digital, analog, or hybrid.

Taken as a whole, we see Wiener's theory as a cleverly interlocked compilation of ideas:

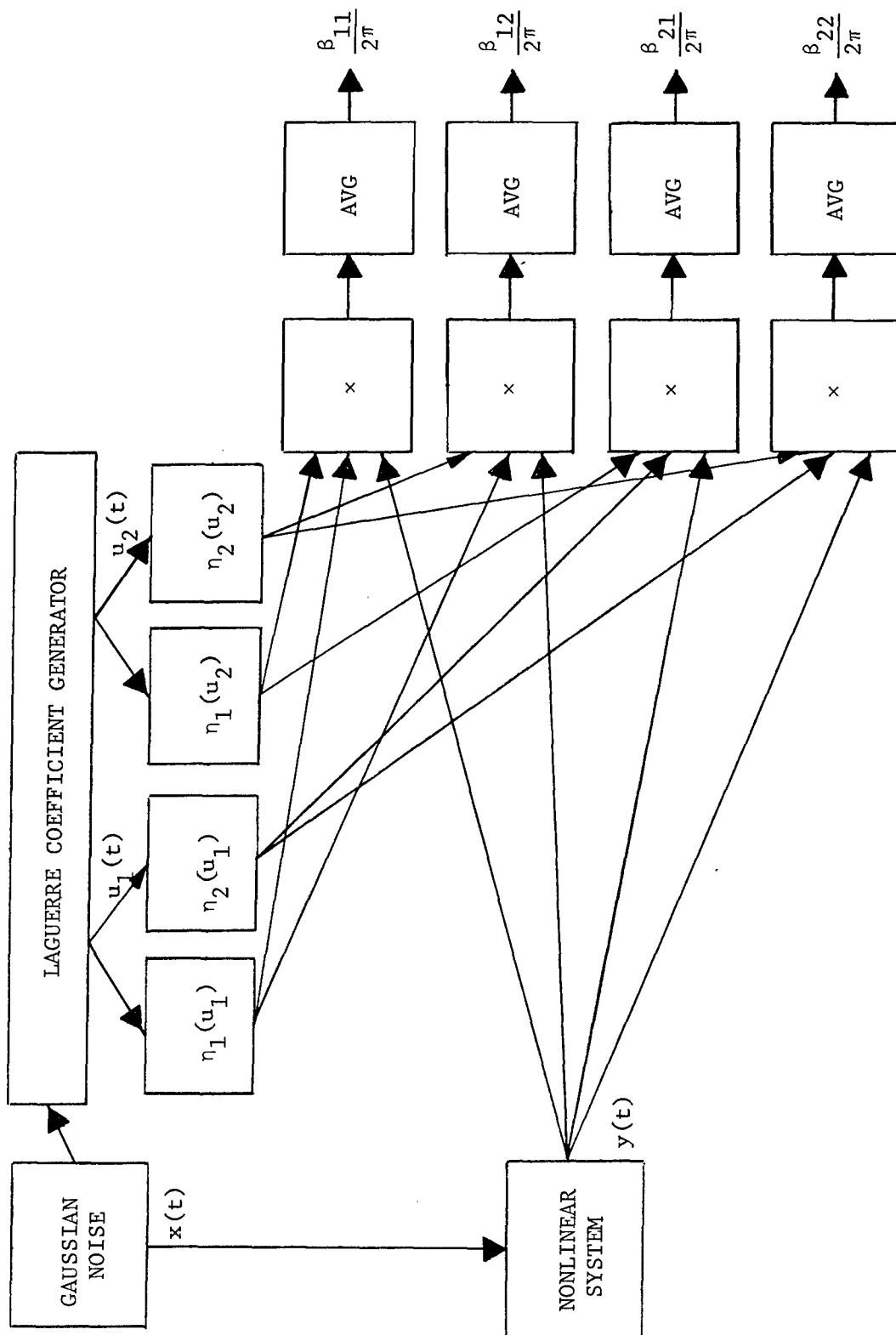


Figure 4 Process Flow for Wiener Analysis

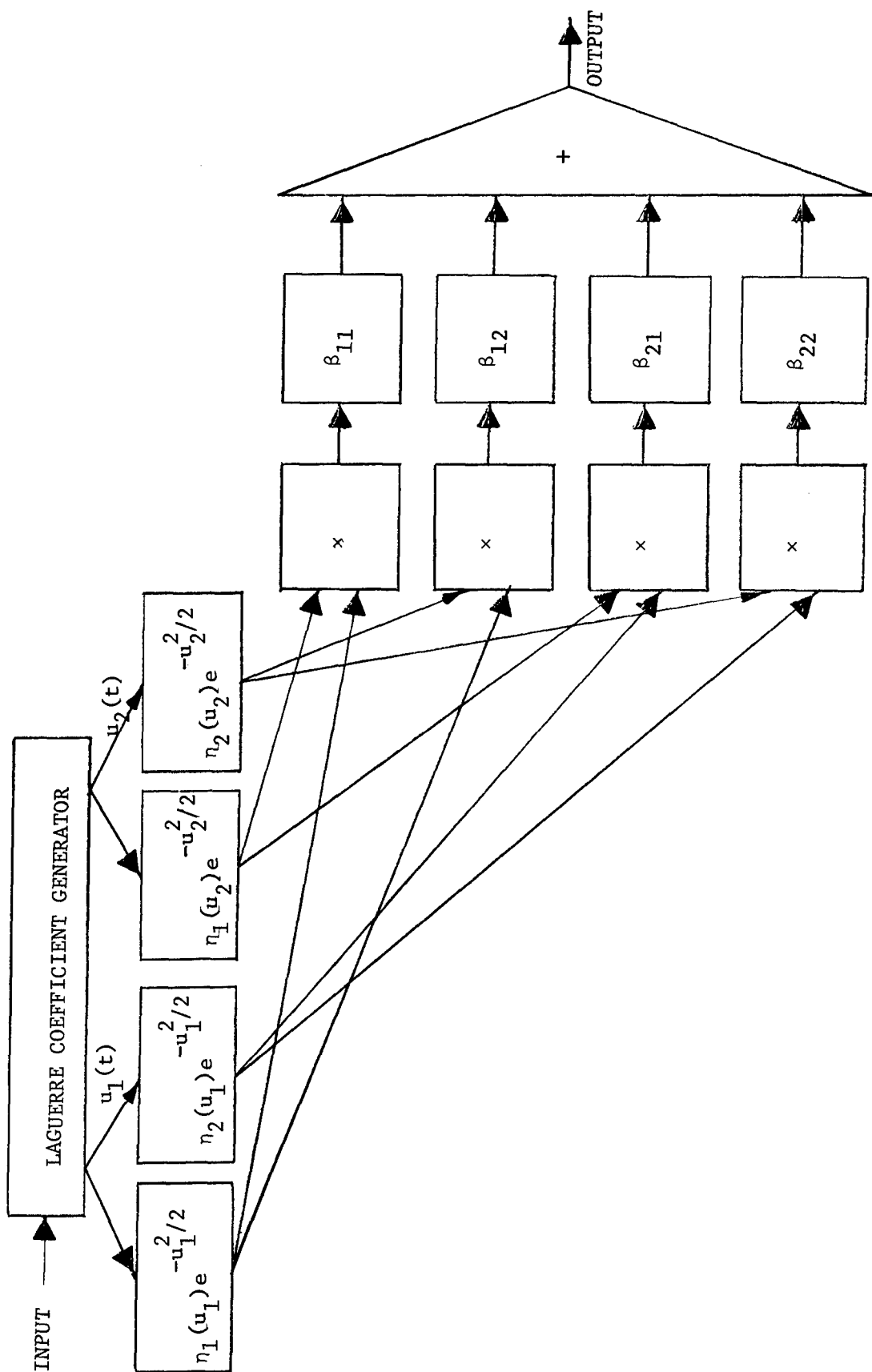
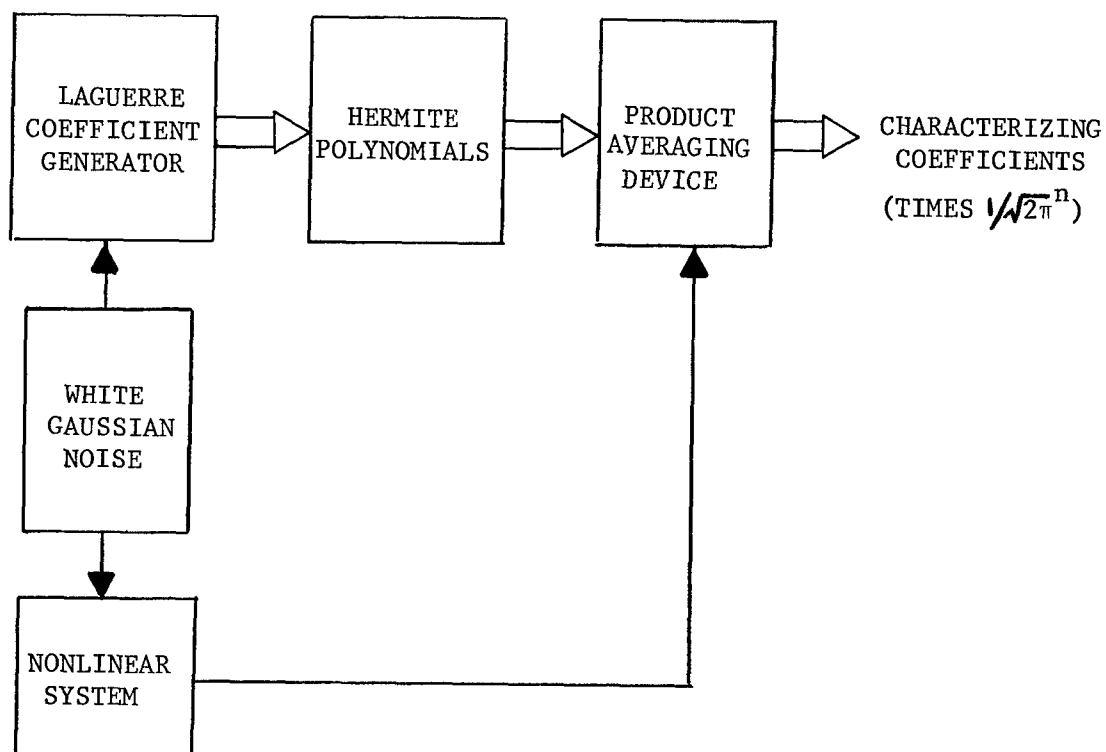
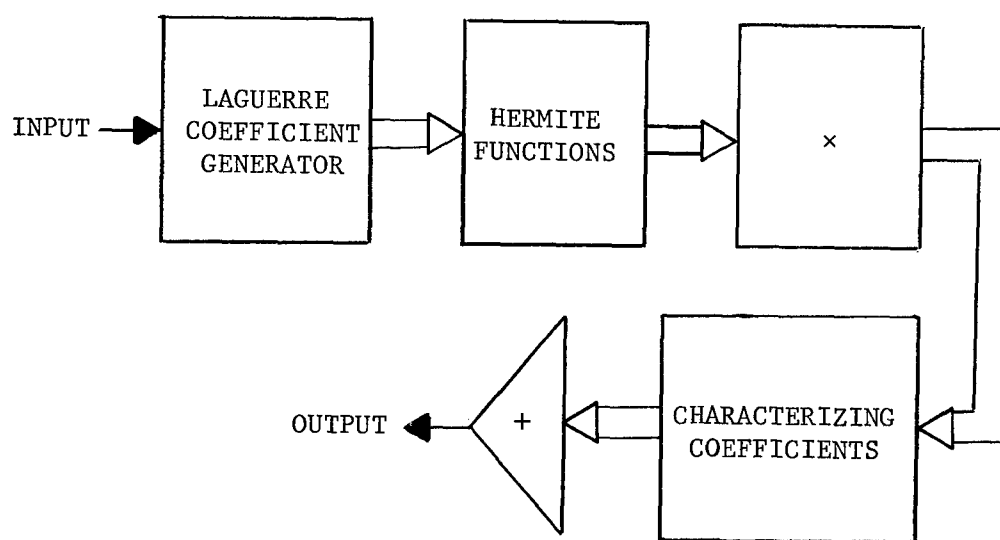


Figure 5 Process Flow for Wiener Synthesis



a. Analysis



b. Synthesis

Figure 6 General Wiener Analysis and Synthesis Procedures

- a. Nonlinear systems are viewed as a cascade of two subsystems. One is linear, of finite memory, and represents the past of the input. The other is nonlinear, of zero memory, and represents the transformation that produces the present output from the past of the input.
- b. The use of Gaussian noise as the probe is an experimentally feasible procedure. Its use requires us to use the Hermite polynomials for expanding the past of the input.
- c. The use of the Laguerre functions to represent the past of the input is reasonable in terms of both analog or digital simulation. It is important for the expansion in Hermite polynomials and the generation of coefficients that the response of each Laguerre coefficient, u_i , to a Gaussian input of given variance also be Gaussian and have the same variance. Harris [7] shows that the Laguerre coefficients have this property when the probe has a constant power spectrum (white Gaussian noise).

It would seem that the only basic constraint to the practical implementation of Wiener's theory is a limit on the number of coefficients that can be used to model a particular system with acceptable effort. But there are other factors which contribute to difficulties in applying the theory:

- a. The Hermite function expansion converges slowly. Representative Hermite functions are shown in figs. 7 and 8. For small arguments they are sinusoidal in character. But their frequencies do not increase as rapidly with the index as

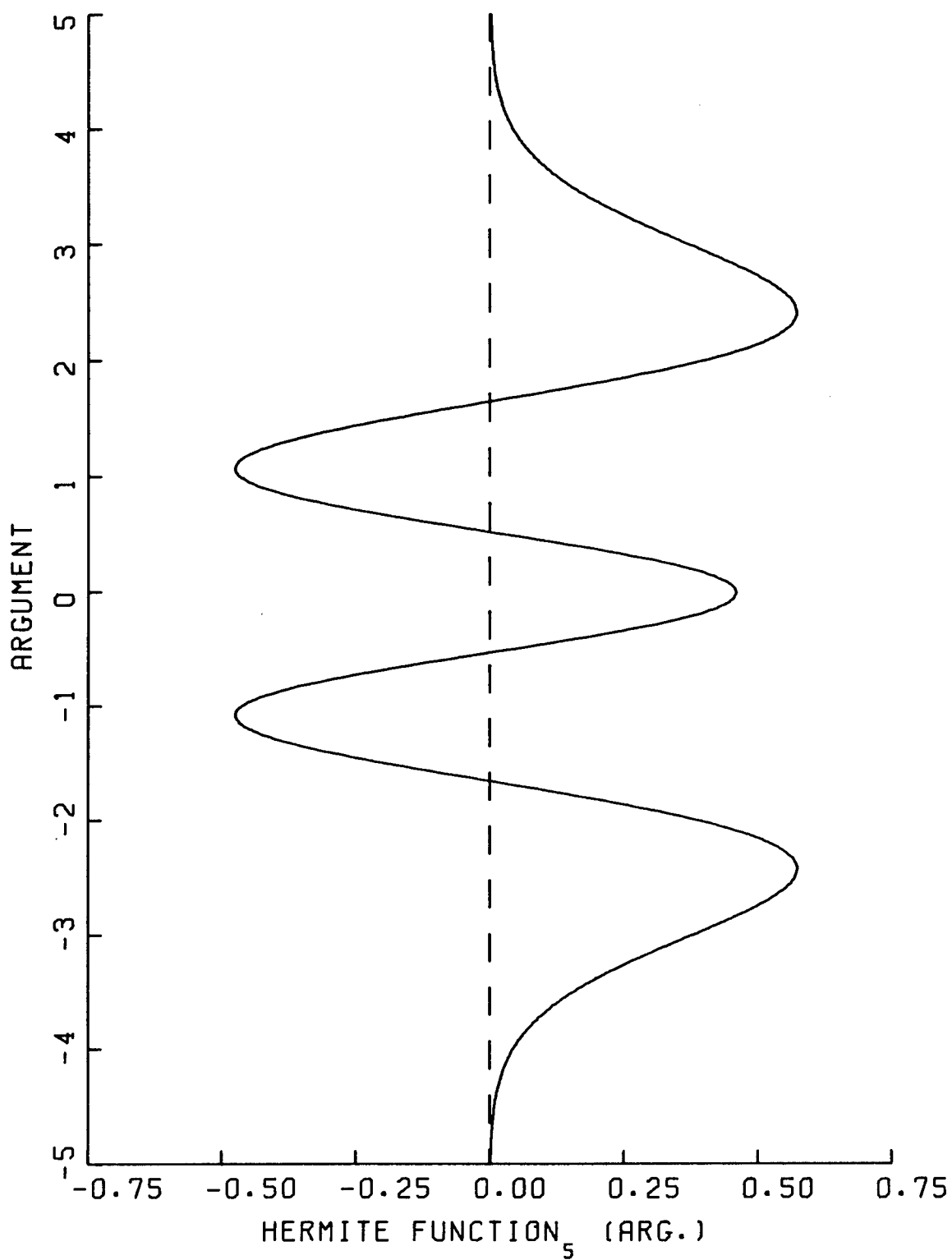


Figure 7 Hermite Function of Index 5

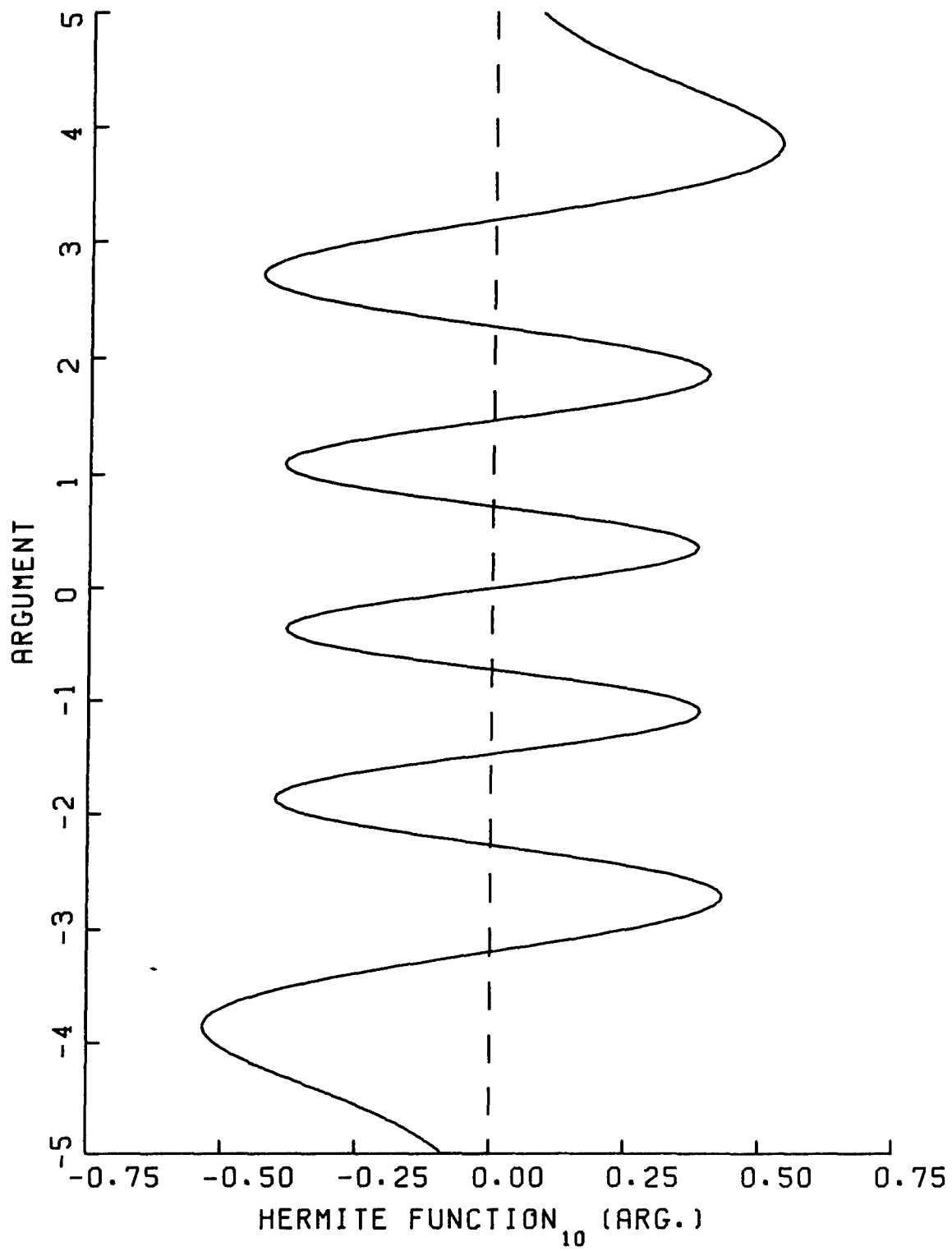


Figure 8 Hermite Function of Index 10

they would in a Fourier expansion, so that the Hermite expansion cannot converge as quickly as would a Fourier expansion. We must expect to use many coefficients to achieve a small error. Furthermore, for large arguments, the weighting function, $\exp(-x^2)$, is so small that large errors in the expansion are possible even within the context of satisfying a minimum weighted mean square error criterion.[12]

- b. Although in principle the Laguerre coefficients for the past of the input, $x(t)$, are Gaussian, independent, and of equal variance when $x(t)$ is white Gaussian noise, in practice this is not true. The chief difficulty is that the variances of the coefficients are significantly different if the input is not exactly white and Gaussian, and no practical input can meet these requirements sufficiently well for proper performance of the Laguerre coefficient generator.

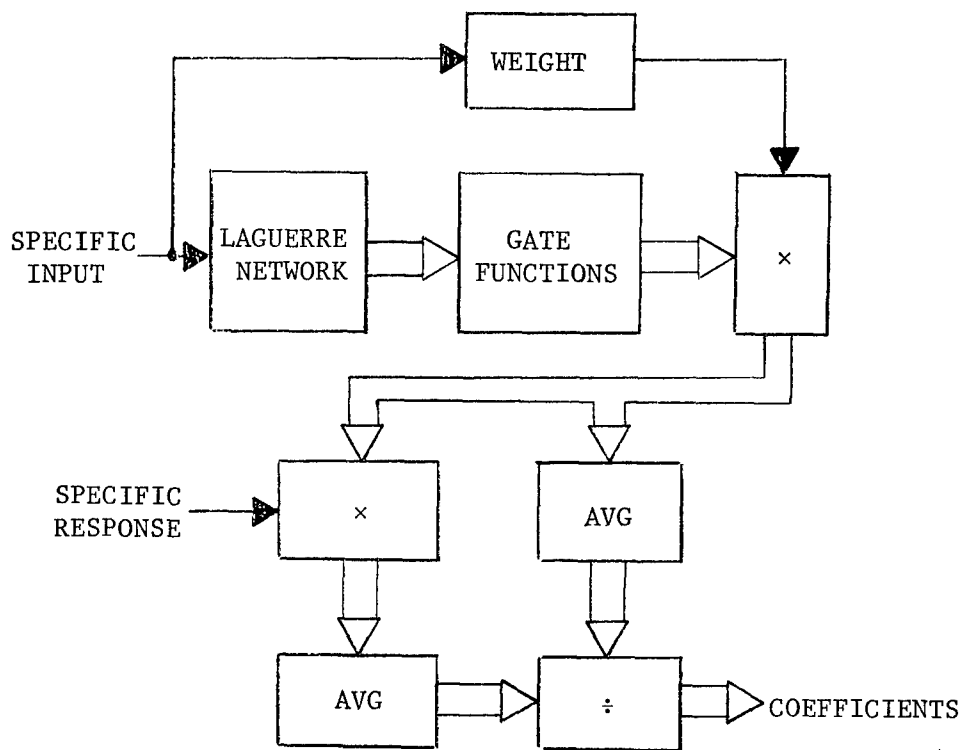
The net result is that the Hermite expansion, already requiring many coefficients to compensate for slow convergence, is further weakened in value by the inability of the Laguerre coefficient generator to produce inputs to the Hermite polynomials that are of the proper variance. This means that the coefficients, $\{\beta_{i,j} \dots, k\}$ cannot be obtained in sufficient quality and quantity to properly implement Wiener's theory of nonlinear systems.

Bose's Contribution to the Wiener Theory

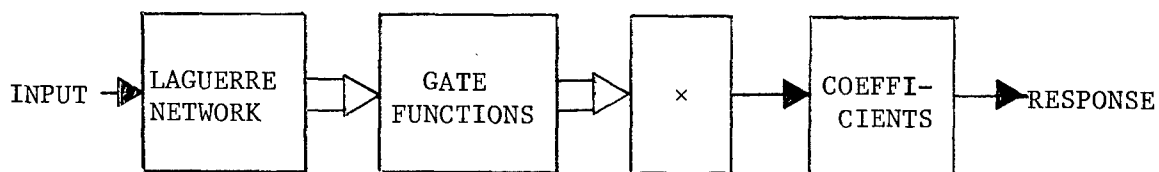
Bose [2] uses Wiener's theory to synthesize a system that is capable of producing a desired response to a given input. The basic idea is to build the system using hardware or computer implementations of the Laguerre coefficient generator and Hermite polynomials once the characterizing coefficients have been determined. Furthermore, it is the intent of his work to determine the coefficients using a representative input-output signal pair in place of the desired system. But the coefficients of a Wiener model must be determined through the use of a Gaussian probe, and in the context of Bose's problem, a given input is not likely to have the correct statistics to serve as the probe. Thus Bose was compelled to abandon the Hermite expansion and to find an expansion whose coefficients could be found regardless of the statistics of the probe. Bose's "gate function" expansion accomplishes this objective.

Bose's analysis and synthesis procedures are illustrated in figs. 9a and 9b. As in Wiener's theory, Laguerre functions represent the past of the input. Each Laguerre coefficient is expanded in a series of gate functions as follows:

- a. Looking at a time history of the i^{th} Laguerre coefficient, $u_i(t)$, we divide the ordinate into many intervals. See fig. 10. The number of divisions and the width and end points of each division are free parameters.
- b. The j^{th} gate function, $\phi_j(u_i)$, is unity whenever $u_i(t)$ is in the j^{th} interval and zero otherwise.



a. Analysis Process



b. Synthesis Process

Figure 9 Bose Analysis and Synthesis Procedures

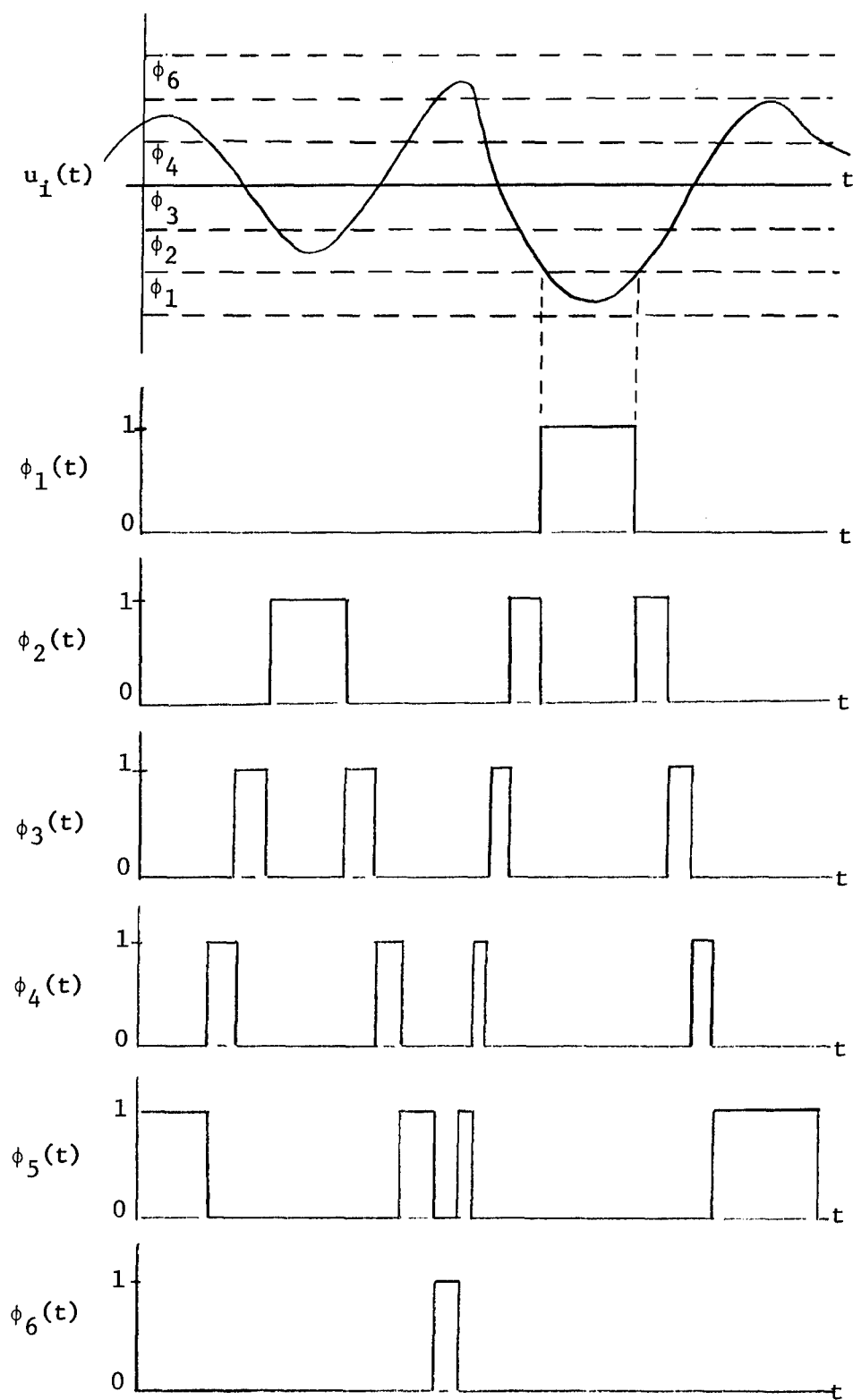


Figure 10 Gate Functions

For example, using six intervals of equal width would produce the time histories for $\phi_j(u_i)$ shown in fig. 10. We must have some idea of the anticipated variation of $u_i(t)$ and ensure that the entire range is covered by the $\{\phi_j\}$.

As defined above, the $\{\phi_j\}$'s are orthogonal over time and orthogonal over the range of u_i :

$$\int_0^T \phi_j(u_i(t)) \phi_k(u_i(t)) dt = \begin{cases} 0 & , j \neq k \\ \text{const.}, j = k \end{cases}$$

$$\int_{u_i \min}^{u_i \max} \phi_j(u_i) \phi_k(u_i) du_i = \begin{cases} 0 & , j \neq k \\ \text{const.}, j = k \end{cases}$$

Note that for any given value of u_i only one gate function is different from zero. Orthogonality over u_i is not altered by including any bounded weighting function, $w(u_i)$:

$$\int_{u_i \min}^{u_i \max} w(u_i) \phi_j(u_i) \phi_k(u_i) du_i = \begin{cases} 0 & , j \neq k \\ \text{const.}, j = k \end{cases}$$

Bose's expansion of the output, $y(t)$, as a function of the past of the input is

$$z_n(t) = \sum_{i=1}^{m_1} \sum_{j=1}^{m_2} \dots \sum_{k=1}^{m_n} a_{i,j,\dots,k} \phi_i(u_1) \phi_j(u_2) \dots \phi_k(u_n)$$

$$y(t) = \lim_{n \rightarrow \infty} z_n(t)$$

There are $\prod_{i=1}^n m_i$ terms in this summation and at any given time only one is different from zero. Each selection of values for u_1, u_2, \dots, u_n corresponds to a single term in the expansion, and that term is nonzero only when the past of the input is such that the selected values of u_i simultaneously occur.

Bose shows that the coefficients $\{a_{i,j, \dots, k}\}$ may be computed according to the rule

$$a_{i,j, \dots, k} = \frac{\text{avg}[y(t)G(x)\phi_i(u_1)\phi_j(u_2) \dots \phi_k(u_n)]}{\text{avg}[G(x)\phi_i(u_1)\phi_j(u_2) \dots \phi_k(u_n)]} \quad (13)$$

where $G[x(t)]$ is a freely chosen nonnegative weighting function. Furthermore, coefficients so computed satisfy the error criterion:

$$\epsilon = \text{avg} \left[G(x(t)) \left\{ y(t) - z_n(t) \right\}^2 \right] = \text{minimum}$$

Bose's modification of Wiener's theory of nonlinear systems is of great importance for two reasons. First, the gate function expansion is independent of the statistics of the signal used to generate the coefficients. Thus we are not committed to white Gaussian noise with its attendant difficulties of processing within the Laguerre coefficient generator. Second, we no longer have a convergence problem. At any instant the output is not the sum of many terms in the expansion but instead is equal to a single term only. Furthermore, the coefficient

on that single nonzero term may be interpreted as the expected value of the output given the past history of the input.

The net outcome is that the effectiveness of the Bose theory is limited only by the number of coefficients used and not by the additional factors of a practical nature that prevent the Wiener theory from being implemented.

III. IMPLEMENTATION OF WIENER-BOSE THEORY

Transition to a Practical Form

The principal motivation for this dissertation has been to learn how to apply in a practical sense Wiener's theory of nonlinear systems, whose principal appeal is the possibility for circumventing detailed knowledge of the physics of the system. We have seen that there are several severe obstacles that prevent practical implementation of this theory. But Bose's form of the theory may be modified and enlarged to accomplish the same purpose. Bose's gate function expansion can be easily implemented, although we will have to be content with discretized step-like responses instead of continuous responses. Although his work was originally couched in terms of building a model for specific input-output pairs, there is no reason why it cannot be recast in terms of the generalized probe and specific response point of view of Wiener. The specific input becomes a rather elaborate probe and the specific output becomes the corresponding response of the system. Bose's original statement of his model was illustrated in fig. 9. An expression of this theory restated from the point of view of Wiener's theory is given in fig. 11. Once coefficients are generated in this way we may find the response to any input of interest.

At this point it should be noticed that in making a transition from Wiener's theory to a practical form of WBT we are beginning a process of degradation of its mathematical elegance. In adapting the gate function expansion we have already given up the ability to model continuous responses; furthermore, the gate functions do not possess the property

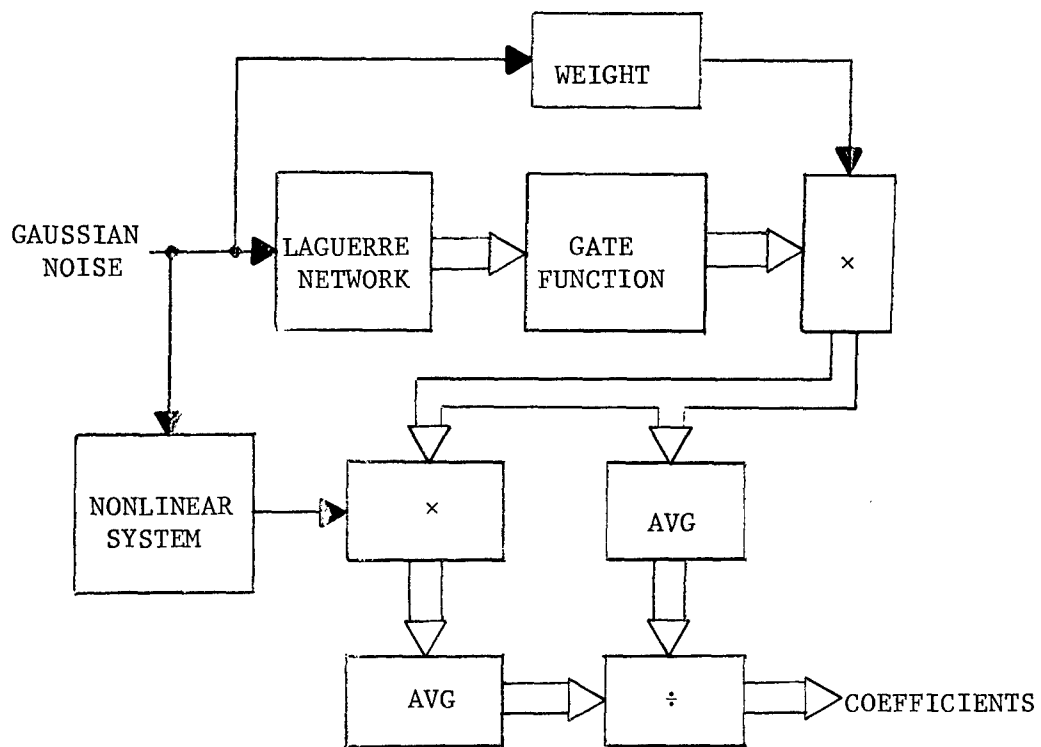


Figure 11 Bose Analysis Process with Generalized Probe

of completeness as do Wiener's Hermite functions. This means that adding more gate functions will not guarantee, in the limit, a zero mean square error. As we continue we must expect more degradation of desirable mathematical properties. But if we do not pay this price, we can expect no practical implementation.

Having chosen gate functions for the expansion of the functional relation between the system output and the past of the input, we want to find other choices for elements of the model that will reduce processing effort. A prime candidate for change is the Laguerre coefficient generator. It is reasonable to expect that most implementations will be accomplished with a digital computer. The Laguerre network will be seen by the computer as a set of simultaneous first-order differential equations whose accurate numerical solution will be accomplished at the expense of considerable processing time. We seek an element capable of representing the past of the input but not characterized by differential equations. A delay line satisfies these requirements; it is easily implemented with a shift register on a digital computer. But the outputs from the delay line taps are not related to any kind of polynomial series expansion of the input, so we have no control over properties such as convergence and completeness. However, we shall use a delay line because it is easy to do and because it satisfies the requirement for retaining some record of the immediate past of the input.

Because the gate function expansion is independent of the statistics of the probe, we may expect that the Gaussian distribution, required by Wiener's Hermite function expansion, will be an unnecessary requirement for a WBT model. As will be discussed below, there is a particular

sequence of input amplitudes corresponding uniquely to certain WBT model parameters that fulfills the probing function more efficiently than white, Gaussian noise. This probe will be referred to as Bose Noise.

The transition from the original Wiener theory to a practical form is now potentially completed and the resultant WBT model is depicted in figs. 12a and 12b.

Example 1. To make ideas more specific, consider the modeling process for a nonlinear system whose output, $y(t)$, is independent of the past of the input, $x(t)$. We want

$$y(t) = \sum_{j=1}^n a_j \phi_j[x(t)]$$

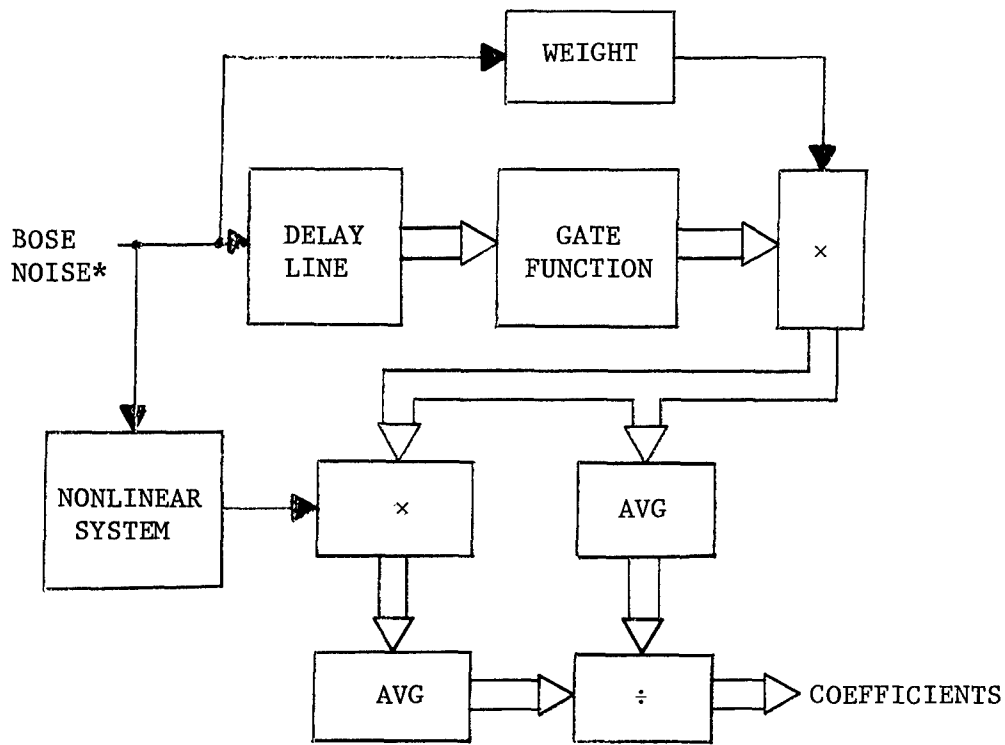
with a_j computed from

$$a_j = \frac{\text{avg}[y(t)G(x)\phi_j(x)]}{\text{avg}[G(x)\phi_j(x)]}$$

If we choose $G(x) = 1$ corresponding to a least mean square error criterion we have

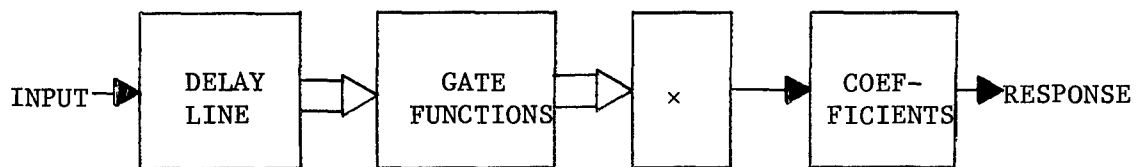
$$a_j = \frac{\text{avg}[y(t)\phi_j(x)]}{\text{avg}[\phi_j(x)]}$$

Thus, as depicted in fig. 13, while the system is being probed with some noise source we want to be continuously smoothing the j^{th} gate function and the product of this gate function with the response of the nonlinear system. As time passes we may expect that these two quantities and their ratio will become substantially constant for each j and will be taken as



*Or Other Probe.

a. Analysis



b. Synthesis

Figure 12 WBT Analysis and Synthesis Procedures

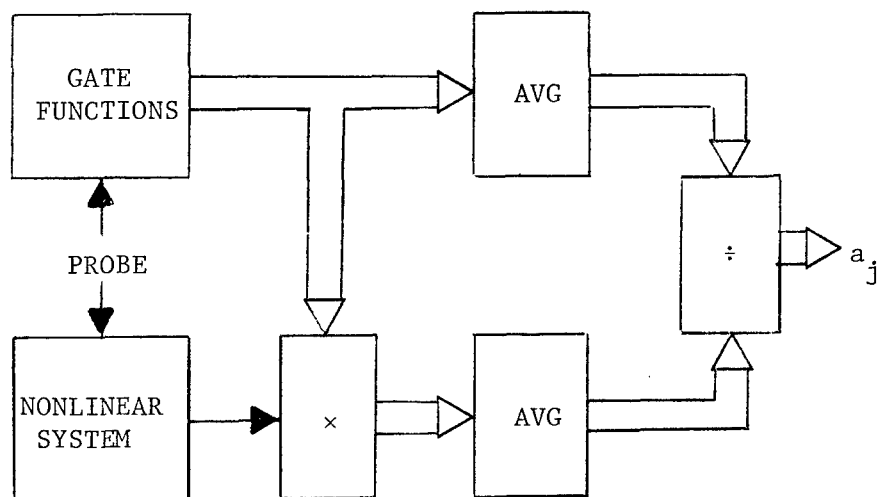
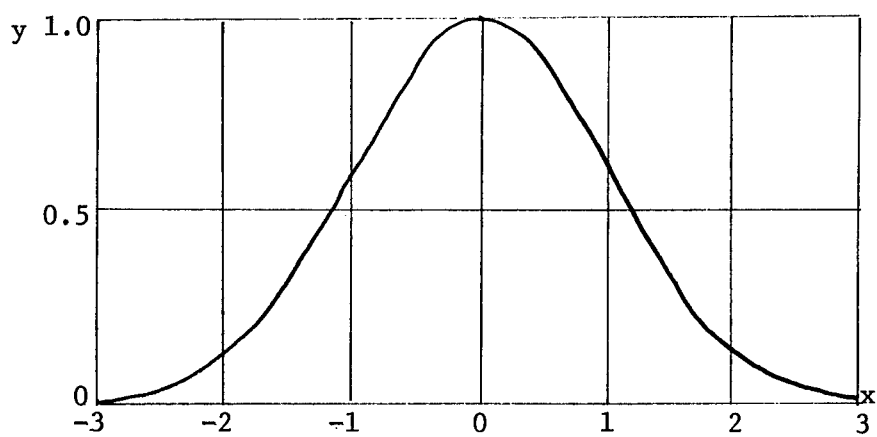


Figure 13 WBT Analysis for Zero-Memory System

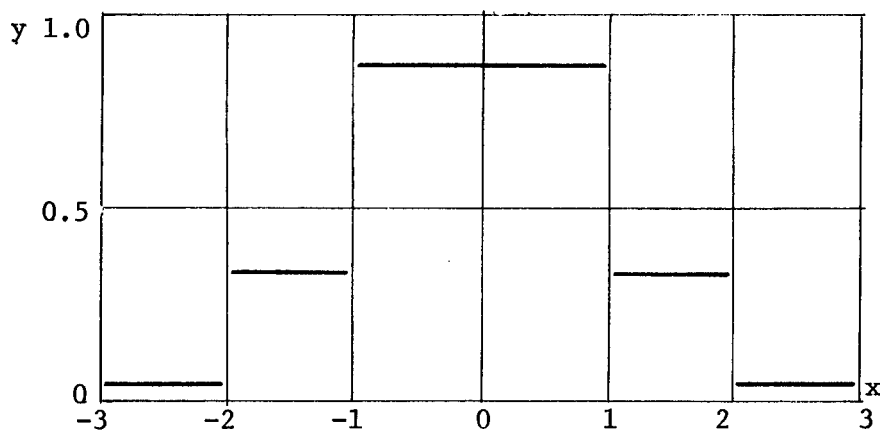
the coefficient, a_j . We do not have, of course, infinite time to conduct the probe and to average the several quantities needed to compute the characterizing coefficients. We must expect that coefficients obtained over a finite averaging interval will produce a WBT model having a mean square error greater than the minimum mean square error that an infinite averaging interval would allow. Harris [7] and Roy, Miller, and DeRusso [13] show that, in fact, the expected value of the mean square error due to finite averaging cannot exceed twice the mean square error due to infinite averaging. The Bose gate function expansion, both in the context of the zero-memory system of this example and in general, is quite tolerant of the very practical limitation of finite processing time.

To continue, suppose that our system has the x - y characteristic depicted in fig. 14a, and that our knowledge of the system consists of the fact of its independence of the past and an estimation that the excursion of inputs of future interest will range over $(-3 < x < 3)$. The WBT characterizing coefficients corresponding to an expansion in six gate functions on the input line are shown in fig. 14b. The coefficients for an expansion in forty gate functions are shown in fig. 14c. The figures show the coefficients, a_j , plotted against the input amplitude. Thus for each input amplitude only one of these coefficients is used to represent the output, and this coefficient is the only one whose corresponding gate function is different from zero.

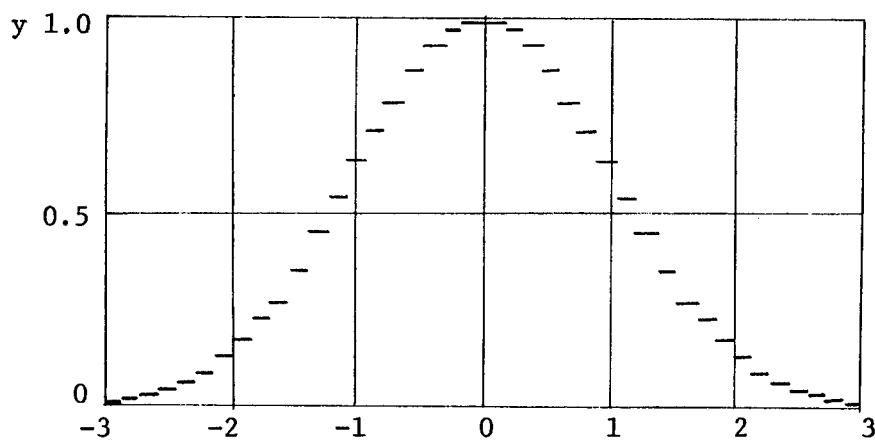
Example 2. Consider a system that displays rate-independent hysteresis. There is a dependence on the past of the input although no characteristic time interval is involved. We want to consider



a. x-y Characteristic



b. Six WBT Coefficients



c. Forty WBT Coefficients

Figure 14 Zero-Memory System of Example 1

the specific system that may be modeled analytically as follows:

Let

$d_1(t)$ = present input, in.

$d_2(t)$ = most recent maximum $d_1(t)$, in.

$d_3(t)$ = most recent minimum $d_1(t)$, in.

$\ell_1(t)$ = present output, lb

$\ell_2(t)$ = most recent maximum $\ell_1(t)$, lb

$\ell_3(t)$ = most recent minimum $\ell_1(t)$, lb

The equations

$$\ell_1 = k_1 d_1^2 + (\ell_2 - k_1 d_2^2) \exp(-k_3[d_2 - d_1]) , \dot{d}_1 < 0$$

$$\ell_1 = k_2 d_1^2 - (k_2 d_3^2 - \ell_3) \exp(-k_3[d_1 - d_3]) , \dot{d}_1 > 0$$

describe the hysteresis characteristic displayed in fig. 15. The system of this example was suggested by the load versus deflection characteristics exhibited by a pneumatic tire when subjected to vertical loads on a flat, nonyielding surface. The example is carried forward for the following selection of constants:

$$k_1 = 10 \text{ lb/in.}^2$$

$$k_2 = 20 \text{ lb/in.}^2$$

$$k_3 = 7.5 \text{ 1/in.}$$

We want to build a WBT model for this system. We will guess that a delay line with two taps, one for the present and the other for the past, will suffice to characterize the past of the input. Other selections of model parameters are listed as follows:

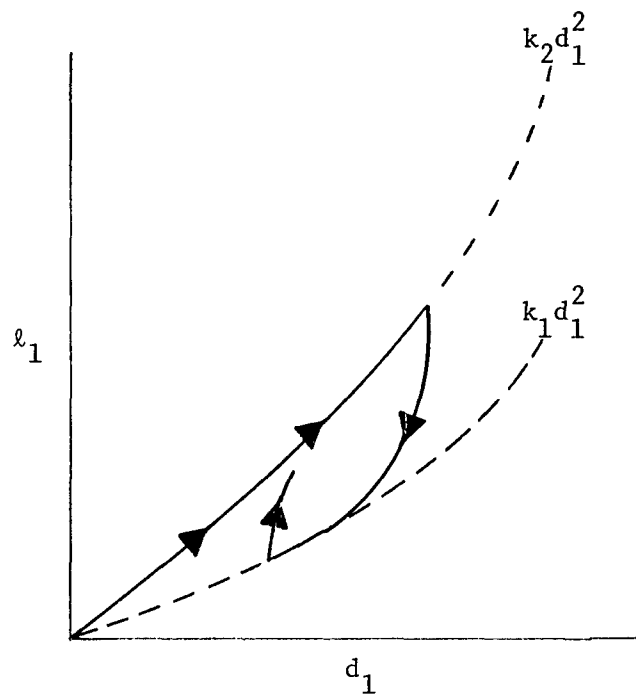


Figure 15 Hysteretic System of Example 2

Number of taps: 2

Number of gate functions: 20 on tap 1, 10 on tap 2

Number of coefficients: 200

Range of future input: $0 < d < 6$ in.

Weighting function, $G(x)$: unity

The coefficients generated by a sustained application of a random input are depicted in fig. 16. The d_1 axis is divided over the interval (0,6) into 20 equal divisions corresponding to the gate function expansion on the first tap of the delay line (the input, in this case). For each of these gate functions there correspond 10 gate functions on the second tap. To each combination of one gate function on the first tap and one on the second, there corresponds one coefficient. Thus each division of (0,6) has 10 coefficients (some identical). When some future input amplitude falls into a given division, the WBT model will give as an output one of the 10 coefficients for that division. Just which of the ten is given will depend on the prior input.

The responses of this system to specific inputs may now be predicted with the WBT model. In fig. 17 is displayed the hysteretic trajectory of the system in response to the following input:

$$d_1(t) = 3.0 \text{ in.}, t < 0$$

$$d_1(t) = (2.73 \sin w t + 3.0) \text{ in.}, \begin{cases} t \geq 0 \\ w > 0 \end{cases}$$

with the initial condition $\ell_1(0) = 134$ lb. The corresponding model

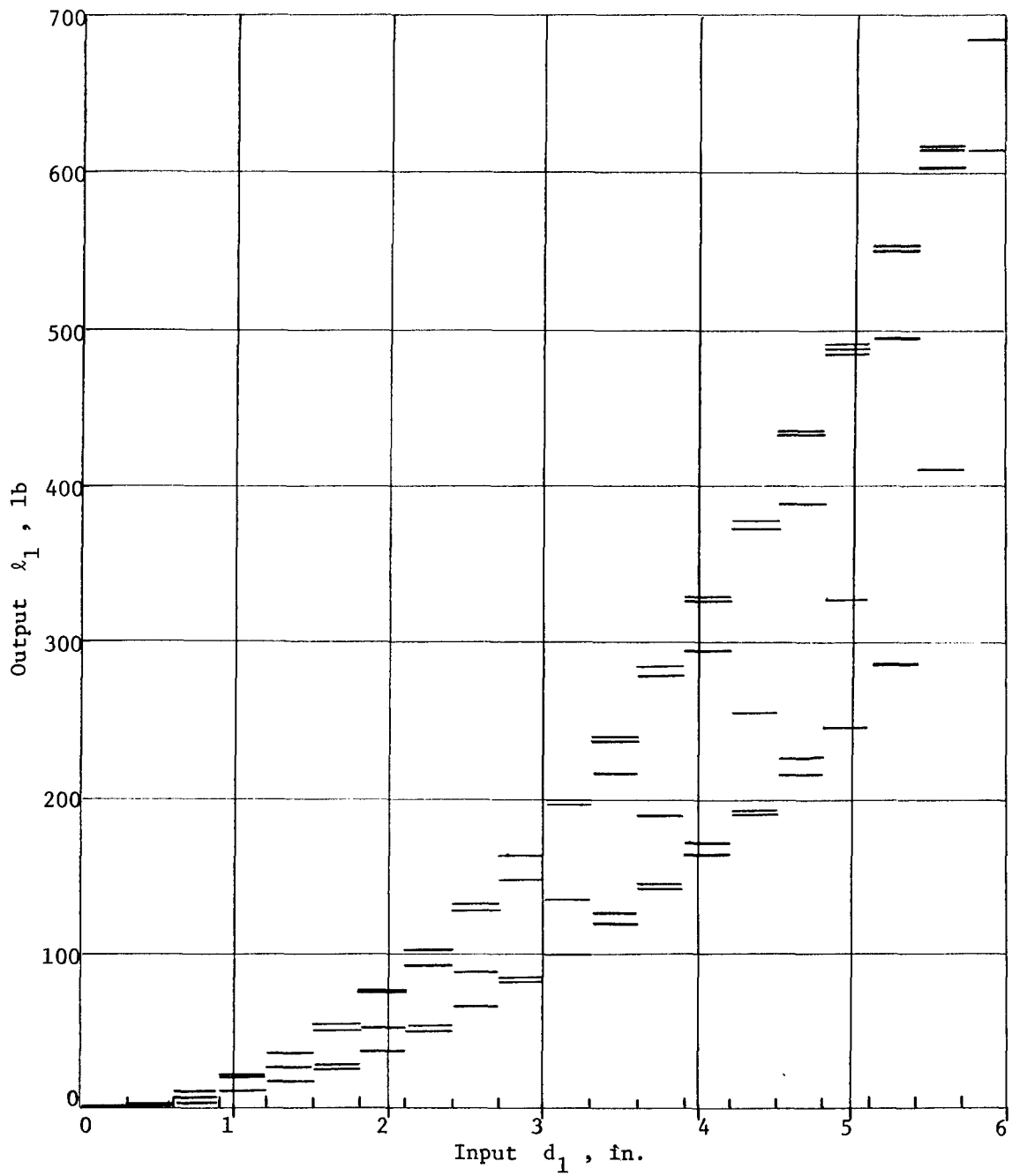


Figure 16 WBT Coefficients, Example 2

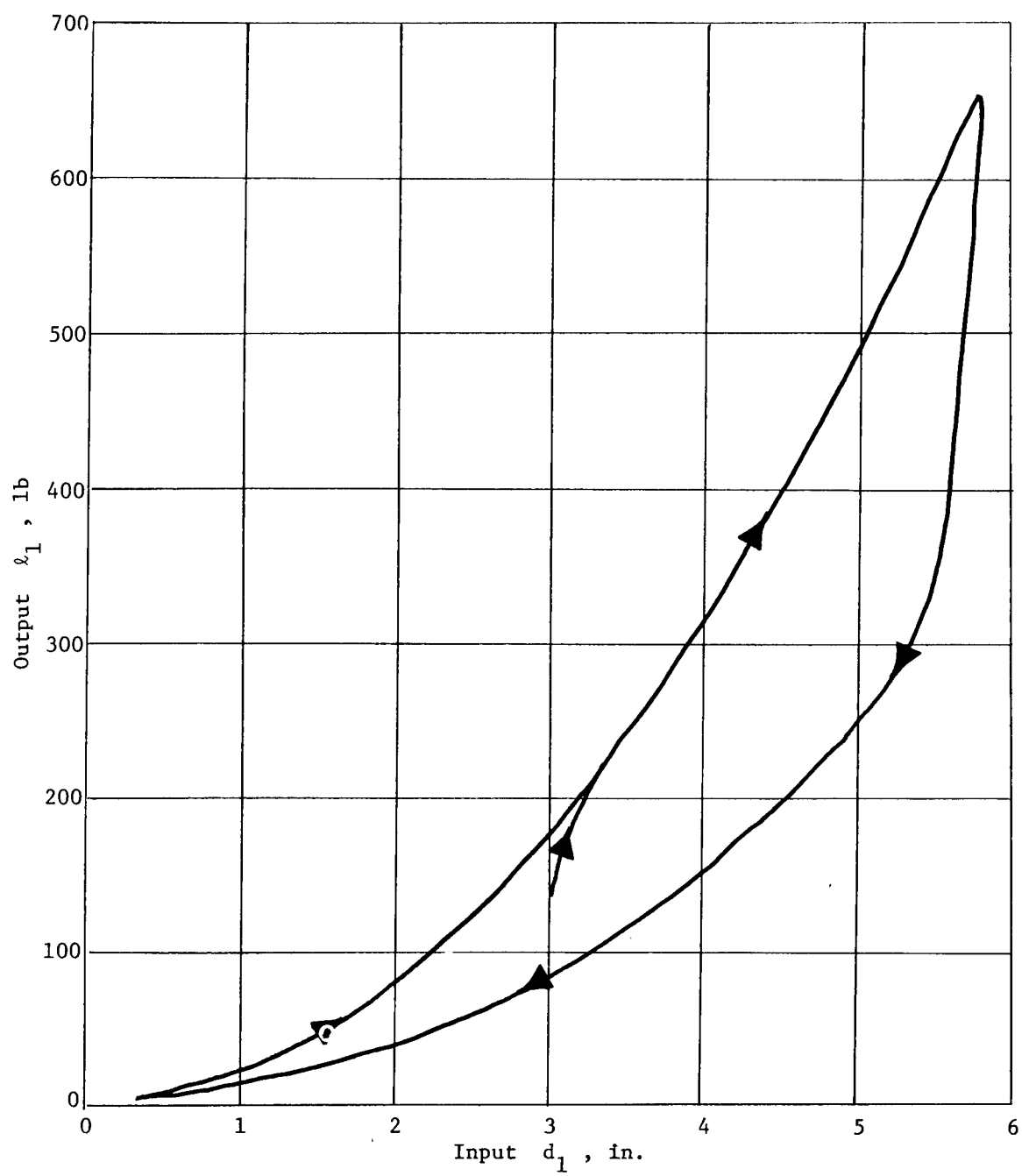


Figure 17 System Response to Specific Input, Example 2

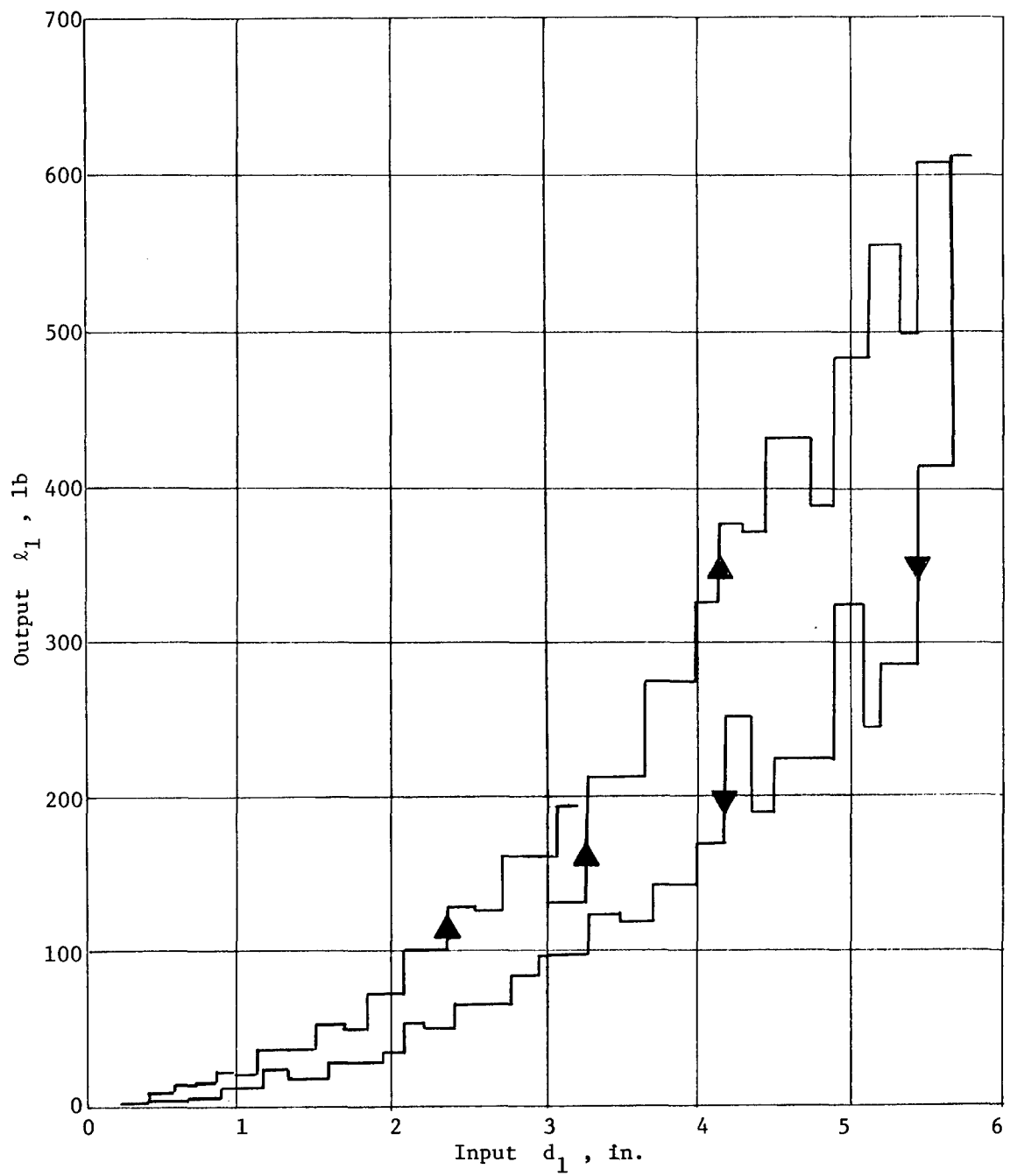


Figure 18 Model Response to Specific Input, Example 2

response is shown in fig. 18. Its discontinuous nature is apparent and is characteristic of all WBT responses. The WBT model does not necessarily give monotonic responses even though the actual system does. This is because the coefficient used to give the present output corresponding to the present input is likely to have been obtained when prior inputs were somewhat different than the specific prior input at hand. If the same number of gate functions were used on each delay line tap, the model would exhibit fewer and smaller nonmonotonic jumps.

Nature and Determination of Characterizing Coefficients

An attractive feature that emerges when Bose's gate function expansion is used is that the characterizing coefficients may be interpreted in an appealing way. They may be regarded as "possible states of the system." Because of the coincidence formulation of the gate function expansion only one product of gate functions is different from zero at any one time and the model output at this time is the coefficient assigned to this product. The displays of coefficients in figs. 14 and 16 may be termed "state diagrams." The model outputs will be states taken from diagrams of this kind.

Another attractive feature appears when we confine the weighting function, $G(x)$, to unity.[2,7] With this condition, the rule for obtaining the characterizing coefficients, equation 13, becomes

$$a_{i,j,\dots,k} = \frac{\text{avg} \left[y(t) \phi_i(u_1) \phi_j(u_2) \dots \phi_k(u_n) \right]}{\text{avg} \left[\phi_i(u_1) \phi_j(u_2) \dots \phi_k(u_n) \right]} \quad (14)$$

We have been assuming all along that we are dealing with random variables whose time averages and ensemble averages may be interchanged. If we do this for the expression in the denominator of equation 14 we have

$$\text{avg} [\phi_i \phi_j \dots \phi_k] = \int_{-\infty}^{\infty} \dots \int_{-\infty}^{\infty} \int_{-\infty}^{\infty} \phi_i \phi_j \dots \phi_k p(u_1, u_2, \dots, u_n) du_1 du_2 \dots du_n \quad (15)$$

where $p(u_1, u_2, \dots, u_n)$ is the probability density function for the joint occurrence of the random variables, u_i , in the intervals $(u_i, u_i + du_i)$. But the gate functions take only the values zero and unity so that contributions to the integral on the right-hand side of equation 15 can occur only when u_1 is in the interval corresponding to ϕ_i , and simultaneously u_2 is in the interval corresponding to ϕ_j , and so forth. Thus

$$\text{avg} [\phi_i \phi_j \dots \phi_k] = \int_{u_k} \dots \int_{u_j} \int_{u_i} p(u_1, u_2, \dots, u_n) du_1 du_2 \dots du_n$$

But this is just the probability, $P(\phi_i, \phi_j, \dots, \phi_k)$ for the joint occurrence of the gate functions $\phi_i, \phi_j, \dots, \phi_k$.

Turning to the numerator of equation 14, we may say

$$\text{avg} [y \phi_i \phi_j \dots \phi_k] = \int_{-\infty}^{\infty} \dots \int_{-\infty}^{\infty} \int_{-\infty}^{\infty} \int_{-\infty}^{\infty} y \phi_i \phi_j \dots \phi_k p(y, u_1, u_2, \dots, u_n) dy du_1 du_2 \dots du_n$$

where $p(y, u_1, u_2 \dots u_n)$ is the probability density function for the joint occurrence of the random variables y and u_i . Once again, because the ϕ 's are zero over most of the range of the u 's we may write

$$\text{avg} [y\phi_i\phi_j \dots \phi_k] = \int_{u_k} \dots \int_{u_j} \int_{u_i}^{\infty} yp(y, u_1, u_2, \dots, u_n) dy du_1 du_2 \dots du_n$$

This may be written as

$$\text{avg} [y\phi_i\phi_j \dots \phi_k] = \int_{u_k} \dots \int_{u_j} \int_{u_i}^{\infty} yp(y|u_1, u_2, \dots, u_n) p(u_1, u_2, \dots, u_n) dy du_1 du_2 \dots du_n$$

where $p(y|u_1, u_2, \dots, u_n)$ is the joint conditional probability density function for y given the u 's [14,15]

Integrating with respect to y we have

$$\text{avg} [y\phi_i\phi_j \dots \phi_k] = \int_{u_k} \dots \int_{u_j} \int_{u_i} E(y|u_1, u_2, \dots, u_n) p(u_1, u_2, \dots, u_n) du_1 du_2 \dots du_n$$

where $E(y|u_1, u_2, \dots, u_n)$ is the conditional expectation of y given the u 's. Integrating again

$$\text{avg} [y\phi_i\phi_j \dots \phi_k] = E(y|u_i, u_j, \dots, u_k) P(u_i, u_j, \dots, u_k)$$

or

$$\text{avg} [y\phi_i\phi_j \dots \phi_k] = E(y|\phi_i, \phi_j, \dots, \phi_k)P(\phi_i, \phi_j, \dots, \phi_k)$$

which expresses the idea that the numerator of equation 14 represents the expected value of the response, y , given that the $(i,j, \dots, k)^{\text{th}}$ coincidence is satisfied onto the probability that it is satisfied.

Thus, we have

$$a_{i,j, \dots, k} = E(y|\phi_i, \phi_j, \dots, \phi_k)$$

which says that the $(i,j, \dots, k)^{\text{th}}$ coefficient is just the mean value of the system response over the time that the $(i,j, \dots, k)^{\text{th}}$ coincidence is satisfied.

This property of the coefficients of Bose's gate function expansion is of great importance for the implementation of WBT. It is an easy task to keep track of times of coincidence and to form averages of responses over those times.

Bose Noise

In the preceding examples, the WBT characterizing coefficients were found during a sustained application of a random input. The nature of this random input was not specified nor did it need to be. This is because the gate function expansion is independent of the statistics of the probe. The only practical requirement is that it have an amplitude spread large enough to cover the anticipated spread of future inputs for which the model is formulated. In addition,

the duration of the probe was not specified. In general, the greater the duration the better the coefficients in the sense of approaching the least possible mean square error. In practice, we want to devote as little time to probing as possible, especially when the WBT model has many coefficients.

It is possible to devise a sequence of input amplitudes that serves efficiently as a probe for coefficient determination. Suppose the number of delay line taps is N_t and there are m_i gate functions on the i^{th} tap. Select any one gate function on the first tap, any one on the second tap, the third tap, and so forth. This particular selection constitutes one "configuration."

There are $\prod_{i=1}^{N_t} m_i$ possible configurations, each of which corresponds

to the simultaneous occurrence of tap outputs within the ranges of the selected gate functions. To each configuration there corresponds one coefficient of the WBT model. For the purpose of coefficient determination the probe should consist of a sequence of input amplitude levels so arranged that each configuration occurs at least once.

This sequence will be called "Bose Noise" and has $N_t \prod_{i=1}^{m_i}$ levels.

Each selection of N_t and the m 's has its own unique sequence.

Bose Noise is set up to produce at least one coincidence for each coefficient. In practice it can produce several coincidences as configurations are shifted down the delay line, but nevertheless, the number is small. Thus the utility of Bose Noise is the relatively

short time required for probing. The coefficients so obtained represent averages of system responses over one, or possibly several, coincidences. Because the total time for averaging is so much less than the very long averaging time implied by equation 14, we must expect that the mean square error will be at or near its maximum value. Just how serious this error is must be judged in each case. However, we may expect that as the number of gate functions used to expand each delay line output increases the error will diminish. In practice, the need to limit probing effort will take a higher priority than will the need to attain the minimum mean square error.

To illustrate a specific Bose Noise sequence, consider a "configuration diagram" for example 2 shown in fig. 19. In this instance we have $N_t = 2$, $m_1 = 20$, and $m_2 = 10$. The fact that this model was intended for the interval $(0 < x < 6)$ means that $(0,6)$, designated the "amplitude spread," s , is divided into 20 equal divisions on the first tap and into 10 equal divisions on the second. Thus, for the gate function numbering scheme shown in fig. 19 we have, for example, that coefficient $a_{1,1}$ corresponds to a simultaneous occurrence of the present input in the range $(0 < x < 0.3)$ and the previous input in the range $(0 < x < 0.6)$. Coefficient $a_{10,7}$ would correspond to the simultaneous occurrence of the present input in the range $(2.7 < x < 3.0)$ and the previous input in the range $(3.6 < x < 4.2)$.

To generate the coefficients from $a_{1,1}$ through $a_{20,10}$ we want to bring in amplitudes that fit into the ranges of the corresponding gate functions. It is convenient (although not necessary) to pick

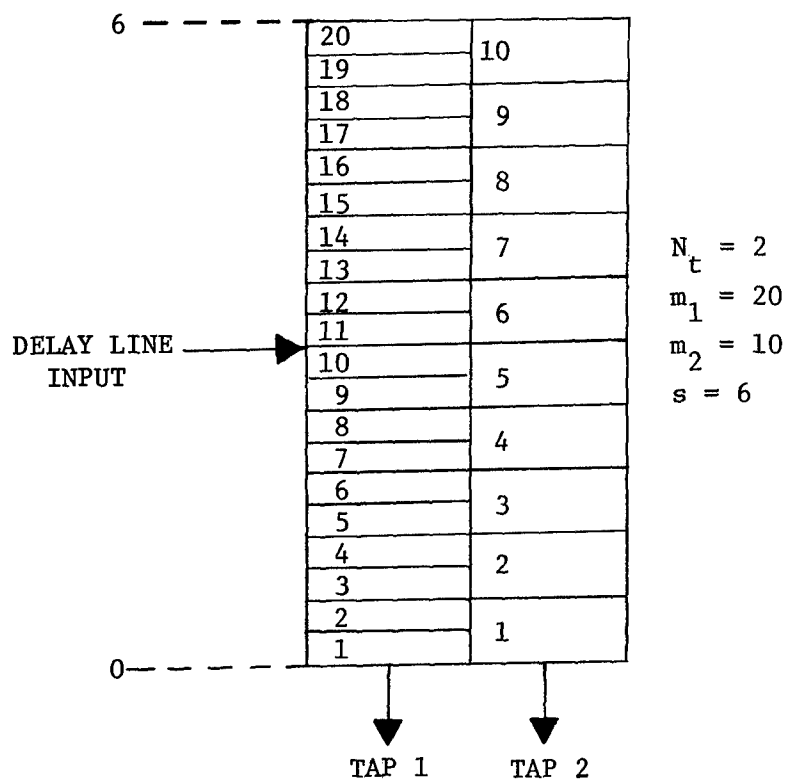


Figure 19 Configuration Diagram, Example 2

amplitudes that fall into the middle of the gate function ranges. For example, for $a_{1,1}$ we want the appearance, at least once, of the combination of 0.15 on the first tap and 0.30 on the second tap simultaneously. For $a_{10,7}$ we want 2.85 and 3.90. It is convenient (although again not necessary) to generate the coefficients by indexing the second subscript. An excerpt from the initial part of the Bose Noise sequence for example 2 is illustrated in fig. 20. This sequence of amplitudes, inserted one after another into the delay line, will systematically satisfy the gate function coincidence requirement of each coefficient. The number of Bose Noise amplitudes for this case is $2 \times 20 \times 10 = 400$. The coefficients for examples 1 and 2 were obtained using Bose Noise.

System Settling Time

Example 1 described a system independent of the past and example 2, a system dependent on past amplitudes regardless of the times of their occurrence. We are now in a position to discuss the more realistic case of dependence on the past of the input in terms of amplitudes and times of occurrence.

WBT requires very little knowledge of specific features of the system under study. But we must know certain basic facts: whether or not there is dependence on the past and, if so, a measure of how much. That measure is conveniently expressed in terms of the "system settling time," T_s . This may be thought of as the time required by the system to regain equilibrium following an impulsive disturbance. A judgement must be made in each case as to just

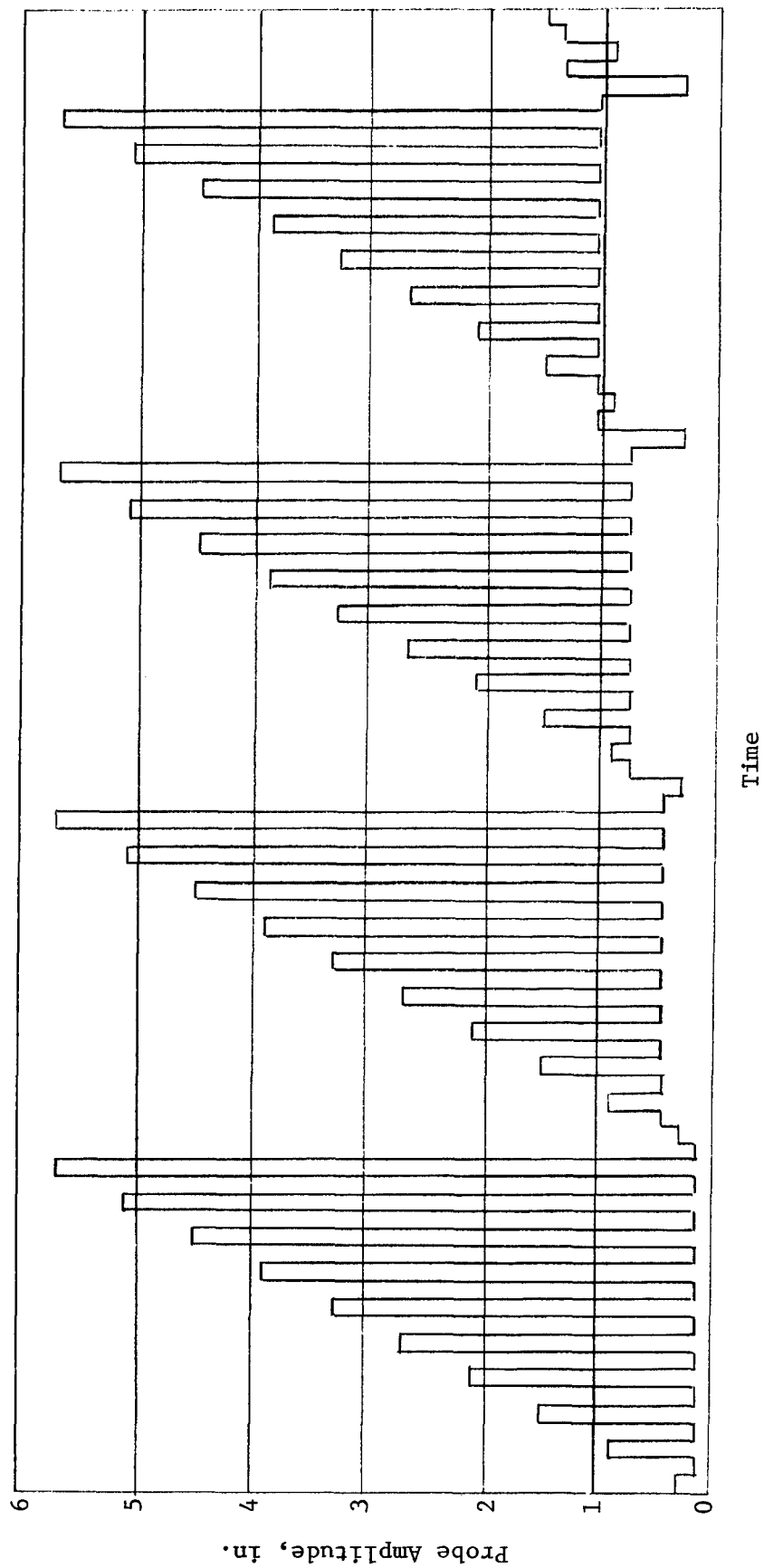


Figure 20 Initial Part of Bose Noise Sequence, Example 2

when, in a practical sense, equilibrium has been regained. For example, if there is one obviously dominant time constant, then a time interval equal to five times this time constant can be used as T_s . If the responses are oscillatory, then the time interval for amplitudes to diminish to one tenth their initial values might be considered as T_s . Indeed, variations on this theme are so numerous that it is difficult to be more specific.

The settling time enters the WBT model as the total time delay of the delay line. After T_s seconds the system has forgotten what the input was and there is no need to retain a record of it for a longer period of time. The time scale for the model is also set by T_s . If we have N_t taps equally spaced along the delay line then the time interval between samples of the input is

$$\Delta T = \frac{T_s}{N_t}$$

In particular, the signal used to probe the system has this time interval between samples. If Bose Noise is used for the probe, the WBT model establishes the sequence of inputs without regard to time and T_s establishes the time scale.

Determination of Coefficients for Bose Noise Probe

When the weighting function, $G(x)$, is selected as unity and Bose Noise is used as the system probe it becomes especially easy to determine the characterizing coefficients. Recall that the basic idea behind the Bose Noise concept is the occurrence at least once

of all possible configurations. We are free to choose the order in which these configurations occur. Once the choice has been made we know in advance when each configuration will occur during the probing process. Because we know this in advance there is no need for the delay line and gate function generator. It suffices to monitor the response of the system during the probing process and mark the time when each configuration is scheduled to appear. When the $(i,j, \dots, k)^{\text{th}}$ configuration appears we determine the average value of the response during the time of occurrence. This average value is the $(i,j, \dots, k)^{\text{th}}$ coefficient.

Another simplification is sometimes possible. If the response of the system during the time of a coincidence is monotonic it will suffice, in a practical sense, to sample the response in the middle of the (prearranged) coincidence interval and to use that single sample as the coefficient, eliminating the averaging process.

Examples

Examples 1 and 2 helped to introduce basic concepts. These concepts have now been presented and some examples will now be useful to consolidate ideas.

Example 3. We will consider a second-order nonlinear system that has been discussed by Harris.[7] This system is illustrated in fig. 21 and is described by the following equations:

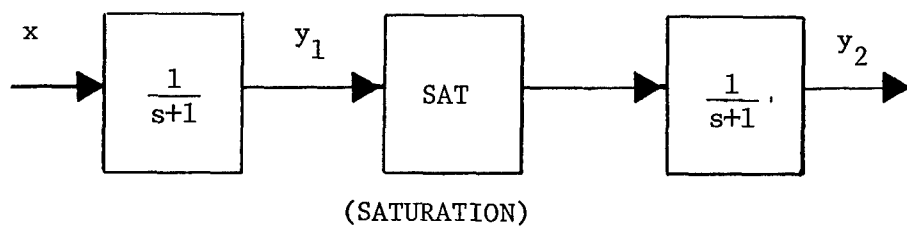


Figure 21 System of Example 3

$$\dot{y}_1 + y_1 = x$$

$$\text{sat}(y_1) = \begin{cases} -0.5, & y_1 \leq -0.5 \\ y_1, & -0.5 < y_1 < 0.5 \\ 0.5, & 0.5 \leq y_1 \end{cases}$$

$$\dot{y}_2 + y_2 = \text{sat}(y_1)$$

We will pretend that we do not have these equations but can probe an actual copy of the system.

We know in advance that the response of this system is dependent on the past of the input and is stable for inputs of interest. We can estimate its settling time as about 5 seconds. Suppose that we are interested in future input amplitudes ranging over the interval $(-1 < x < 1)$. We now want to select the number of delay line taps and the number of gate functions on each tap. In general we want these numbers as large as possible; in practice computation and probing efforts set the limit. It would be useful at this point for the reader to select some numbers and see the consequences in terms of coefficient count,

$$N_c = \prod_{i=1}^{N_t} m_i$$

and in terms of probe length,

$$N_B = N_t N_c$$

We will pursue this example with selections made by the author as

directed by available computer capacity and time for processing:

$$N_t = 5$$

$$m_1 = 20$$

$$m_2 = 8$$

$$m_3 = 6$$

$$m_4 = 4$$

$$m_5 = 2$$

These choices give

$$N_c = 7680$$

$$N_B = 38400$$

We have estimated

$$s = 2$$

The configuration diagram for these selected parameters is shown in fig. 22. We have also estimated

$$T_s = 5.0 \text{ sec}$$

This corresponds to the total delay of the delay line. Thus the delay between the equally spaced taps is

$$\Delta T = \frac{5.0}{5.0} = 1.0 \text{ sec}$$

Corresponding to these parameter selections is a unique Bose Noise probe. Excerpts from the beginning, middle, and end of this sequence are illustrated in figs. 23a, 23b, and 23c, respectively. As discussed earlier, because we know in advance when the system is to be probed

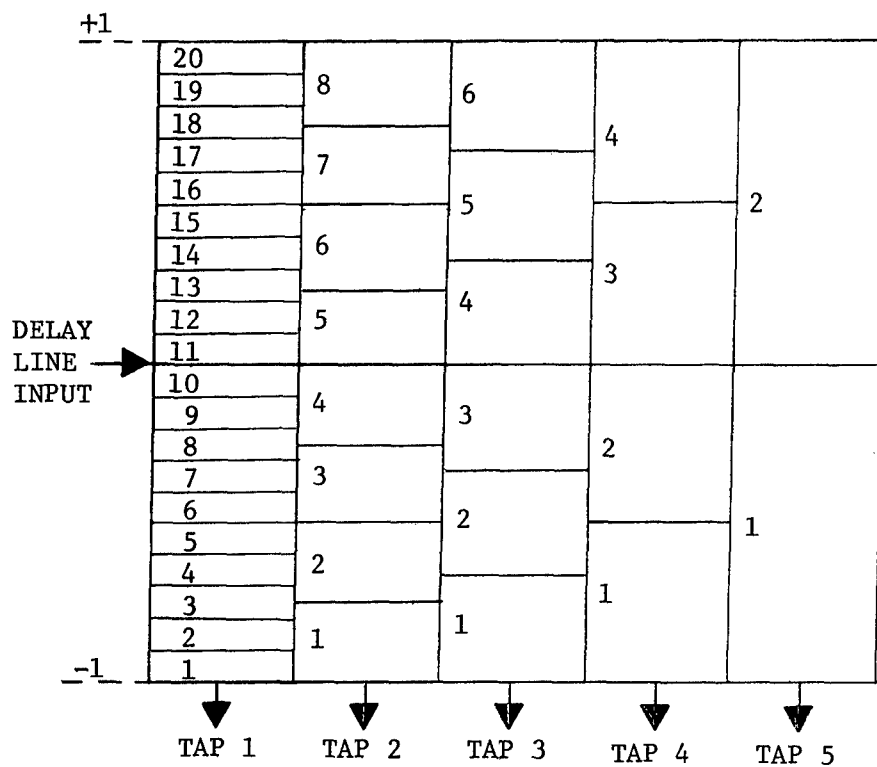
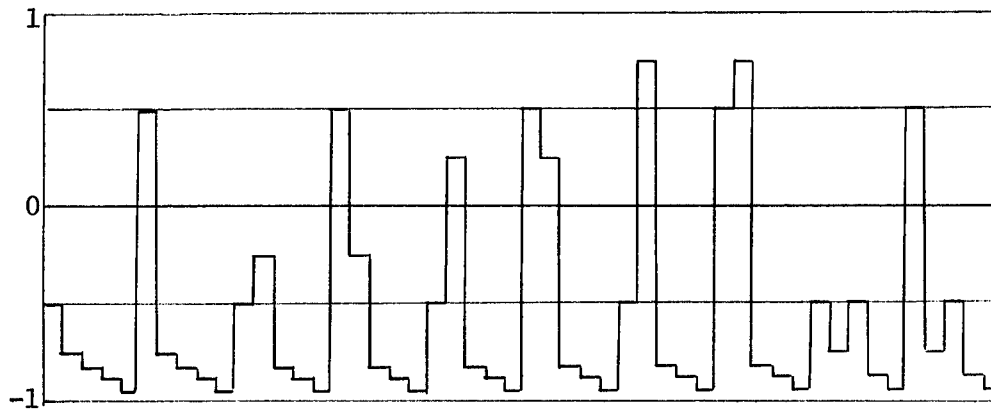
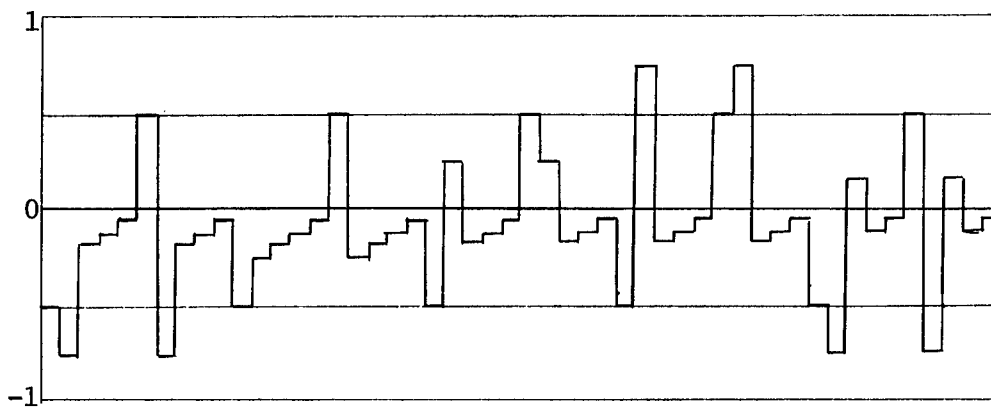


Figure 22 Configuration Diagram, Example 3

a. Beginning



b. Near Middle



c. Near End

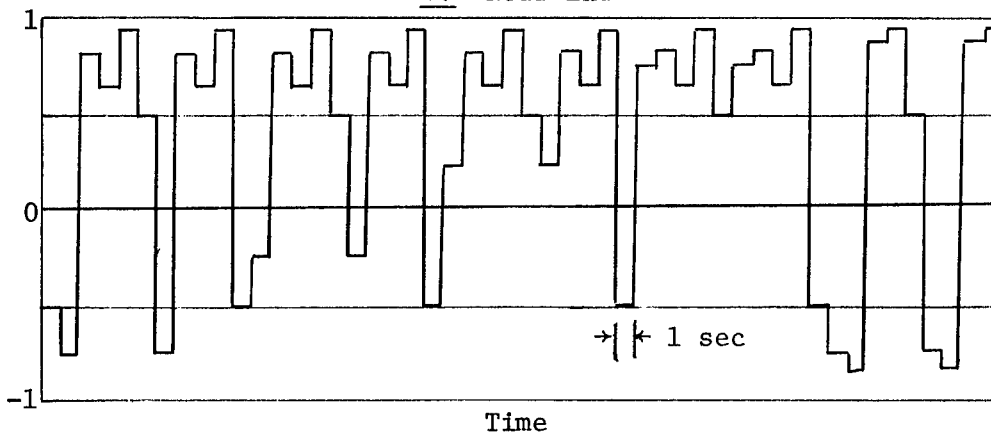


Figure 23 Excerpts from Bose Noise Sequence, Example 3

for a certain coefficient, we may monitor its response at that time. The average of the response over the time of coincidence is the coefficient.

A state diagram for this system is illustrated in fig. 24. The abscissa of this diagram represents the amplitude of the present input and has been divided into 20 equal intervals over the range $(-1 < x < 1)$. When the input falls into any one interval, the model output is one of 384 $(= 8 \times 6 \times 4 \times 2)$ possible states.

We may now synthesize a response to any input, $x(t)$, whose amplitude remains in the range $(-1 < x < 1)$. For example, consider the input depicted in fig. 25a. This input runs across the amplitude spread parameter, s , at different rates and will give insight into model performance for inputs of different rates. The response of the model to this input is shown in fig. 25c together with the responses of the differential equations of the system. We see immediately the staircase response characteristic of WBT models. The form of the model response compares favorably with the "actual" response. The initial part of the input is a step function sustained for a time equal to T_s . In the WBT response to this part of the input, there are as many steps as delay line taps as the input is shifted down the delay line. This part of the response represents the poorest performance of the WBT model and makes it apparent that responses improve with increasing N_t . The remainder of the input consists of ramps of decreasing slope. The fastest of these

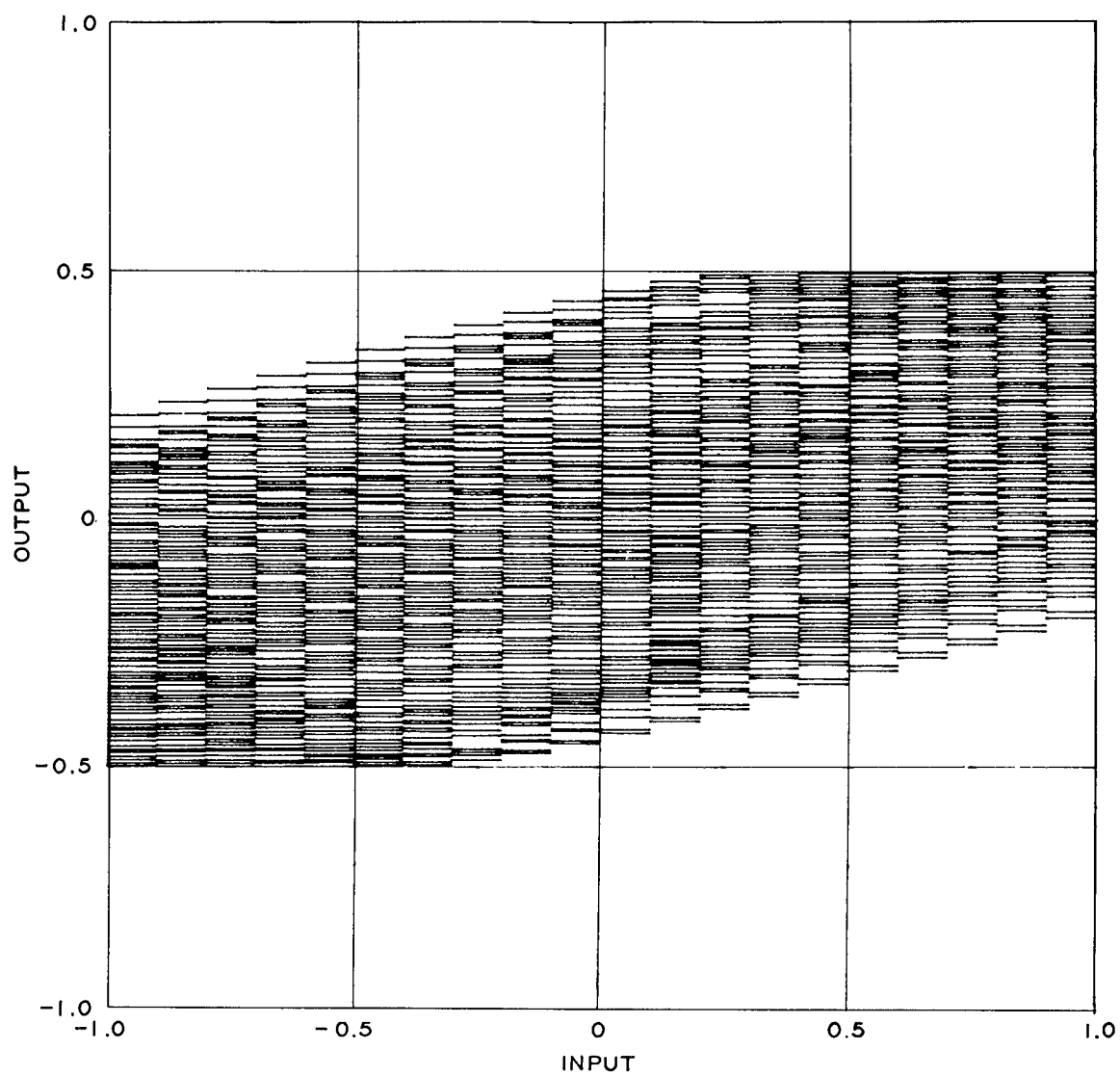


Figure 24 State Diagram, Example 3

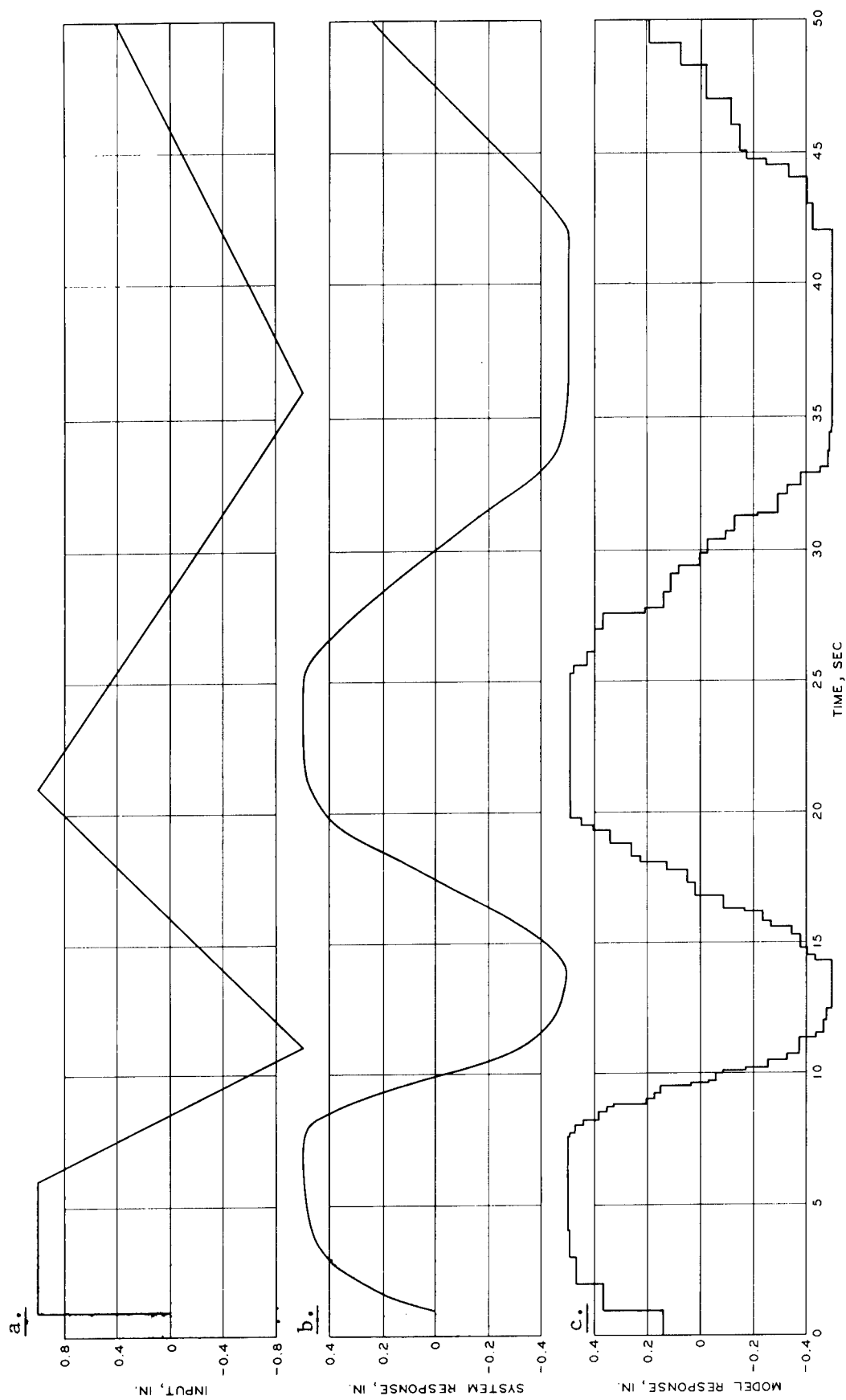


Figure 25 Comparison of System and Model Responses, Example 3

goes from $+s/2$ to $-s/2$ in a time equal to T_s , and the WBT response appears, qualitatively, to be satisfactory in this area and remains satisfactory for the rest of the input.

To quantify this idea the input can be partitioned into intervals as follows:

<u>Interval</u>	<u>Time, sec</u>
1	0 to 1
2	1 to 6
3	6 to 11
4	11 to 21
5	21 to 36
6	36 to 56

The first interval corresponds to the equilibrium state of the model and the second corresponds to the step-function response. The remaining intervals correspond to the ramps of decreasing slope.

In each interval we may compute the mean square error between the WBT and "actual" responses:

<u>Interval</u>	<u>MSE</u>
1	0.0209
2	0.0614
3	0.0007
4	0.0024
5	0.0044
6	0.0073

We see that, as expected, the second interval corresponding to the step-function response has the greatest mean square error. All other errors are less than the step response error. This fact suggests

that we might take the step response error as an indicator (pessimistic) of the quality of the model. Having selected WBT model parameters, it is easy to determine, using the configuration diagram, what specific coefficients would be summoned by the model to predict the step response. The system can be probed to determine just those coefficients (N_t in number). The model prediction can be compared to the actual step response to determine the mean square error and a decision made whether to proceed with the determination of the remainder of the coefficients or to revise the model parameters.

The equilibrium state seen in the first interval compares poorly with that of the actual system. This is an outcome of the fact that our estimate of T_s is somewhat low (Harris computed a settling time of 5.4 seconds). As a result, the system had not yet come to equilibrium during the probing process at the time when the equilibrium coefficient was determined.

As mentioned above, this particular system was studied extensively by Harris. We have already come to appreciate how quickly the number of coefficients of a WBT model increases with increases in the number of gate functions selected. Harris' contribution was to find a way to drastically reduce the coefficient count at the expense of certain restrictions on the nature of the input. He studied inputs that were constrained to switching between two constant levels, and that were limited to no more than two switches in a time interval equal to T_s seconds and separated by no less than $T_s/2$ seconds. These are realistic constraints for the chemical engineering context of his work. They are not realistic for the

ride dynamics context of this work. With inputs so restricted, Harris was able to consider delay lines with as many as 54 taps, not necessarily equally spaced. Furthermore, he needed only to use two gate functions on each tap. The net outcome is that for the specific nonlinear system of this example, Harris' WBT model gives a much better fit for step function inputs than did the model used above. However, his model is inherently incapable of handling arbitrary inputs and has no way of producing responses such as shown in fig. 25.

Example 4. In this example we will consider a mechanical system having four degrees of freedom. The example was formulated as part of the evolutionary process leading toward the application of WBT to ride dynamics. The nonlinear system to be studied is illustrated in fig. 26 and could represent a wheeled vehicle having identical displacement inputs to the front and rear wheels. Such a collection of masses, springs, and dashpots is representative of the current modeling technique for simulating a mechanical system of this kind.

For the purpose of ride dynamics studies, the system of this example is unrealistic and would not be used. Our interest in it is as a nonlinear system in its own right, representable by a set of differential equations. We want to apply the WBT modeling strategy to it, using the differential equations as a stand-in for an actual copy of the system. However, several WBT model parameters will be selected with the knowledge that this system can be made to behave in some ways similar to a vehicle.

Parameter selections for the mass-spring-dashpot model were

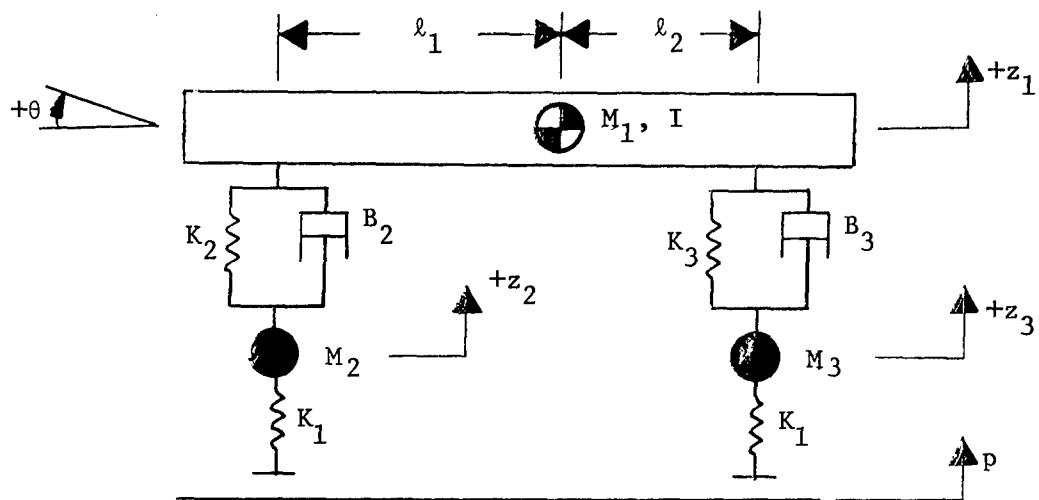


Figure 26 System for Example 4

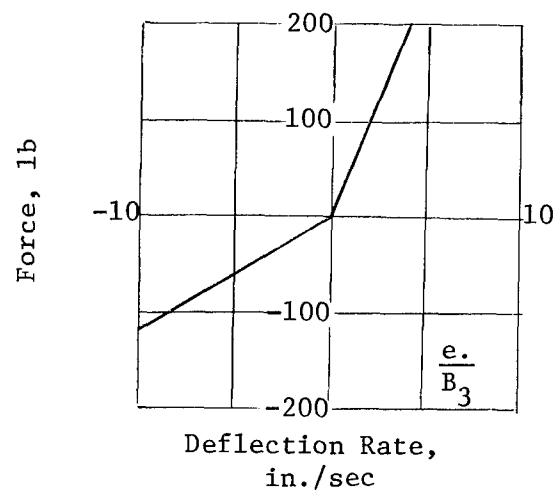
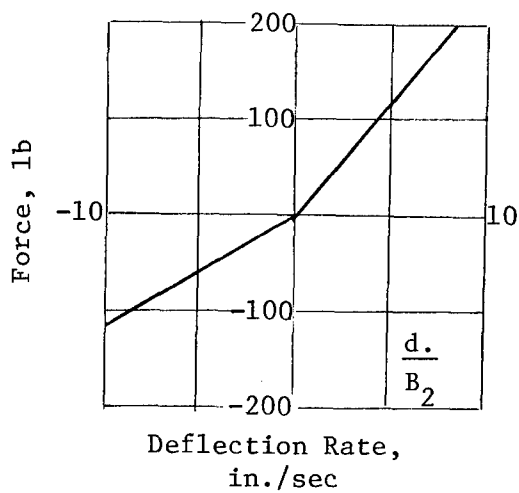
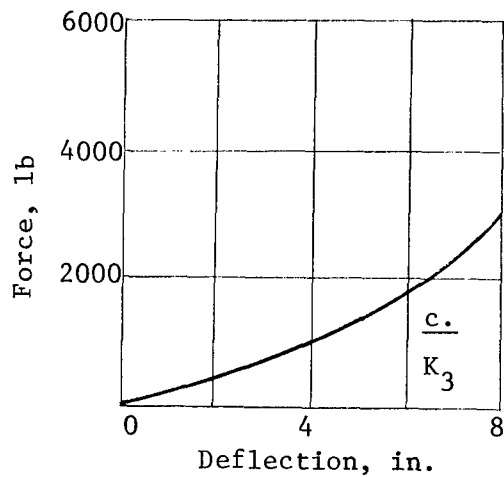
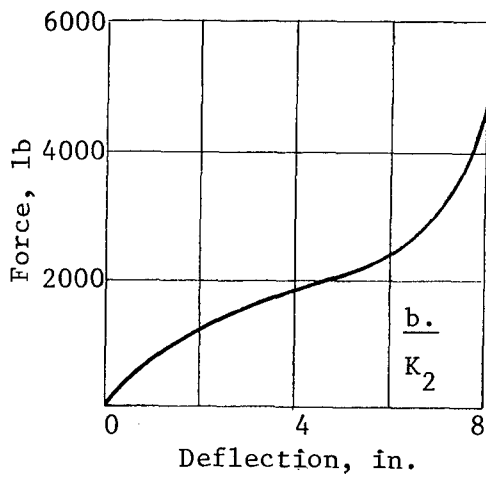
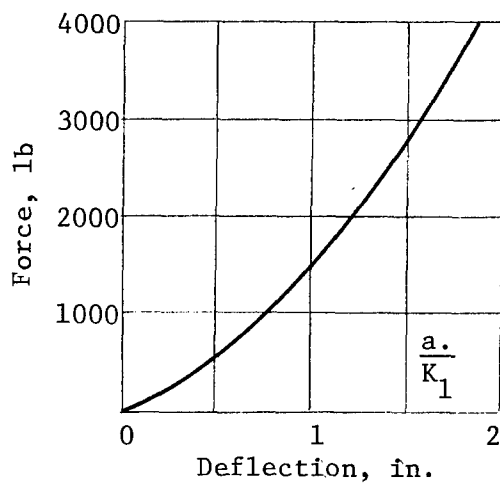


Figure 27 Model Parameters, Example 4

as follows:

$$M_1 = 8.10 \text{ lb-in./sec}^2$$

$$I = 2551.0 \text{ lb-in.}^3/\text{sec}^2$$

$$M_2 = 0.94 \text{ lb-in./sec}^2$$

$$M_3 = 0.80 \text{ lb-in./sec}^2$$

$$l_1 = 64.80 \text{ in.}$$

$$l_2 = 47.20 \text{ in.}$$

Nonlinear force-deflection characteristics for springs K_1 ,

K_2 , K_3 ; see figs 27a, b, and c.

Nonlinear force-velocity characteristics for dashpots B_2 ,

B_3 ; see figs. 27d and e.

With this selection of parameters, the differential equations for this mass-spring-dashpot model are as follows:

Deflections of compliance elements

$$\Delta_{11} = \begin{cases} p - z_2 , & p - z_2 \leq 0 \\ 0 & , p - z_2 > 0 \end{cases}$$

$$\Delta_{12} = \begin{cases} p - z_3 , & p - z_3 \leq 0 \\ 0 & , p - z_3 > 0 \end{cases}$$

$$\Delta_2 = z_2 - z_1 - 64.8 \theta$$

$$\Delta_3 = z_3 - z_1 + 47.2 \theta$$

Forces due to deflections of compliance elements

$$F_{K_{11}} = f(\Delta_{11}) \quad \text{See fig. 27a}$$

$$F_{K_{12}} = f(\Delta_{12}) \quad \text{See fig. 27a}$$

$$F_{K_2} = f(\Delta_2) \quad \text{See fig. 27b}$$

$$F_{K_3} = f(\Delta_3) \quad \text{See fig. 27c}$$

$$F_{B_2} = f(\dot{\Delta}_2) \quad \text{See fig. 27d}$$

$$F_{B_3} = f(\dot{\Delta}_3) \quad \text{See fig. 27e}$$

Dynamics

$$\begin{aligned} \ddot{z}_1 &= 0.124 \left[F_{K_2} + F_{K_3} + F_{B_2} + F_{B_3} - 3107.3 \right] \\ \ddot{\theta} &= 0.000392 \left[64.8 (F_{K_2} + F_{B_2}) - 47.2 (F_{K_3} + F_{B_3}) \right] \\ \ddot{z}_2 &= 1.0638 \left[F_{K_{11}} - F_{K_2} - F_{B_2} - 367.8 \right] \\ \ddot{z}_3 &= 1.25 \left[F_{K_{12}} - F_{K_3} - F_{B_3} - 308.8 \right] \end{aligned}$$

We want to formulate a WBT model for this system. We will identify the input as the displacement forcing function, $p(t)$, common to both springs, K_1 . The output will be the vertical displacement, z_1 , of mass, M_1 , at the center of gravity. As a consequence of studying the response of this system to step functions of several magnitudes, it is possible to estimate

$$T_s = 2.0 \text{ seconds.}$$

Because the system is capable of oscillatory responses we want as large a number of delay line taps as possible for good resolution in time. WBT model parameters were selected as follows:

$$N_t = 6$$

$$m_1 = 8$$

$$m_2 = 6$$

$$m_3 = 4$$

$$m_4 = 4$$

$$m_5 = 2$$

$$m_6 = 2$$

These choices give

$$N_c = 3072$$

$$N_B = 18,432$$

$$\Delta T = 0.333 \text{ sec}$$

The range of future inputs of interest was selected as $(-3 < x < 3)$ or

$$s = 6$$

The configuration diagram for this model is shown in fig. 28. The state diagram of coefficients determined by probing with the Bose Noise sequence is shown in fig. 29.

The performance of the WBT model was studied using the same kind of input as was used in the previous example--a step followed by ramps of different slopes ranging over the entire spread, s , of the model. Model and system responses to this input are shown as departures from equilibrium in fig. 30. We see that the basic form

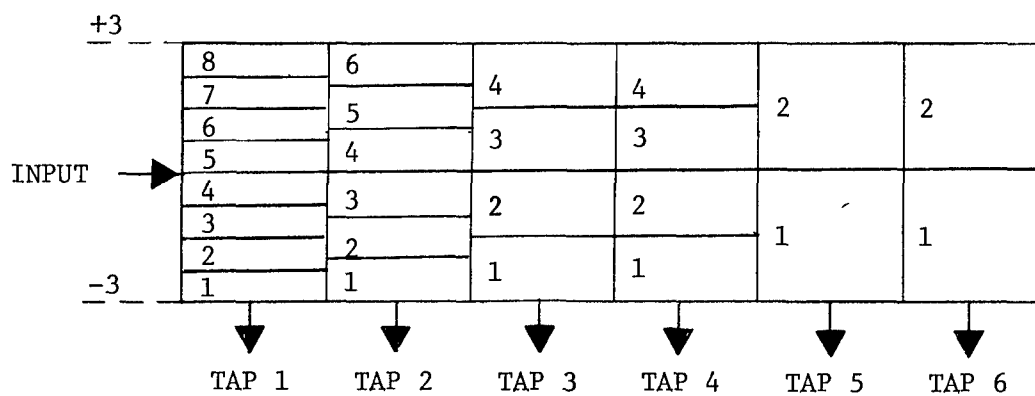


Figure 28 Configuration Diagram, Example 4

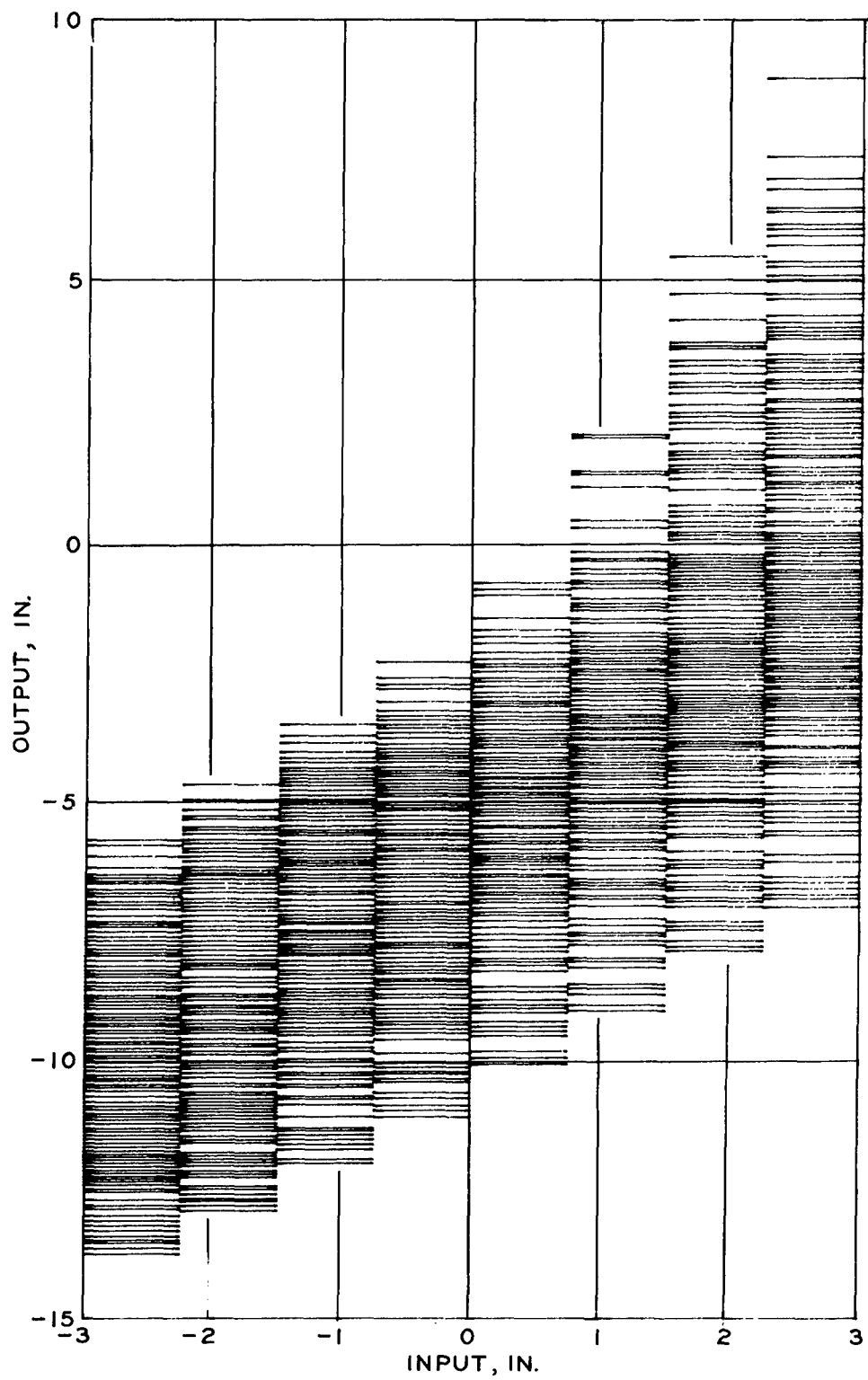


Figure 29 State Diagram, Example 4

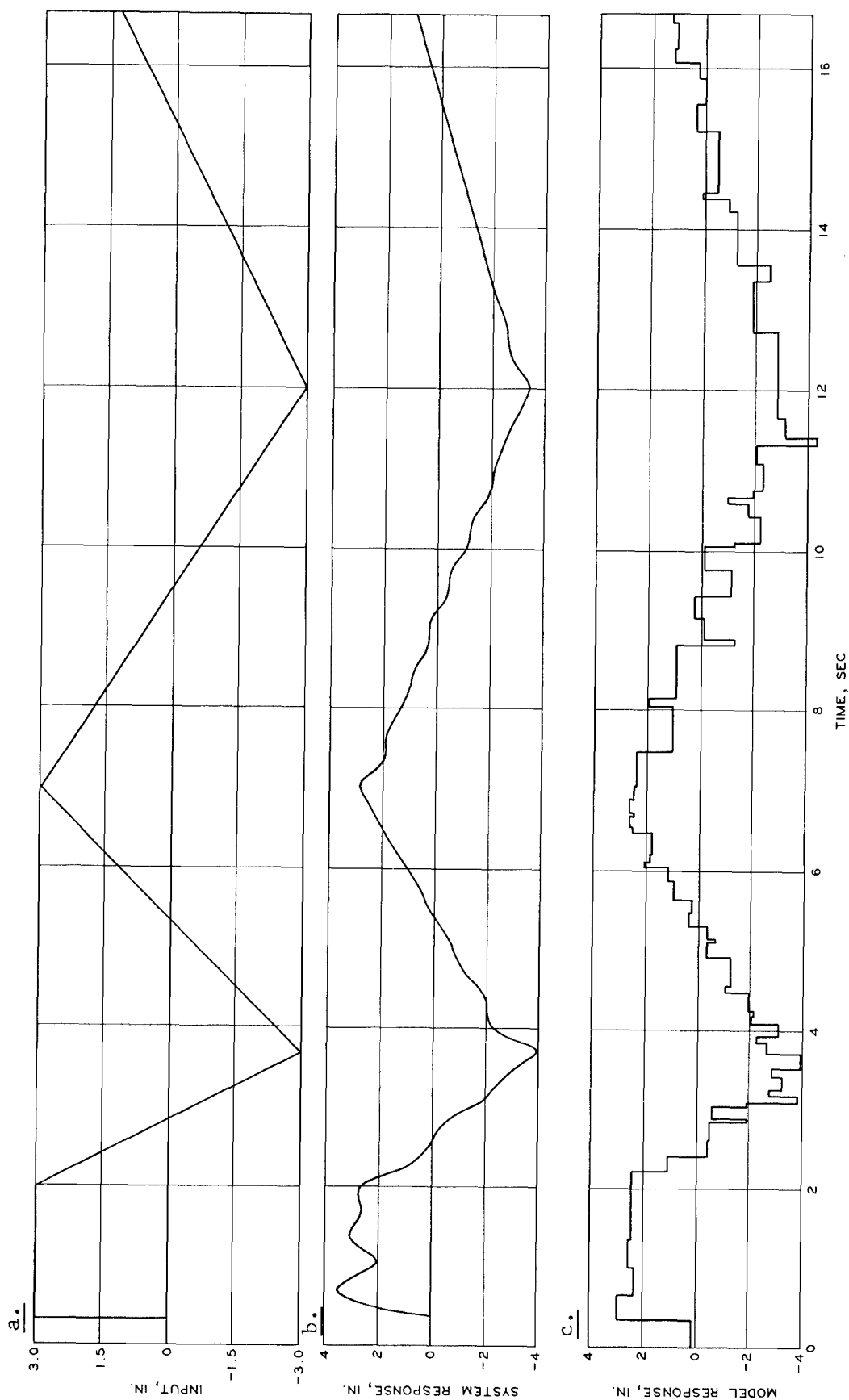


Figure 30 Comparison of System and Model Responses, Example 4

of the system response is displayed by the model, although there are many seemingly erratic jumps. Such jumps would be removed by using more gate functions on each delay line tap at the expense of increased probing effort to determine the greater number of coefficients.

We may study the mean square error by once again partitioning the input into time intervals as follows:

<u>Interval</u>	<u>Time, sec</u>
1	0 to 0.333
2	0.333 to 2.00
3	2.00 to 3.667
4	3.667 to 7.00
5	7.00 to 12.00
6	12.00 to 16.667

The mean square errors in these intervals are as follows:

<u>Interval</u>	<u>MSE, in.²</u>
1	0.189
2	0.3753
3	0.4029
4	0.1734
5	0.3871
6	0.1143

It appears at first glance that in this case the step response error (interval 2) is not the upper bound on the other errors. However, we must realize that this particular system can exhibit quite different dynamics depending on whether the compliance elements are being compressed or released from compression. Also, the system is capable of being "launched" in the sense that it can lose contact with the displacement forcing function, $p(t)$, and this is more likely to occur during a period of release from compression than

during a period of compression. The net outcome is that intervals 2, 4, and 6 should be regarded separately from intervals 3 and 5. If we do this, we see that the step response error of interval 2 is indeed greater than the errors in intervals 3 and 5. In addition, the response of the model to a downward-going step of 3-inches amplitude was determined to be 1.1637 in.² which is larger than the errors of intervals 3 and 5.

This WBT model could be improved by the use of more gate functions, especially on the first tap. That this was not done was due to the constraint imposed on computer effort by the need to process the several differential equations representing the nonlinear system.

IV. APPLICATION TO RIDE DYNAMICS

General Considerations

To ascertain factors of a practical nature in the application of Wiener-Bose Theory, and to carry out the second principal goal of this dissertation, the empirical probing process was carried out on a wheeled vehicle. With reference to ride dynamics, a vehicle is a satisfactory system for Wiener-Bose characterization. It is basically a constant-parameter system; the inputs are terrain profiles at the wheels, and the outputs are dynamic properties of interest such as accelerations and pitch angles at selected points on the vehicle. Present outputs do not depend upon the remote past of the inputs; the natural responses of most vehicles to impulsive inputs are similar to highly damped sinusoids.

There is one basic conceptual problem in applying Wiener-Bose Theory to a vehicle. To this point we have discussed single input-single output systems. A four-wheeled vehicle is a four-input system. There are several ways in which WBT can be brought to bear on this problem. Bose shows how multiple input systems may be treated. Using the methods of this dissertation, we would employ four delay lines, one for each wheel, to keep track of the past of each input. Then Bose's gate function expansion would be enlarged by using more gate functions so that we would be looking for particular configurations of the past of the inputs occurring simultaneously. If we have N_c configurations for each wheel, then the total number of configurations would be $(N_c)^4$. A model so constructed would represent a completely

unconstrained vehicle and be capable of predicting bounce, pitch, and roll motions.

Although this method of extending the theory to multiple inputs is attractive because of its conceptual clarity and represents the correct way of accomplishing the task, its cost in probing and computing effort would be prohibitive at the present time.

There are many instances in which profitable ride dynamics studies may be accomplished even when roll motion is suppressed. If we constrain our model to pitch and bounce motions then our input problem is considerably lessened because we are saying that the right and left sides of the vehicle are excited by the same terrain input. Thus we are now dealing with a two-input system: front wheels and rear wheels.

It is tempting to go further and reason that because the rear wheel input is a time-delayed version of the front wheel input we really have a single-input system and we may apply WBT directly. This fails to work out, however, when we think about the meaning of the settling time, T_s , in this context. The settling time becomes dependent on the vehicle velocity and reflects the time lag between front and rear inputs rather than the dynamic responses to those inputs. So that we have, in effect, a time varying parameter and cannot apply WBT in this way.

Returning to the two-input case, the analysis can be carried forward by constructing separate models for front wheel excitation and for rear wheel excitation and superposing the predicted responses with the time delay between inputs taken into account. This approach

has the advantage of being reasonable in the number of coefficients required. The utility of using superposition in the process of modeling a nonlinear system must be determined in each case.

Selection of the Vehicle and the Wiener-Bose Models

The vehicle selected for Wiener-Bose characterization was the military 3/4-ton truck designated M37. This vehicle has an unloaded weight of 6000 lb and is equipped with four-wheel drive. Several ride dynamics studies have been conducted using it [16,17], and much field data has been collected.

The formulation of a suitable Wiener-Bose model was influenced by two conflicting requirements: the desire for high resolution in amplitude and time on one hand which calls for many coefficients and the need to limit coefficient probing effort on the other. The model parameters finally selected are listed below:

$$N_t = 4$$

$$m_1 = 16$$

$$m_2 = 8$$

$$m_3 = 4$$

$$m_4 = 2$$

$$N_c = 1024$$

$$N_B = 4096$$

$$s = 6 \text{ in.}$$

By reviewing existing ride dynamics data for the M37, the settling time was estimated as

$$T_s = 1.75 \text{ seconds}$$

The configuration diagram for these parameters is illustrated in fig. 31.

The net outcome of these selections is a coefficient count that is rather small for ride analysis requirements but not too small to make a judgment of the overall effectiveness of the method.

The principal effort in applying WBT to this mechanical system is obtaining the characterizing coefficients. As discussed earlier our strategy is to use one WBT model for front wheel inputs and a second for rear wheel inputs. Both models are the same and have 1024 coefficients. They will have the same Bose Noise sequence for determining the coefficients. The probing process will involve traversal of an obstacle course configured to represent the Bose Noise sequence. In addition we must recognize that front and rear wheels are probed alternately and that the rear wheels must be isolated when the front wheels are being probed and the front wheels isolated when the rear wheels are probed. This means that the Bose Noise sequence is to be interrupted by isolation intervals.

The hardware realization of these probing requirements begins by recognizing that the Bose Noise sequence for each coefficient is a series of four steps (one for each delay line tap). Thus, each obstacle is to be configured in this series of steps and is to be impacted simultaneously by right and left sides of the vehicle. The average of the dynamic response of the vehicle as, say, the front wheels traverse the last step of this obstacle is interpreted as the desired characterizing coefficient for the front wheel model. The overall length of this obstacle is dictated by tire footprint

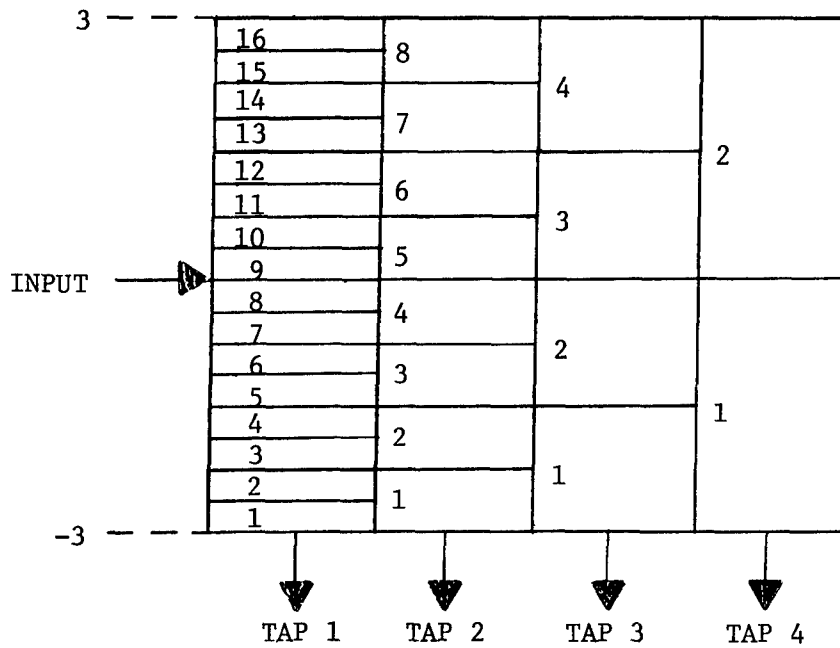


Figure 31 Configuration Diagram, M37 Model

geometry and desired operating velocity. The basic requirement is that the wheels traverse this obstacle in 1.75 seconds. This can be done at high speed with a wide obstacle or at low speed with a narrow one. Previous experience with the M37 suggested that reasonably constant velocity could be maintained with four-wheel drive at about 4 feet per second. For ease of assembly the total obstacle width was set at 8 feet. An isolation interval of 8 feet between obstacles was selected.

Now when we consider that 1024 such obstacles are required and that each is separated by 8 feet from its neighbor we can see the effort required to probe. The total length of such an obstacle course would be about 2.5 miles.

Test Setup and Procedures

The 1024 coefficients required for the selected WBT models were determined on a specially constructed obstacle course. Each obstacle was constructed of stacks of 3/8-in. plywood cut in 2 ft by 2 ft squares. Three such obstacles are shown in figs. 32, 33, and 34. They differ in the heights of the individual stacks. Each obstacle produces a different characterizing coefficient. Each coefficient was obtained as the average response of the vehicle during the time of traversal of the last step of an obstacle as shown in fig. 35. The average response was approximated by sampling the instantaneous response in the middle of the last step. Between each two obstacles is a runway 8 ft long whose purpose is to provide the isolation interval mentioned above. The elevation of the runway sets the reference



Figure 32 Representative Obstacle



Figure 33 Representative Obstacle

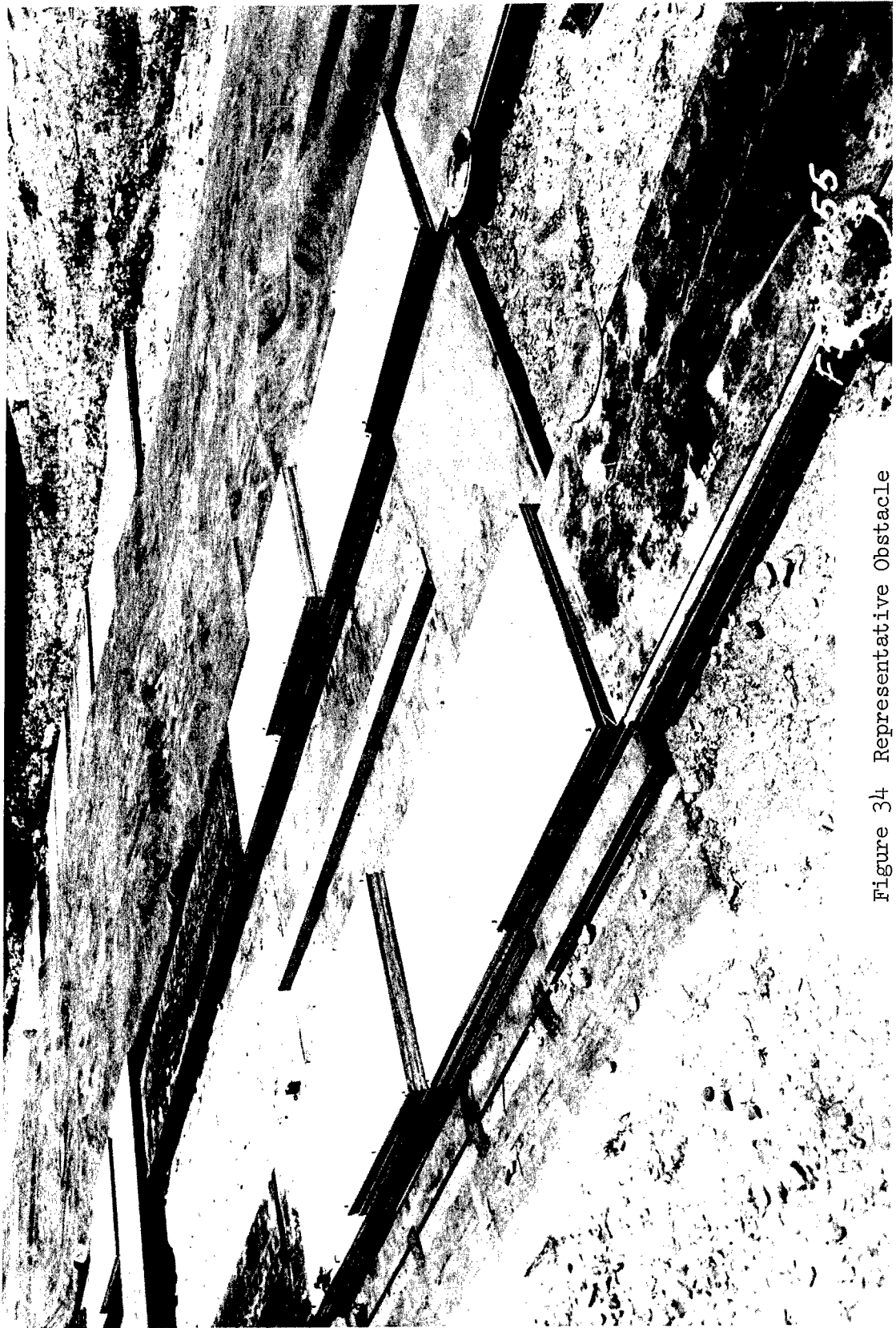


Figure 34 Representative Obstacle

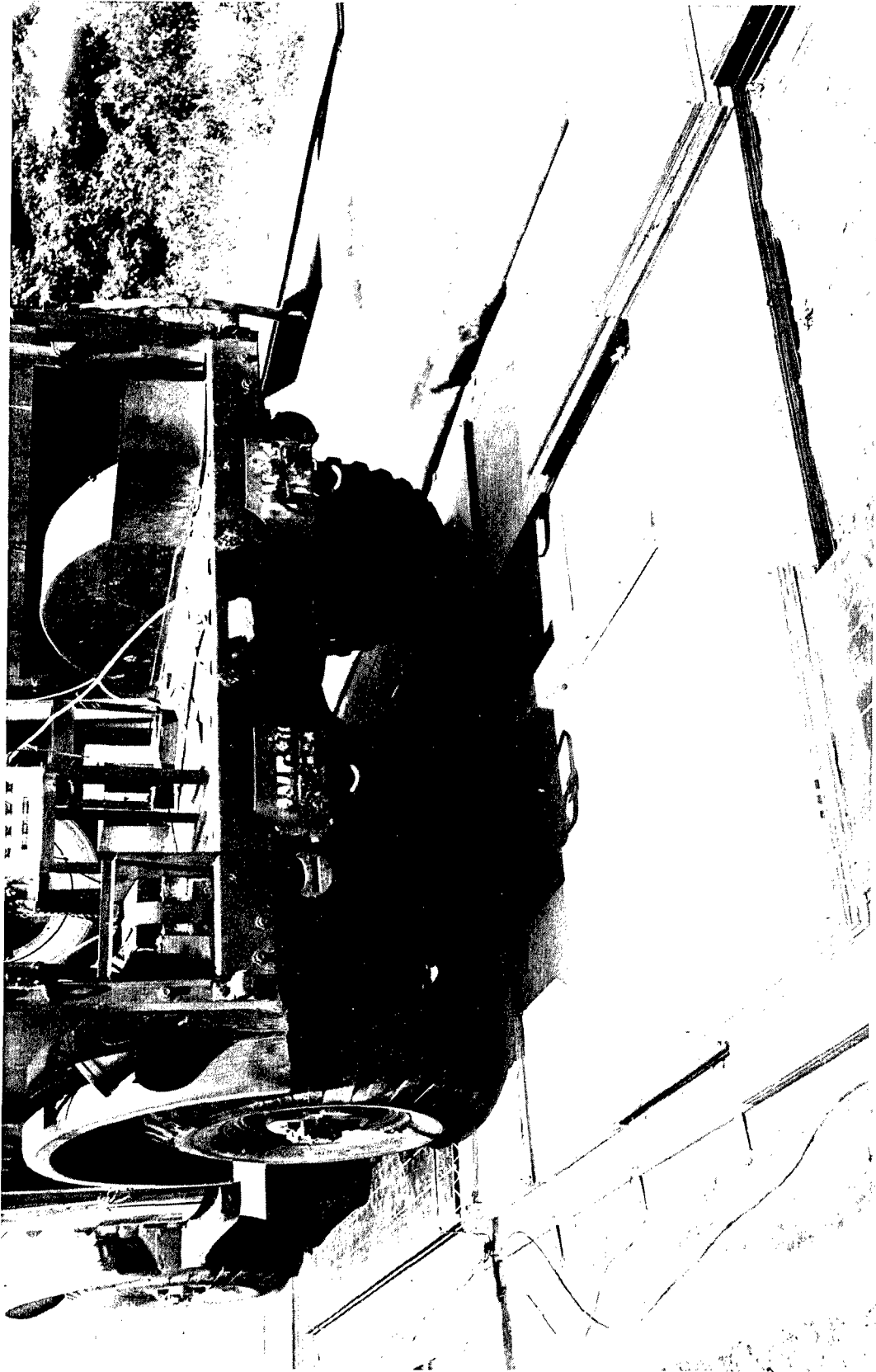


Figure 35 Traversal of Last Step of an Obstacle



Figure 36 12-Obstacle Test Course.

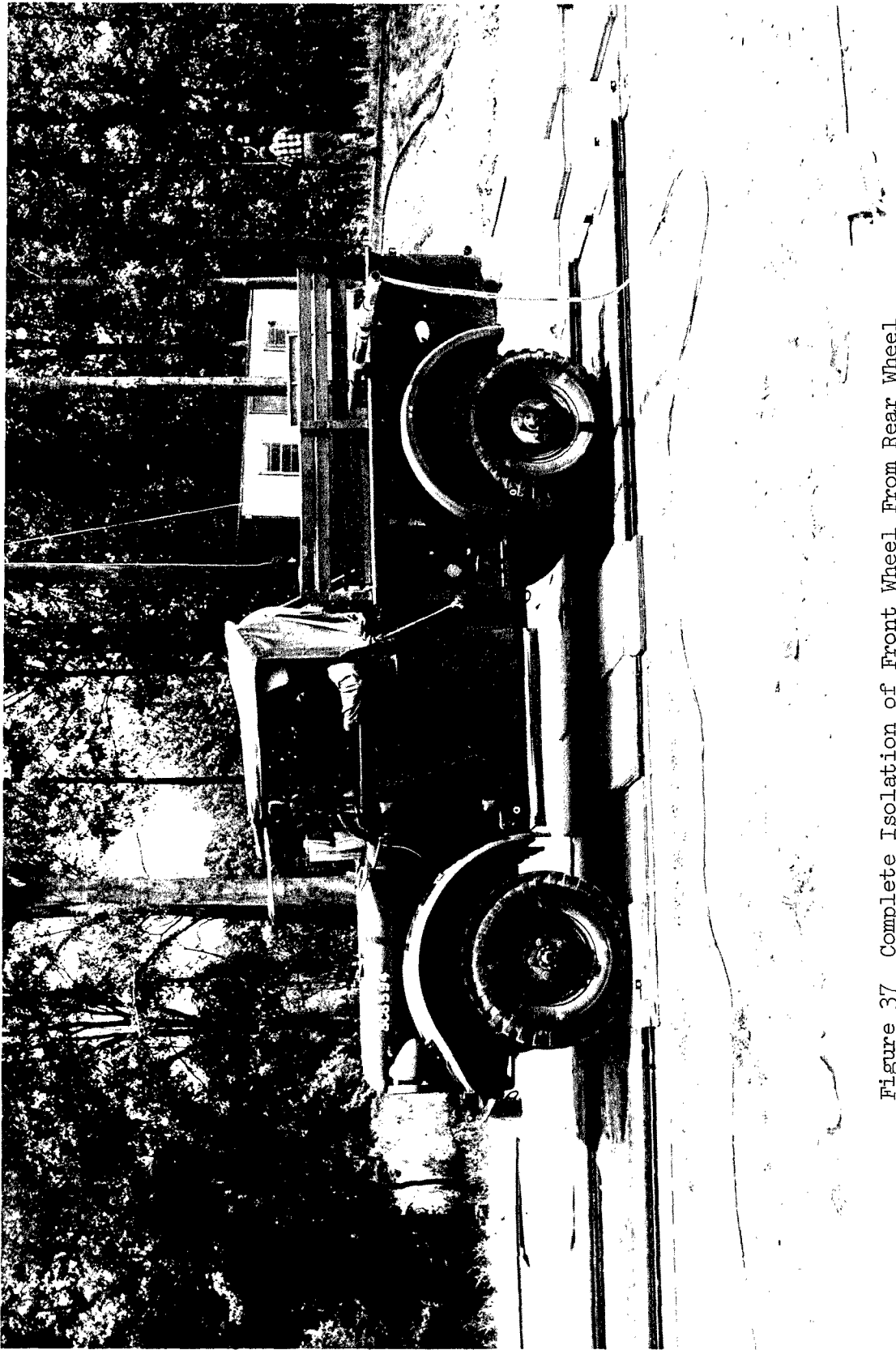


Figure 37 Complete Isolation of Front Wheel From Rear Wheel

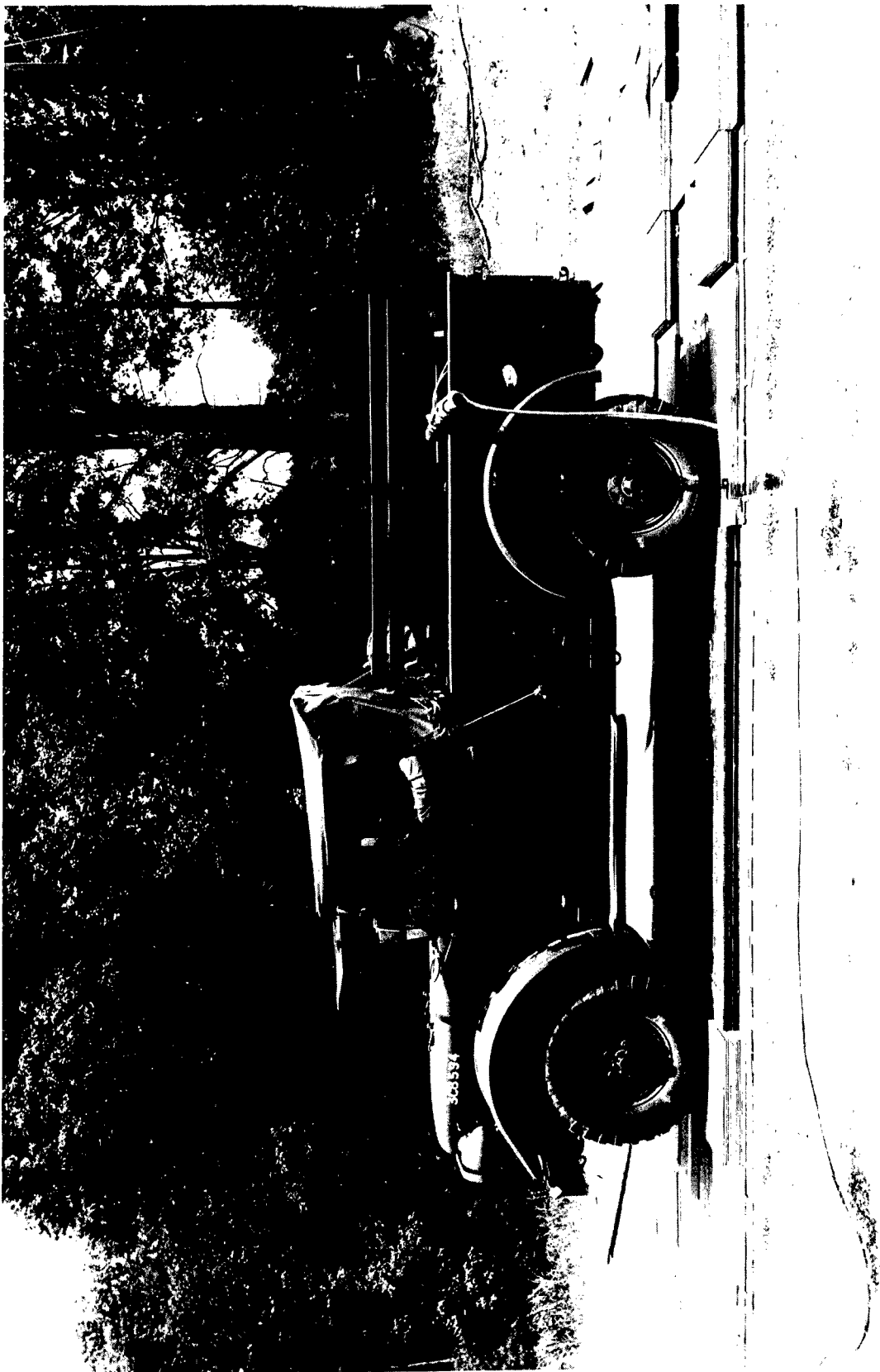


Figure 38 Incomplete Isolation of Rear Wheel From Front Wheel

level for displacements. Obstacle stack heights are both higher and lower than this level.

Twelve such obstacles and their neighboring isolation zones were assembled at any one time. These are shown in fig. 36. The total length of this obstacle course was 184 ft and corresponded to the length of preexisting hard-surface test lanes to which the obstacles were secured. When these twelve obstacles were traversed and analog data obtained, they were replaced by another set of twelve obstacles. It required 86 such replacement and traversal processes to probe the vehicle for the 1024 characterizing coefficients.

The role of the isolation intervals is illustrated in figs. 37 and 38. In fig. 37, a coefficient for the front wheel model is about to be determined as the front wheel nears the completion of its traverse of the obstacle. At that time there is no significant contribution to dynamics from the rear wheels. In fig. 38 a coefficient for the rear wheel model is about to be determined. Ideally there should be no contribution from front wheel dynamics. In practice we can see that the isolation is not complete. The distance of 8 ft chosen for the isolation interval represented a compromise between coefficient isolation on the one hand and the number of obstacles that could be placed in the available 184-ft test lanes on the other.

The vehicle was instrumented to record analog data as follows:

Pitch angle at center of gravity

Vertical acceleration at center of gravity

Horizontal acceleration at center of gravity

Horizontal velocity.

These analog time histories were recorded on magnetic tape and oscillograph paper. In addition, elapsed distance was monitored and event marks recorded to identify the instant of traversal of the middle of the last stack in each obstacle.

The testing procedure consisted of setting up twelve obstacles and traversing them at each of three constant speeds while recording analog responses. Then the next twelve obstacles were set up and the process repeated. The use of three traversal speeds was intended to show how sensitive the characterizing coefficients were to significantly different traversal velocities. Such fluctuations in velocity are unavoidable. There is also some uncertainty in the estimate of the settling time that can be simulated by traversing the fixed obstacle length at different velocities. The velocities used are listed as follows, where the settling time is the same as the time to traverse 8 ft at the indicated velocity:

<u>Velocity</u> <u>ft/sec</u>	<u>Settling Time</u> <u>sec</u>
3.50	2.28
4.00	2.00
4.56	1.75

The analog tapes were processed using a computer-controlled data acquisition system. The analog responses were sampled at instants dictated by the recorded event marks. These sampled data points were the desired coefficients.

Results

As mentioned earlier, the WBT model parameters selected within

the constraints of materiel and labor available for probing the vehicle results in a rather coarse model for purposes of ride dynamics studies. The net outcome is that of all analog data recorded, only the pitch motions of the vehicle were suitable for modeling; the accelerations were too oscillatory (and noisy) for effective modeling with only four delay line taps. Data reduction efforts were limited to determining the coefficients for the front- and rear-wheel-input models of pitch motion.

Because, to the author's knowledge, WBT had never been applied to a mechanical system like a wheeled vehicle, and because it was by no means certain that the outcome of a difficult field test program for probing the vehicle would yield results of any value, a computer study of the probing process was made. A mass-spring-dashpot model for the vehicle was formulated and coefficients for front and rear wheel WBT pitch models were determined by simulating responses for the traversal of exactly the obstacle course proposed for the actual vehicle. The mass-spring-dashpot model used is illustrated in fig. 39 and is clearly an enlargement of the system of example 4 that makes use of a segmented-wheel concept [18] for realistically simulating the transmission of forces through pneumatic tires. This model was referred to as the "bench-mark" model. In essence, the application of WBT to the bench-mark model produced a model of a model, a fact of no particular virtue. Nevertheless, by pretending that the bench-mark model was our wheeled vehicle and proceeding with the WBT probing process, state diagrams were produced, as illustrated in fig. 40, that identified trends and served as a guide for judging the

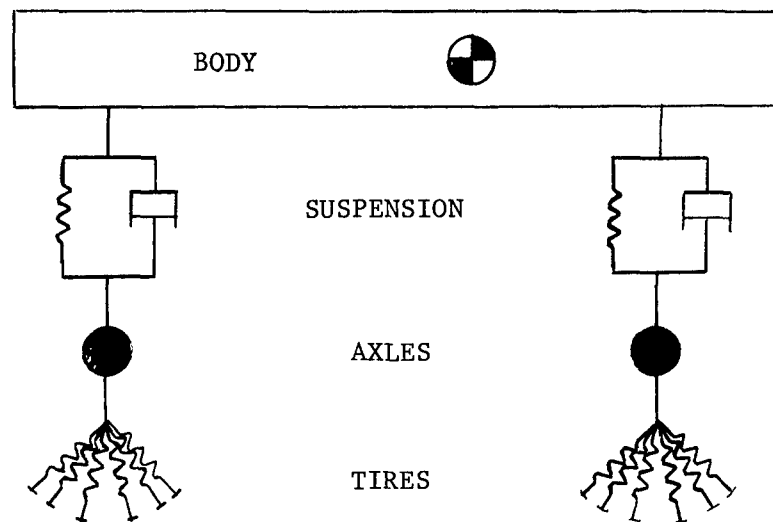


Figure 39 Benchmark Model

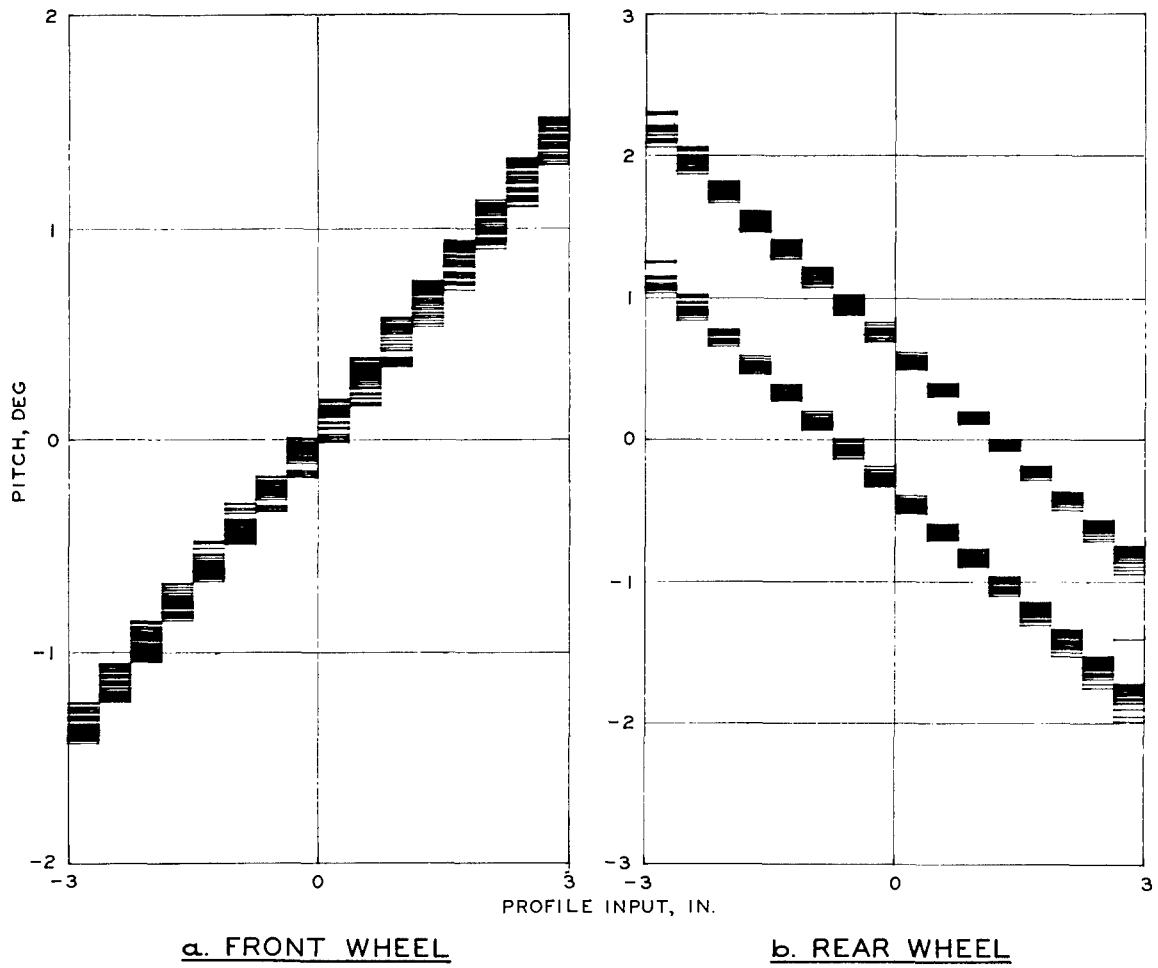


Figure 40 Benchmark State Diagrams

reasonableness of the field test data.

It is interesting to note the separation of the rear wheel coefficients into two clearly distinct groups. This is an outcome of the incomplete isolation of the rear wheels from the front wheels during the probing process.

To study the ability of the WBT model to synthesize responses to specific inputs, two input profiles were selected for simulated traversal at 4.56 feet per second. These are shown in fig. 41. A field test was conducted with the M37 in which the vehicle traversed these profiles at the same speed. These traverses were simulated with the bench-mark model and the model parameters "tuned," as usual for mass-spring-dashpot models, to give good pitch responses in comparison to the field data. With the bench-mark model optimized in this manner, the WBT probing process was carried out as mentioned above. Once the coefficients were determined, they, in turn, were used to simulate responses to the inputs of fig. 41. The responses predicted by the WBT models are illustrated in figs. 42 and 43 and are compared to the actual vehicle responses. Such predicted responses are satisfactory for ride dynamics studies and suggested that it would indeed be profitable to proceed with the test program for determining the characterizing coefficients of the M37.

The outcome of the test program was the determination of the 1024 coefficients shown assembled into a state diagram in fig. 44. Three diagrams, one for each test traversal speed, are shown for the front and rear wheel models. The coefficients were used to predict the pitch time history of the vehicle during traversal of the input profile of fig. 41. The predicted responses, using the three sets of coefficients, are compared to the actual response in figs. 45 and 46. In addition, the coefficients were used to

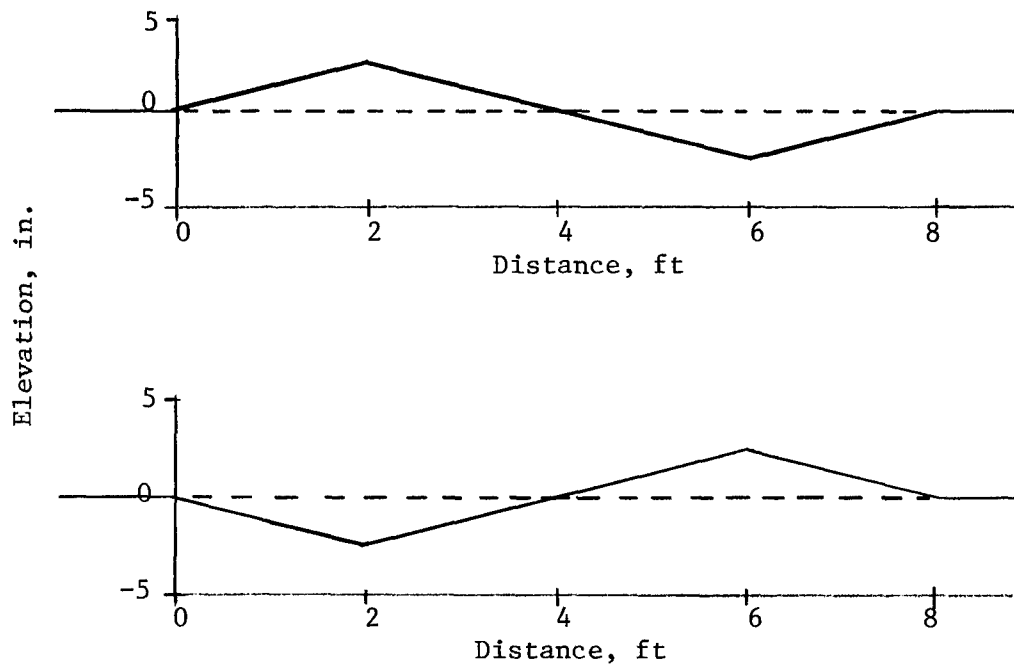


Figure 41 Specific Inputs for Benchmark and WBT Models

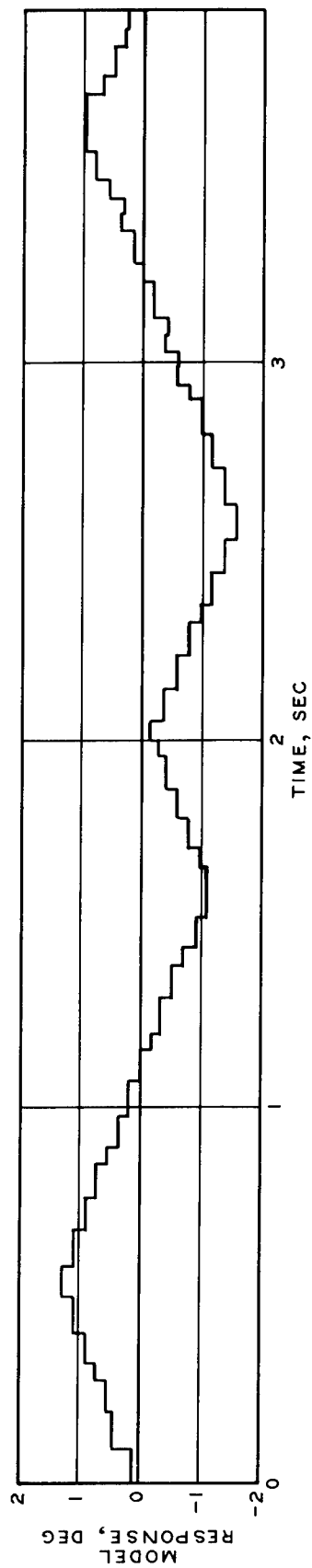
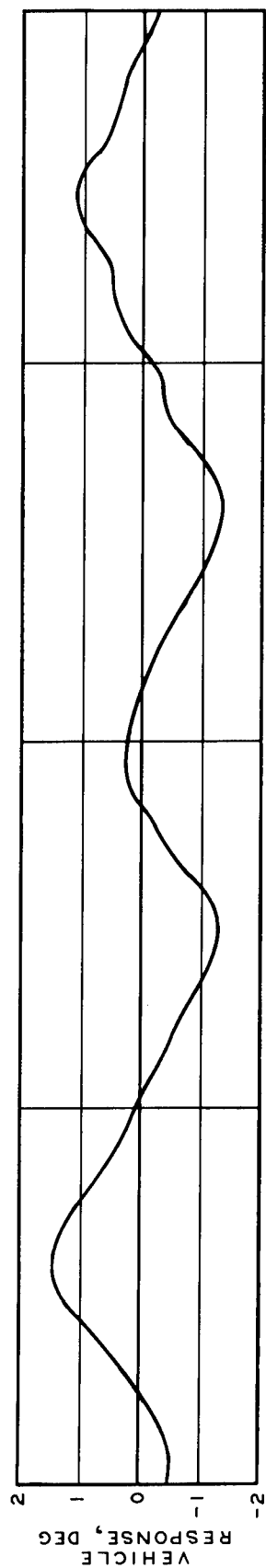
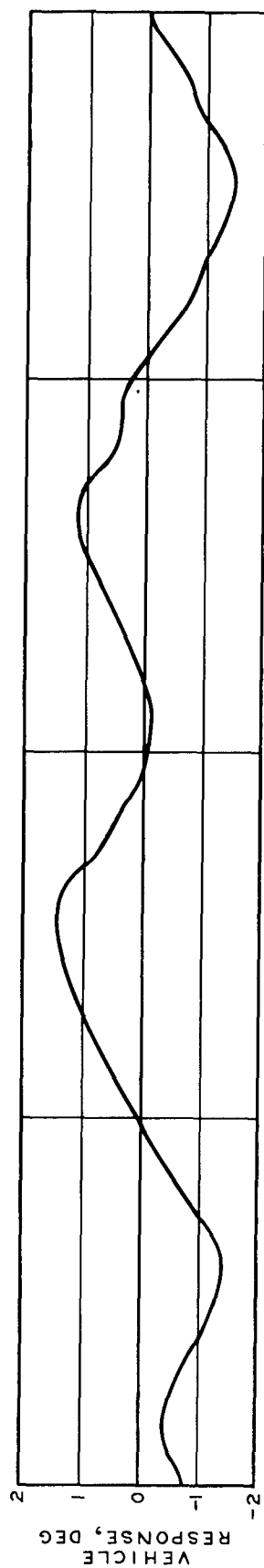


Figure 42 Vehicle and WBT (Benchmark) Responses



101

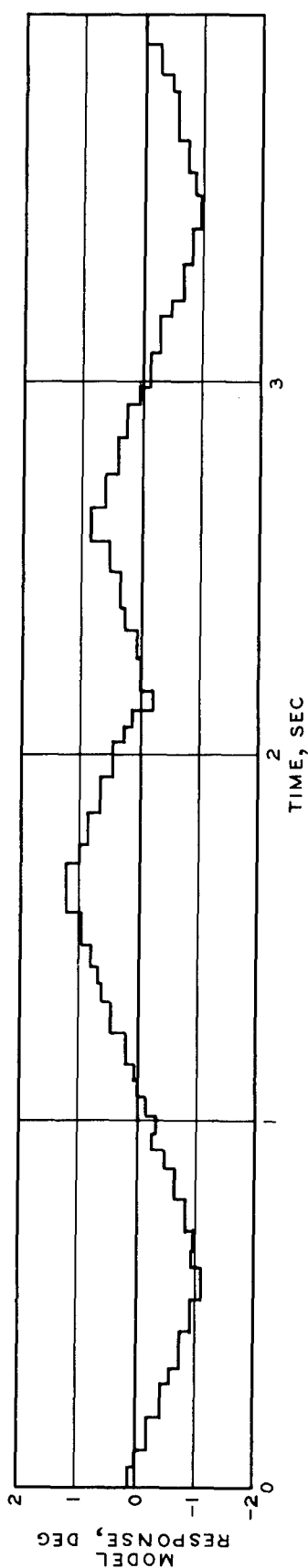


Figure 43 Vehicle and WBT (Benchmark) Responses

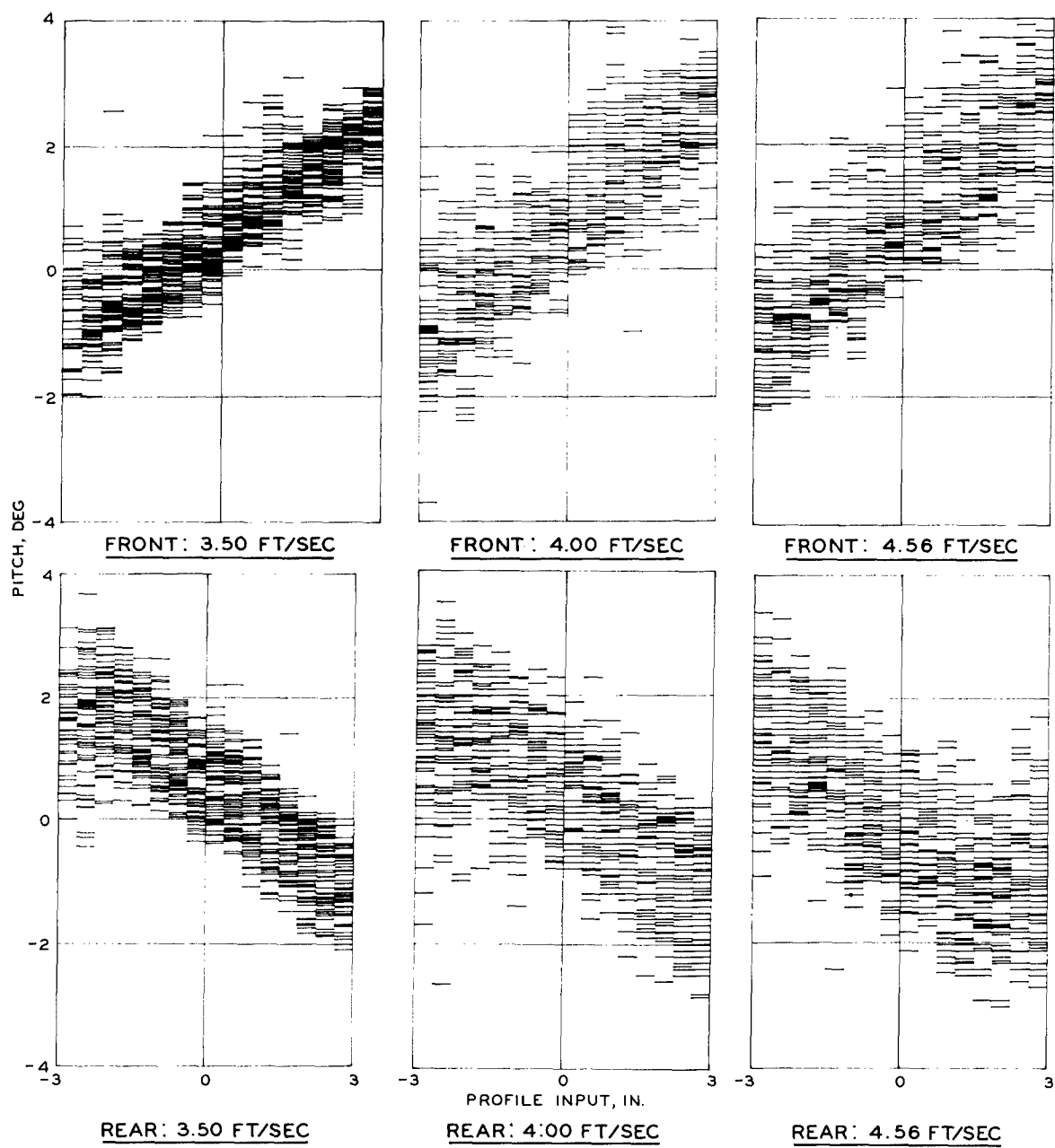


Figure 44 M37 State Diagrams

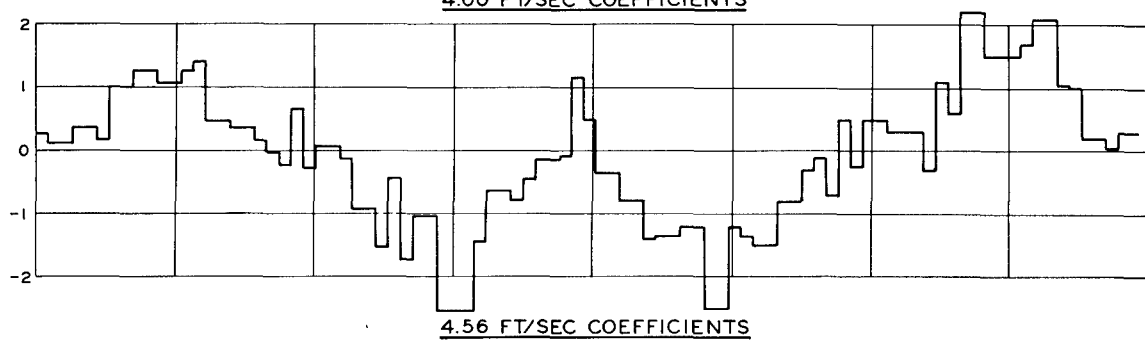
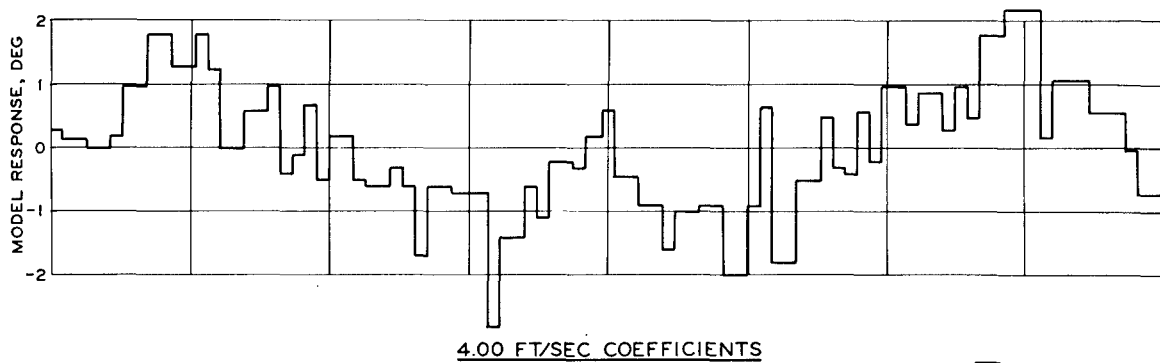
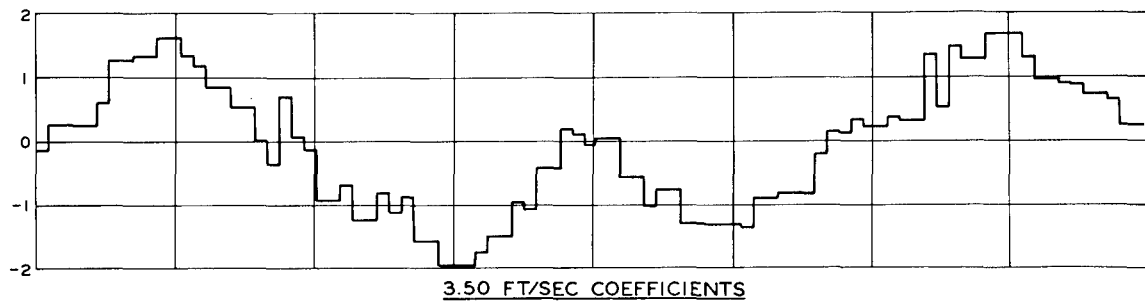
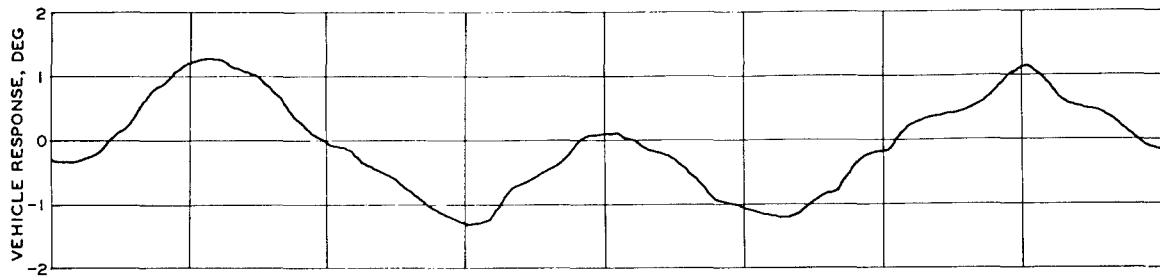


Figure 45 M37 Responses

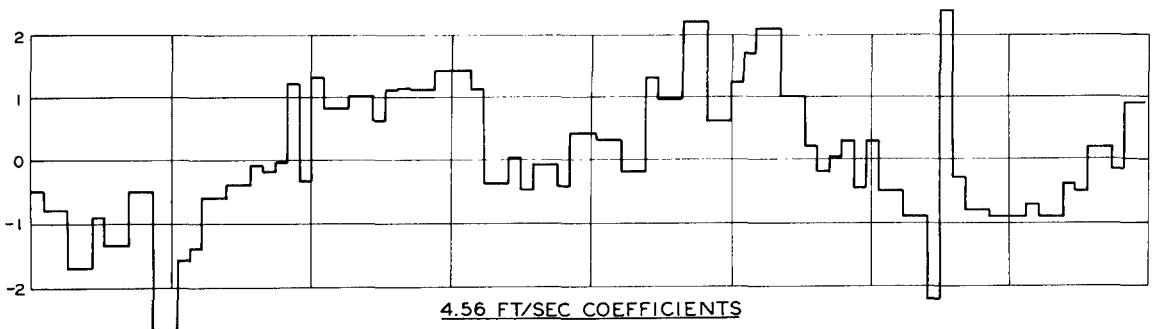
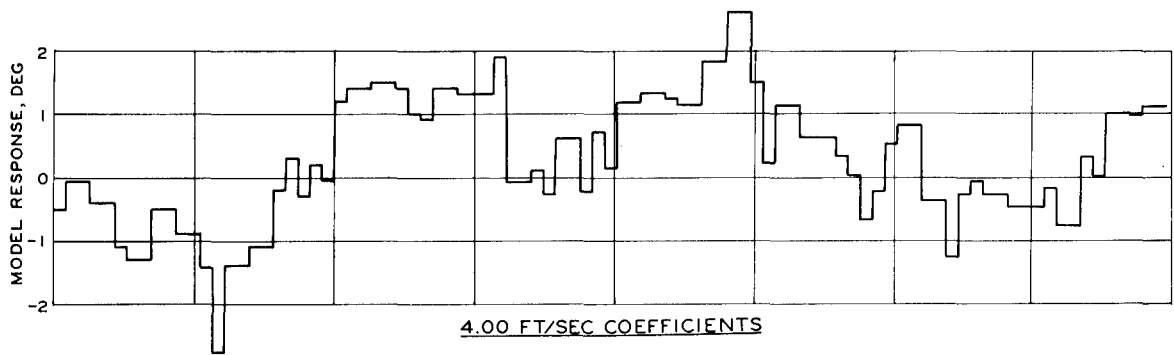
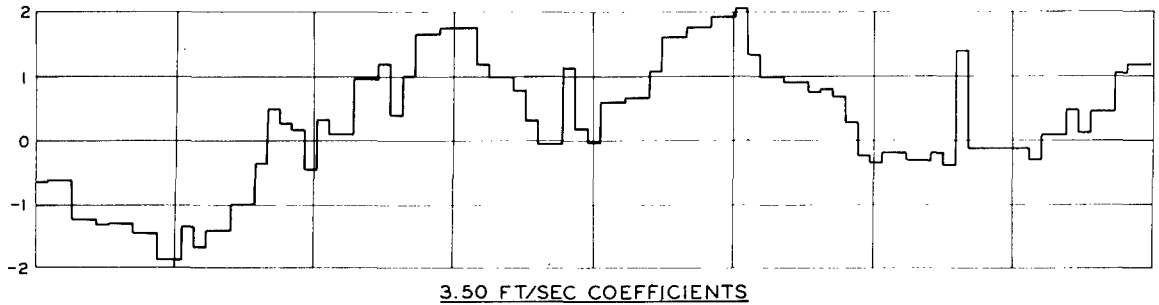
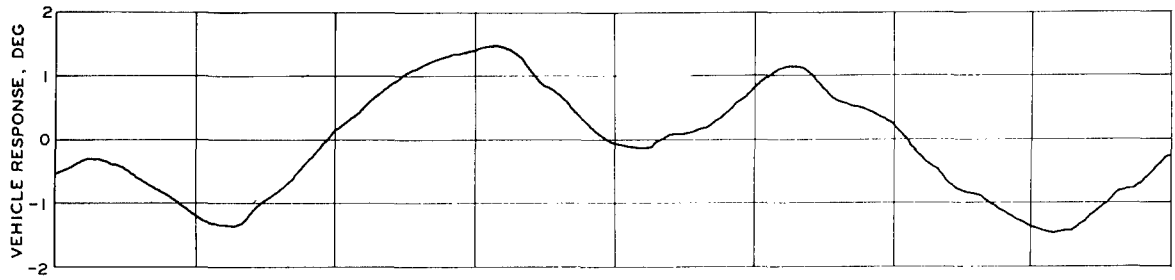


Figure 46 M37 Responses

predict the RMS pitch motion of the vehicle during traversal of a profile corresponding to one of the 12-obstacle setups of the test program. This profile is shown in fig. 47. The predicted and actual RMS pitch responses are also shown in fig. 47. The predicted responses were obtained by computing separately the responses at the center of gravity for front wheel inputs and rear wheel inputs with the time lag between these inputs accounted for. The two separate responses were superimposed and the RMS time history computed for the resulting response.

Discussion

It was necessary to make two corrections to the sets of coefficients obtained during the test program. The first correction was needed to minimize the effect of some drift in the gyro pitch sensor. At the beginning and end of the obstacle course were known locations at which the vehicle was in an attitude of zero pitch. These locations were determined on the oscillograms of pitch motion and identified the zeroes of pitch at beginning and end of the tests. The zero of pitch during the test was assumed to vary linearly between these two points. The coefficients shown in the state diagrams of fig. 44 were determined with reference to this zero of pitch.

The second correction was invoked after comparisons were made of the benchmark and M37 state diagrams (figs. 40 and 44). These diagrams are similar with respect to their linear trend across the input axis. If each of these state diagrams were fitted with a linear regression line, it would be seen that, in the case of the rear wheel coefficients, the y-intercepts of the lines would be about the same for both the benchmark and M37

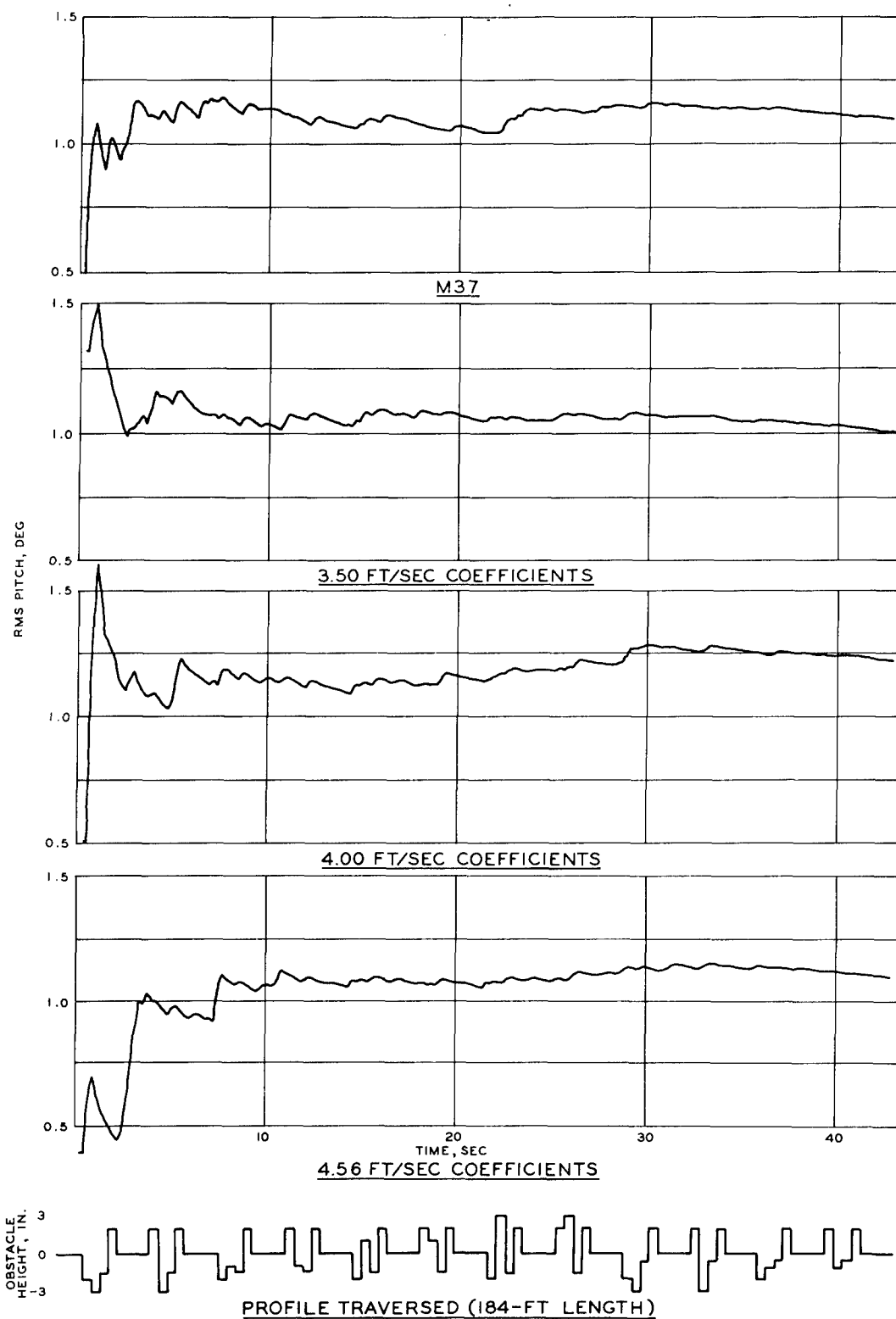


Figure 47 Comparison of Actual and Predicted RMS Pitch Time Histories

coefficients. However, for the case of the front wheel coefficients these y-intercepts would be distinctly different. For the benchmark coefficients the regression line would pass through the origin, but for the M37 coefficients it would pass well above the origin. It was decided that in utilizing the M37 coefficients to predict pitch responses, the front wheel coefficients would be decremented by an amount equal to the y-intercept of their respective regression lines. Figures 45, 46, and 47 were obtained with the front wheel coefficients used in this way.

A comparison of the predicted and actual pitch time histories shown in figs. 45 and 46 suggests, qualitatively, that WBT is capable of capturing the main features of the dynamic responses of the actual vehicle. It should be borne in mind that the coefficients used to assemble these predicted responses were obtained during traversal of an obstacle course that bore no resemblance to the input profile corresponding to these responses.

There will be little merit in formulating quantitative measures of model performance with respect to deterministic time histories. It is more realistic to study the statistical performance of the model. In comparing the predicted and observed RMS pitch responses, fig. 47, a satisfactory match may be seen. It is this outcome that suggests that WBT is capable of satisfactory performance for ride dynamics studies.

It is pertinent at this point to comment on some of the practical problems encountered in determining the WBT coefficients. The test program required four months to accomplish. Work proceeded intermittently, slowed by weather conditions, personnel changes, and higher priority projects. Thus, the vehicle which we tacitly assume to be invariant in its mechanical properties is never quite the same from test to test when driven by different

men, undergoing maintenance, and operating in the open. These facts, of course, can be anticipated prior to doing any testing and we are interested in knowing how sensitive the WBT coefficients are to these perturbing factors.

As mentioned earlier, the coefficients were studied under three different conditions of traversal speed, knowing that an absolutely constant speed cannot be maintained. Thus, to use three speeds separated by approximately 15 percent exaggerates the effect of variations in test speed and gives a clue to the sensitivity of the WBT coefficients to this factor. In general, the obstacle course corresponding to the Bose Noise sequence for our WBT model was rather rough on the vehicle, even though the maximum peak-to-peak obstacle height was never greater than 6 inches. The net outcome was that although the overall traversal speed could fairly easily be held to the desired value, deviations from this speed could be significant. In some cases it was necessary to put small blocks in front of the higher obstacles to prevent the vehicle from being stopped dead in its tracks. Most of the coefficients were obtained with the desired condition of traversal speed, but others were obviously in error because of too great deviations in speed at the wrong time.

Another perturbing factor was the nonsimultaneous impacting of obstacles by the right and left wheels. The WBT models were predicated on the absence of any roll motion. This condition was observed to be maintained most of the time but could become a problem especially when traversing the rougher segments of the Bose Noise sequence.

Notwithstanding these problems, the WBT coefficients, as indicated by the state diagrams in fig. 44, would seem to be fairly tolerant of the practical aspects of probing. Moreover, the predicted responses of figs. 45 and 46, are reasonably similar in view of the fact that the coefficients of which they are constructed were determined at significantly different speeds. It is interesting to note that the greatest errors occur on the right-hand side of these figures corresponding to the response of the rear wheel model, and the coefficients of the rear wheel model were the ones that were obtained under the condition of incomplete isolation from the front wheels (see fig. 38).

In retrospect, the test procedures and obstacle course construction are capable of much refinement. For example, it required about 20 minutes to run the vehicle at three speeds over a completed obstacle course, thereby securing another 12 coefficients. Then it required some 2 hours to change the configuration of the obstacles prior to another run. Because of the considerable overall expenditure of time and effort on probing the vehicle, test procedures must be significantly refined before WBT can easily be applied to ride dynamics problems.

These refinements can be carried out in two ways. First, effort expended in designing and constructing a quick-change obstacle course will offset the testing slowdown incurred with the rudimentary obstacle course employed in this study. Second, it may be possible to reduce the generality of the model and so reduce the coefficient count significantly. This comment is suggested by the observation that in assembling specific responses to specific inputs, the model summons only a small number of coefficients from the available stockpile. Thus, if it were possible to

say that only a certain class of inputs were likely to be studied in the future, it may be possible to decide in advance what coefficients were likely to be used. Those coefficients that would see little use need not be found. This approach represents a middle ground between a completely general model like WBT provides and a completely empirical strategy for determining vehicle responses to a few profiles of interest.

V. CONCLUSION

Some Guidelines for Constructing WBT Models

The experience gained during this study of the implementation of WBT is most usefully summarized in the form of guidelines for selecting WBT model parameters. The principal utility of such guidelines is to remind the investigator of the many options at his disposal and to suggest priorities for his selection of parameters. Figure 48 attempts a graphic illustration of the flow of ideas to be discussed below.

- a. Although it was actually within the context of the original Wiener theory to inject a probing signal into the nonlinear system without any knowledge of its nature other than its lack of spontaneous oscillation or combustion, we should, in fact, know more than this. We must be able to prod, poke, or otherwise tamper with the system so that an estimate may be made of a settling time, T_s . The settling time is an important parameter in the WBT model and an effort should be made to learn the peculiarities of the system in its different regimes in order to make a good estimate. If the selection of T_s is too small, the equilibrium states of the model will be in error; if too large, too long a record of the past of the input is retained and many coefficients will be wasted in the expansion of unnecessary delay line taps. A possible way to check the correctness

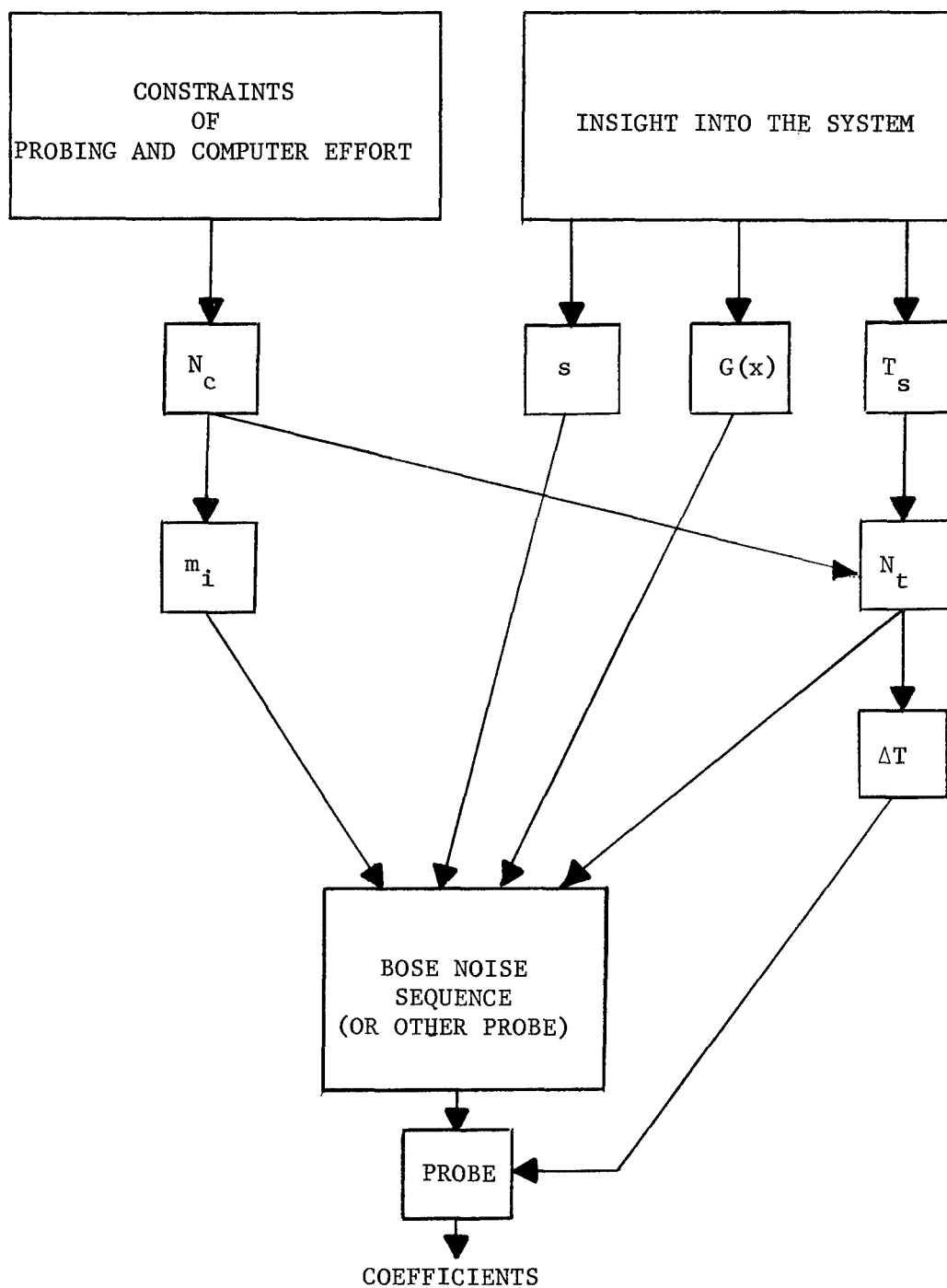


Figure 48 WBT Parameter Selection Flow Chart

of the estimate of T_s is to determine, using the configuration diagram for the WBT model, just which configuration determines the coefficient representing the equilibrium state (assuming, for example, only one). The system may be probed to find this coefficient and the mean square error between the model and system equilibrium levels determined. A large error suggests that T_s has been selected too small and, in fact, a very small error should alert the investigator to the possibility of too large a value for T_s . It should be borne in mind that other factors contribute to equilibrium level errors. Specifically, there are the number and widths of the gate functions, and the spacing of the taps along the delay line. Thus the procedure suggested above does not completely isolate the error due to the estimate of T_s but can serve as a guide.

- b. In reference, once again, to the original Weiner theory, there was no expressed limit to the amplitude of the probe or to the amplitude of inputs to be handled by the model. In WBT, there is a limit to such amplitudes, especially when Bose Noise is used as the probe. In fact this limit is fixed by the investigator as the amplitude spread parameter, s , and represents the maximum peak-to-peak excursions of the input for which the WBT model is valid. We must be able to estimate the range of amplitudes for future inputs of interest.

This estimate is based upon our knowledge of the nature of the nonlinear system under study. We want to be certain that the WBT model is not more elaborate than necessary; too large an estimate of s will usually result in more coefficients than needed for most future inputs.

- c. The weighting function, $G(x)$, is completely unspecified in WBT except for the requirement that it be non-negative. Throughout this dissertation we have used

$$G(x) = 1$$

Aside from the fact that this choice results in simple formulas for coefficient determination, the selection of unity is necessary if Bose Noise is to be used as the probe and the coefficients are to be determined by averaging responses over predetermined times of coincidence. This method offers important savings in data processing effort. In addition, the choice of unity corresponds to the production of coefficients capable of producing minimum mean square error model responses, although this capability is degraded by using short averaging times. Thus the choice of unity for the weighting function is quite effective in its own right and we may expect that this choice will often be made automatically with no more thought given to it. However, in establishing WBT model parameters

the investigator should recall that $G(x)$ is a free choice and can possibly play a decisive role in dealing with the peculiarities of his particular nonlinear system.

d. Many theories are born clamoring for great amounts of time, effort, and computing machinery so that they may grow, prosper, and bring forth good results. Few do so more loudly than WBT. We have two principal constraints upon the implementation of WBT: the effort required to probe the system to determine the characterizing coefficients and the limitations on processing speed and storage capacity of the computer that will hold all these coefficients and assemble specific responses from them. With regard to probing effort, nothing can be said here as to how much will be required because it depends completely on the nature of the system to be modeled and upon the error requirements placed upon the model. As mentioned above, the probing effort required for the mechanical system studied in this dissertation was very great and must be reduced before WBT can be applied routinely. Furthermore, the constraint imposed by probing effort will be just as severe in the future as at present, in contrast to what we may expect of the second constraint. It is entirely reasonable to expect that the constraint imposed by speed and capacity of computers will diminish to the point of essentially

becoming no constraint at all and that the probing effort to determine model coefficients will be the only factor that fixes their number.

- e. The net outcome of dealing with the factors discussed above is the selection of values for the parameters T_s , N_c , s , and $G(x)$. Two more basic parameters are at our disposal, the number of delay line taps, N_t , and the number of gate functions, m_i , used to expand each tap. In essence, N_t controls resolution in time and the m 's control resolution in amplitude.

Throughout this dissertation, we have used equal spacings of delay line taps, a configuration especially easy to implement. But we are not restricted to keeping track of particular instants in the past of the input and may tap the delay line at will. Harris, with his special form of WBT, has used some unequal tap spacings with improvement in the error performance of his models.[7] Thus the investigator may want to consider the possibility of strategically located taps on the delay line as suggested by features (such as transport lag) of his nonlinear system.

On each tap of the delay line of the models used in this dissertation, we have used gate functions of equal width. Once again this choice is prompted by ease of implementation but is not a basic requirement of WBT. As long as the partitioning of the amplitude

of the waveform emerging from the delay line tap is nonoverlapping, the partition intervals may be chosen at will.

In this dissertation we have used diminishing numbers of gate functions to expand taps positioned later and later along the delay line. The motivation was to reduce the total number of coefficients in comparison to the number that would be required if all taps were expanded with the same number of gate functions as used on the first. This procedure was also suggested by the nature of the nonlinear systems studied whose dependence on the past diminishes as we go farther into the past, and which would seem to require less detailed knowledge of past amplitudes to determine present responses. But we should be aware of the fact that the choice of numbers of gate functions is free and may suit the convenience of the investigator.

f. Having gone on to select values for N_t and the m 's, we have fixed the time interval between delay line taps, ΔT , and the Bose Noise sequence for the model. We are now ready to determine the characterizing coefficients to complete the model. Recall that the principal advantage in using Bose Noise is the relatively short time required for probing. But we are by no means committed to using it and may use any kind of probing signal, perhaps one suggested by the nature of the system or the future

inputs to be studied.

Conclusions

- a. The original theory of nonlinear systems suggested by Wiener is not suitable for engineering applications because of excessive numbers of coefficients required and practical difficulties incurred in their determination with a nonideal Gaussian probe.
- b. The gate function expansion suggested by Bose is an important factor in developing a practical theory. This factor, together with the concept of Bose Noise, contributes to a workable strategy for modeling nonlinear systems.
- c. The principal constraint on the application of the theory is the effort required to probe the system to determine the characterizing coefficients.
- d. With respect to the application of WBT to ride dynamics, the modeling strategy gives responses that compare favorably with those of the actual wheeled vehicle considered in this dissertation. The probing process for coefficient determination is extensive and better field test procedures must be worked out before WBT can be applied in a routine way.

Recommendations

- a. Strategies for coefficient reduction based upon elimination of coefficients unlikely to be used should be formulated.

- b. With reference to vehicle ride dynamics, quick-change obstacle courses for probing the vehicle should be used.

REFERENCES

1. Wiener, N., Nonlinear Problems in Random Theory (New York: John Wiley and Sons, Inc., 1958).
2. Bose, A. G., "A Theory of Nonlinear Systems," Technical Report 309, Research Laboratory of Electronics, Massachusetts Institute of Technology, May, 1956.
3. Taylor, A. E., Advanced Calculus, (New York: Ginn and Co., 1955).
4. Mishkin, E. and Braun, L., Adaptive Control Systems (New York: McGraw-Hill Book Co., 1961).
5. Flake, R. H., "Volterra Series Representation of Nonlinear Systems," Transactions of the A.I.E.E., Vol 81, Part 2, pp 330-335, Jan 1963.
6. Cameron, R. H. and Martin, W. T., "The Orthogonal Development of Nonlinear Functionals in Series of Fourier-Hermite Functionals," Annals of Mathematics, Vol 48, No. 2, pp 385-392, April 1947.
7. Harris, G. H., The Identification of Nonlinear Systems with Two-Level Inputs, Dissertation, Princeton University, 1966.
8. Rula, A. A. and Nuttall, C. J., "Analysis of Mobility Models," Technical Report (being prepared for publication), U. S. Army Engineer Waterways Experiment Station, CE, Vicksburg, Miss.
9. Lee, Y. W. and Schetzen, M., "Some Aspects of the Wiener Theory of Nonlinear Systems," Proceedings of the National Electronics Conference, Chicago, Ill., Vol 21, pp 759-764, Oct 1965.
10. Kautz, W. H., "Network Synthesis for Specified Transient Response," Technical Report No. 209, Research Laboratory of Electronics, Massachusetts Institute of Technology, April 1952.
11. Morrison, N., "Smoothing and Extrapolation of Continuous Time Series Using Laguerre Polynomials," SIAM Journal of Applied Mathematics, Vol 16, No. 6, pp 1280-1304, Nov 1968.
12. Hildebrand, F. B., Introduction to Numerical Analysis (New York: McGraw-Hill Book Co., 1956).
13. Roy, R. J., Miller, R. W., and DeRusso, P. M., "An Adaptive-Prediction Model for Nonlinear Processes with Two-Level Inputs," Proceedings of the Fourth Joint Automotive Control Conference, Minneapolis, Minn., pp 204-210, 1963.
14. Hogg, R. V. and Craig, A. T., Introduction to Mathematical Statistics (New York: The MacMillan Co., 1965).

15. Pfeiffer, P., Theory of Probability (New York: McGraw-Hill Book Co., 1965).
16. Van Deusen, B., "Experimental Verification of Surface Vehicle Dynamics," NASA Contract Report NASW-1607, Oct 1968.
17. Switzer, G. G., "Effects of Obstacle Geometry and Traversal Speed on the Dynamic Response of a Wheeled Vehicle," Technical Report (being prepared for publication), U. S. Army Engineer Waterways Experiment Station, CE, Vicksburg, Miss.
18. Lessem, A. S., "A Mathematical Model for the Traversal of Rigid Obstacles by a Pneumatic Tire," Technical Report M-68-1, May 1968, U. S. Army Engineer Waterways Experiment Station, CE, Vicksburg, Miss.

ABSTRACT

Allan S. Lessem, Doctor of Philosophy, August, 1970

Major: Electrical Engineering, Department of Electrical Engineering

Title of Dissertation: Implementation of Wiener-Bose Theory and
Application to Ride Dynamics

Directed by: Dr. Willie L. McDaniel, Jr.

Pages in dissertation, 123. Words in abstract, 361.

ABSTRACT

Wiener-Bose Theory is a strategy for identifying nonlinear systems in terms of a set of "characterizing coefficients." These are obtained through the agency of a certain probing process carried out on each system. Once the coefficients have been determined they must be used in a rational synthesis procedure to predict responses to inputs of interest. The principal appeal of Wiener-Bose Theory is that it requires very little knowledge of the physics of the system. No dynamical equations need be written. In essence the physics of the system is incorporated into the characterizing coefficients.

It is this property of Wiener-Bose Theory that makes its application to vehicle ride dynamics studies attractive. The present strategy for ride dynamics studies invokes the use of structure-oriented mass-spring-dashpot models based on rigid body mechanics. These models are characterized by the need for repeated "tuning" in which model parameters are altered in a basically irrational way when comparisons are made to

different sets of responses of actual vehicles.

A computer study was conducted to discern problems of implementation of the theory. Several systems of increasing complexity were studied and a practical form of Wiener-Bose Theory evolved. The systems studied were as follows: (a) a zero-memory system, (b) rate-independent hysteresis, (c) a second-order system with saturation, and (d) a fourth-order mechanical system with nonlinear compliances. The experience gained during this study was summarized in a set of guidelines for the construction of Wiener-Bose models.

A program of testing was carried out to ascertain the practicality and utility of Wiener-Bose Theory for ride dynamics studies. A military M37, 3/4-ton truck was selected for characterization using a Wiener-Bose model having 1024 coefficients. The characterizing coefficients were obtained by utilizing the responses of the vehicle recorded during traversal of a specially configured obstacle course whose total length was 2.5 miles. Once the coefficients were obtained, they were used to synthesize responses to specific terrain profiles. These predicted responses compared favorably with counterpart responses of the vehicle traversing the same profiles.

It was concluded that Wiener-Bose Theory is capable of satisfactory performance in the analysis of many nonlinear systems. The principal difficulty in its practical application is the extensive probing effort required for characterizing the system.

DISTRIBUTION LIST A

(For Distribution of TR's and MP's on Trafficability and Mobility Studies
and Related Investigations)

Address*	No. of Copies
<u>Army</u>	
Chief of Engineers, Department of the Army, Washington, D. C. 20314	
ATTN: ENGME-RD	1
ENGME-RO (For Engineer Standardization Program)	4
ENGAS-I	2
ENGMC-ER	2
ENGSA (Dr. G. G. Quarles)	1
ENGME-S (U. S. Army Topographic Command, 6500 Brooks Lane, Washington, D. C. 20315)	2
ENGRD	1
Deputy Director for Operations/Environmental Services, Organization of the Joint Chiefs of Staff, Washington, D. C. 20301	1
Assistant Chief of Staff for Force Development, Department of the Army, Washington, D. C. 20310	1
ATTN: FOR DS SSS	
Chief of Research and Development, Department of the Army, Washington, D. C. 20310	
ATTN: Director of Army Technical Information	3 copies of Form 1473
Chief, Combat Materiel Division	1
CRDES	1
Commandant, Command and General Staff College, Fort Leavenworth, Kans. 66027	1
ATTN: Archives	
Commander, U. S. Army Combat Developments Command Engineer Agency, Fort Belvoir, Va. 22060	1
ATTN: CSGEN-M	
Commander, U. S. Army Forces Southern Command, APO New York 09834	1
ATTN: Engineer	
Commander, U. S. Army Picatinny Arsenal, Dover, N. J. 07801	1
ATTN: SMUPA-VC1	
Commanding General, XVIII Airborne Corps, Fort Bragg, N. C. 28307	2
ATTN: Corps Engineer	
Commanding General, U. S. Army Tank-Automotive Command, Warren, Mich. 48090	
ATTN: AMSTA-UL	2
AMSTA-BSL	2
AMSTA-RU	2
Commanding General, U. S. Continental Army Command, Fort Monroe, Va. 23351	
ATTN: Engineer Division, DSCLOG, ATLOG-E-MB	2
ATIT-RD	1

* Addressees please notify USA Engineer Waterways Experiment Station, Vicksburg, Miss. 39180 of corrections or changes in address.

Address	No. of Copies
<u>Army (Continued)</u>	
Commanding General, U. S. Army Materiel Command, Washington, D. C. 20315 ATTN: AMCRD-TV AMCRD-G	2 1
Commanding General, U. S. Army Weapons Command, Rock Island, Ill. 61201 ATTN: AMSWE-RDR	1
Commanding Officer, U. S. Army Arctic Test Center, APO Seattle, Wash. 98733	1
Commanding Officer, U. S. Army Combat Developments Command Transportation Agency, Fort Eustis, Va. 23604 ATTN: Mr. Earl S. Brown	1
Technical Library, USACDC Institute of Land Combat, Taylor Drive, Alexandria, Va. 22314	1
Commanding Officer, U. S. Army General Equipment Test Activity, Fort Lee, Va. 23801	1
Commanding Officer, U. S. Army Mobility Equipment Research and Development Center, Fort Belvoir, Va. 22060 ATTN: Technical Documents Center, Building 315	2
Commanding Officer, USA Cold Regions Research and Engineering Laboratory, Hanover, N. H. 03755 ATTN: Library	1
President, U. S. Army Armor and Engineering Board, Fort Knox, Ky. 40121	1
President, U. S. Army Artillery Board, Fort Sill, Okla. 73503	1
President, U. S. Army Infantry Board, Fort Benning, Ga. 31905	1
Senior Engineer Instructor, Office of Military Instruction, United States Corps of Cadets, West Point, N. Y. 10996	1
Technical Library, Branch No. 4, U. S. Army Limited War Laboratory, Aberdeen Proving Ground, Md. 21005	1
U. S. Army Engineer School, Fort Belvoir, Va. 22060 ATTN: Heavy Construction Branch	1
The Librarian, U. S. Army Engineer School Library, Thayer Hall, Fort Belvoir, Va. 22060	2
U. S. Army Continental Army Command Intelligence Center, Fort Bragg, N. C. 28307 ATTN: Library, IPO	2
U. S. Army Transportation Engineer Agency, Military Traffic Management and Terminal Service, Fort Eustis, Va. 23604	1
Chief, Crops Division, U. S. Army Biological Laboratories, Fort Detrick, Md. 21701	1
Commanding General, U. S. Army Electronics Command, Fort Monmouth, N. J. 07703 ATTN: AMSEL-GG-DD	1
Director, U. S. Army Engineer Topographic Laboratories (TPCTL-GSA), Fort Belvoir, Va. 22060 ATTN: Scientific and Technical Information Center Geographic Application Branch, Geographic Science Division Research Institute (701 Prince St., Alexandria, Va. 22314)	1 1 1

Address	No. of Copies
<u>Army (Continued)</u>	
Commanding Officer, Yuma Proving Ground, Yuma, Ariz. 85364 ATTN: STEYP-TGM	1
Commanding General, U. S. Army Test and Evaluation Command, Aberdeen Proving Ground, Md. 21005	1
ATTN: STEAP-DS-TU	1
STEAP-DP-LU	2
Technical Library, Building 313	
District Engineer, U. S. Army Engineer District, Sacramento, 650 Capitol Mall, Sacramento, Calif. 95814	1
ATTN: The Hydrologic Engineering Center	
<u>Navy</u>	
Commander, Naval Facilities Engineering Command (NFAC-03), Department of the Navy, Washington, D. C. 20390	2
Commander, Naval Ship Systems Command (PMS 384-2), Department of the Navy, Washington, D. C. 20360	1
Commanding Officer, U. S. Naval Photographic Center, Washington, D. C. 20390	1
Commanding Officer, PHIBCB One, U. S. Naval Amphibious Base, Coronado, San Diego, Calif. 92118	1
Commanding Officer, PHIBCB Two, U. S. Naval Amphibious Base, Little Creek, Norfolk, Va. 23521	1
Commanding Officer and Director, Naval Civil Engineering Laboratory, Port Hueneme, Calif. 93041	1
Director, Naval Warfare Research Center, Stanford Research Institute, Menlo Park, Calif. 94025	1
Office of Naval Research, Department of the Navy, Washington, D. C. 20390	1
ATTN: Geography Branch, Earth Sciences Division	
United States Army Attaché, American Embassy, U. S. Navy 100, Box 36, Fleet Post Office, New York 09510	2
U. S. Naval Academy, Annapolis, Md. 21402	2
ATTN: Library, Serials Division	
Chief, Combat Service Support Division, Marine Corps Landing Force Development Center, Marine Corps Schools, Quantico, Va. 22134	1
<u>Air Force</u>	
Air Force Weapons Laboratory, Kirtland AFB, N. Mex. 87117	2
ATTN: Civil Engineering Branch, WLDC	
Commander, Armament Development and Test Center, Eglin AFB, Fla. 32542	1
ATTN: ADBRL-2	
Commander, 3800th AB Wing, AU, Maxwell AFB, Ala. 36112	1
ATTN: BDCE-ED	

Address	No. of Copies
<u>Air Force (Continued)</u>	
Commander, Air Force Systems Command, Aeronautical Systems Division (ASNMS-20), Wright-Patterson AFB, Ohio 45433	1
Commander, Hqs, Military Airlift Command, Scott AFB, Ill. 62225 ATTN: MAMCE/FS	1
Commander, U. S. Strike Command, McDill AFB, Fla. 33608 ATTN: J4-E	1
Chief, Concepts and Evaluation Group	1
Headquarters, U. S. Air Force, Washington, D. C. 20330 ATTN: Astronautics Division, DCS/Research and Development (AFRSTC)	1
Director of Civil Engineering (AFOCE-KA) 20333	2
Base Structures Branch, Directorate of Civil Engineering (AFOCE-GC) 20333	1
Headquarters, Air Force Systems Command, Directorate of Civil Engineering (SCOC), Andrews AFB, Washington, D. C. 20331	2
Headquarters, Tactical Air Command, Langley AFB, Va. 23365 ATTN: DEPL	2
Director, Terrestrial Sciences Laboratory (CRJT), Air Force Cambridge Research Laboratories, L. G. Hanscom Field, Bedford, Mass. 01730	1
<u>Colleges and Universities</u>	
University of Arkansas, College of Engineering, Fayetteville, Ark. 72701 ATTN: Mr. Henry H. Hicks, Jr.	1
University of California, Institute of Transportation and Traffic Engineering Library, Richmond, Calif. 94804	1
University of Detroit, Detroit, Mich. 48221 ATTN: Mr. David Sloss, Civil Engineering Department	1
University of Kansas, Center for Research and Engineering Science, Lawrence, Kans. 66044	1
Louisiana State University, Coastal Studies Institute, Baton Rouge, La. 70803	1
University of Michigan, Ann Arbor, Mich. 48104 ATTN: Professor L. C. Stuart	1
University of New Mexico, Eric H. Wang Civil Engineering Research Facility, Box 188, University Station, Albuquerque, N. Mex. 87106	2
New York University, University Heights, Bronx, N. Y. 10453 ATTN: Engineering Library, School of Engineering and Science	1
Stevens Institute of Technology, Davidson Laboratory, Hoboken, N. J. 07030 ATTN: Dr. I. R. Ehrlich	1
<u>Others</u>	
Stanford Research Institute, Menlo Park, Calif. 94025 ATTN: Mr. John J. Emanski	1

Address	No. of Copies
<u>Others (Continued)</u>	
Chief, World Soil Geography Unit, Soil Conservation Service, USDA, Room 233A Federal Center Building, Hyattsville, Md. 20782	1
Cornell Aeronautical Laboratory, Inc., P. O. Box 235, Buffalo, N. Y. 14221	1
Defense Documentation Center, Cameron Station, Alexandria, Va. 22313 ATTN: Mr. Myer Kahn	12
Defense Intelligence Agency, Washington, D. C. 20301 ATTN: DIAAP-4B	1
Director, Pacific Southwest Forest and Range Experiment Station, Berkeley, Calif. 94704 ATTN: Mr. Henry W. Anderson	1
Engineering Societies Library, 345 E. 47th Street, New York, N. Y. 10017	1
Director, OSD/ARPA Regional Field Office, APO New York 09205 ATTN: ARMISH-MAAG (RFO-I)	1
Chief, Crops Protection Branch, Crops Research Division, Agricultural Research Service, Beltsville, Md. 20705	1
Highway Research Board, 2101 Constitution Ave., Washington, D. C. 20001	1
Federal Highway Administration, U. S. Department of Transportation, Washington, D. C. 20591	1
Library, Division of Public Documents (NO CLASSIFIED REPORTS TO THIS AGENCY), U. S. Printing Office, Washington, D. C. 20401	1
Library of Congress, Documents Expediting Project, Washington, D. C. 20450	1
National Tillage Machinery Laboratory, U. S. Department of Agriculture, Auburn, Ala. 36830	1
Research Analysis Corporation, McLean, Va. 22101 ATTN: Library	1
Space Sciences Laboratory, Code RSSL-N, George C. Marshall Spaceflight Center, National Aeronautics and Space Administration, Huntsville, Huntsville, Ala. 35812 ATTN: Dr. Nicholas C. Costes	1
U. S. Geological Survey, Washington, D. C. 20242 ATTN: Chief, Source Material Unit, Branch of Military Geology	2
WNRE, Inc., Chestertown, Md. 21620 ATTN: Library	1

Unclassified
Security Classification

DOCUMENT CONTROL DATA - R & D		
(Security classification of title, body of abstract and indexing annotation must be entered when the overall report is classified)		
1. ORIGINATING ACTIVITY (Corporate author) U. S. Army Engineer Waterways Experiment Station Vicksburg, Mississippi		2a. REPORT SECURITY CLASSIFICATION Unclassified
		2b. GROUP
3. REPORT TITLE DYNAMICS OF WHEELED VEHICLES; Report 2, IMPLEMENTATION OF WIENER-BOSE THEORY AND APPLICATION TO RIDE DYNAMICS		
4. DESCRIPTIVE NOTES (Type of report and inclusive dates) Report 2 of a series		
5. AUTHOR(S) (First name, middle initial, last name) Allan S. Lessem		
6. REPORT DATE March 1971	7a. TOTAL NO. OF PAGES 134	7b. NO. OF REFS 18
8a. CONTRACT OR GRANT NO.		9a. ORIGINATOR'S REPORT NUMBER(S) Technical Report M-68-1, Report 2
b. PROJECT NO. LT061102B52A Task 01		9b. OTHER REPORT NO(S) (Any other numbers that may be assigned this report)
c.		
d.		
10. DISTRIBUTION STATEMENT This document has been approved for public release and sale; its distribution is unlimited.		
11. SUPPLEMENTARY NOTES Report was also submitted as thesis for degree of Doctor of Philosophy in Engineering to Mississippi State University, State College, Miss.		12. SPONSORING MILITARY ACTIVITY U. S. Army Materiel Command Washington, D. C.
13. ABSTRACT Wiener-Bose Theory is a strategy for identifying nonlinear systems in terms of a set of "characterizing coefficients." These are obtained through the agency of a certain probing process carried out on each system. Once the coefficients have been determined they must be used in a rational synthesis procedure to predict responses to inputs of interest. The principal appeal of Wiener-Bose Theory is that it requires very little knowledge of the physics of the system. No dynamical equations need be written. In essence the physics of the system is incorporated into the characterizing coefficients. It is this property of Wiener-Bose Theory that makes its application to vehicle ride dynamics studies attractive. The present strategy for ride dynamics studies invokes the use of structure-oriented mass-spring-dashpot models based on rigid body mechanics. These models are characterized by the need for repeated "tuning" in which model parameters are altered in a basically irrational way when comparisons are made to different sets of responses of actual vehicles. A computer study was conducted to discern problems of implementation of the theory. Several systems of increasing complexity were studied and a practical form of Wiener-Bose Theory evolved. The systems studied were as follows: (a) a zero-memory system, (b) rate-independent hysteresis, (c) a second-order system with saturation, and (d) a fourth-order mechanical system with nonlinear compliances. The experience gained during this study was summarized in a set of guidelines for the construction of Wiener-Bose models. A program of testing was carried out to ascertain the practicality and utility of Wiener-Bose Theory for ride dynamics studies. A military M37, 3/4-ton truck was selected for characterization using a Wiener-Bose model having 1024 coefficients. The characterizing coefficients were obtained by utilizing the responses of the vehicle recorded during traversal of a specially configured obstacle course whose total length was 2.5 miles. Once the coefficients were obtained, they were used to synthesize responses to specific terrain profiles. These predicted responses compared favorably with counterpart responses of the vehicle traversing the same profiles. It was concluded that Wiener-Bose Theory is capable of satisfactory performance in the analysis of many nonlinear systems. The principal difficulty in its practical application is the extensive probing effort required for characterizing the system.		

DD FORM 1473
1 NOV 65

REPLACES DD FORM 1473, 1 JAN 64, WHICH IS OBSOLETE FOR ARMY USE.

Unclassified
Security Classification

14.	KEY WORDS	LINK A		LINK B		LINK C	
		ROLE	WT	ROLE	WT	ROLE	WT
	Mathematical models Nonlinear systems Ride dynamics Vehicle dynamics Wiener-Bose Theory						